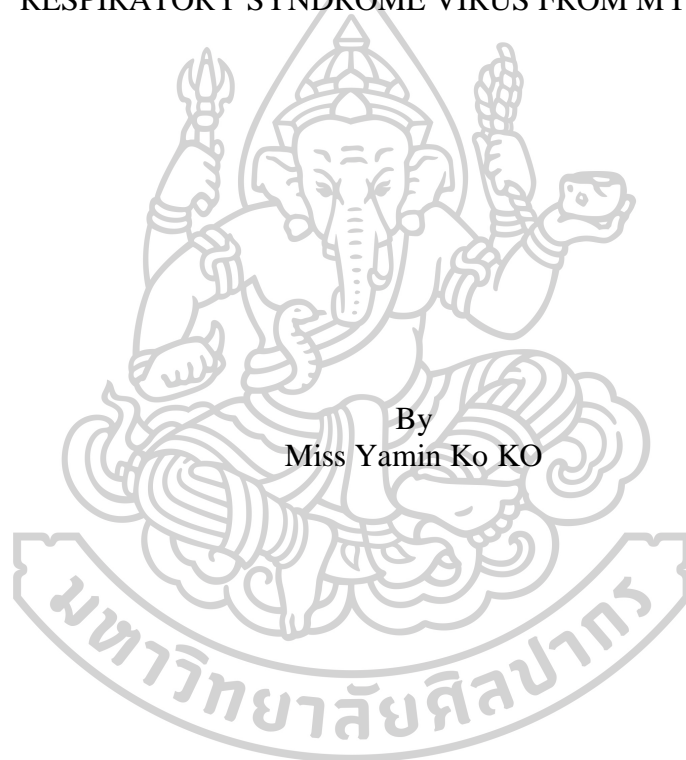


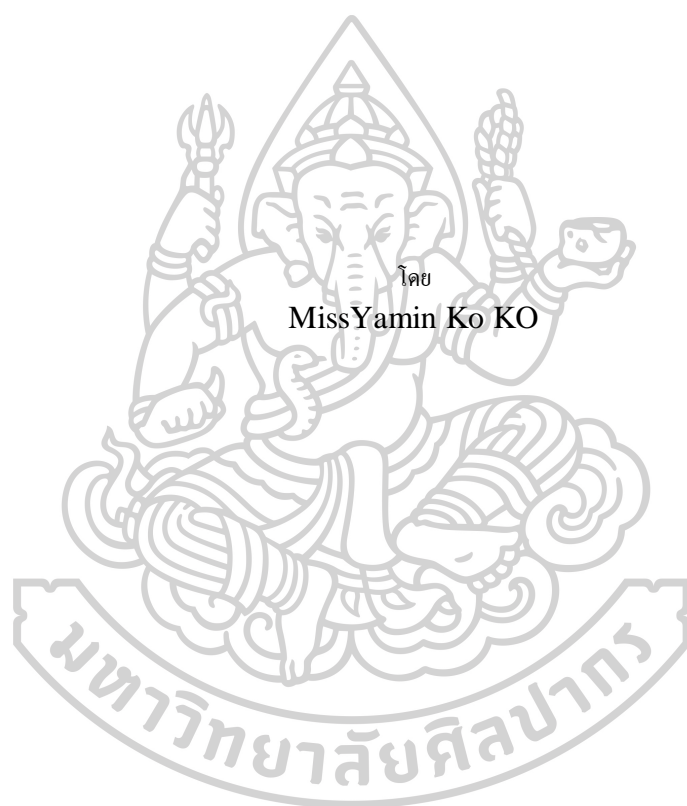


MOLECULAR CHARACTERIZATION AND *IN SILICO* EPITOPE PREDICTIONS  
OF NSP2-HVII, GP5, AND NP OF PORCINE REPRODUCTIVE AND  
RESPIRATORY SYNDROME VIRUS FROM MYANMAR



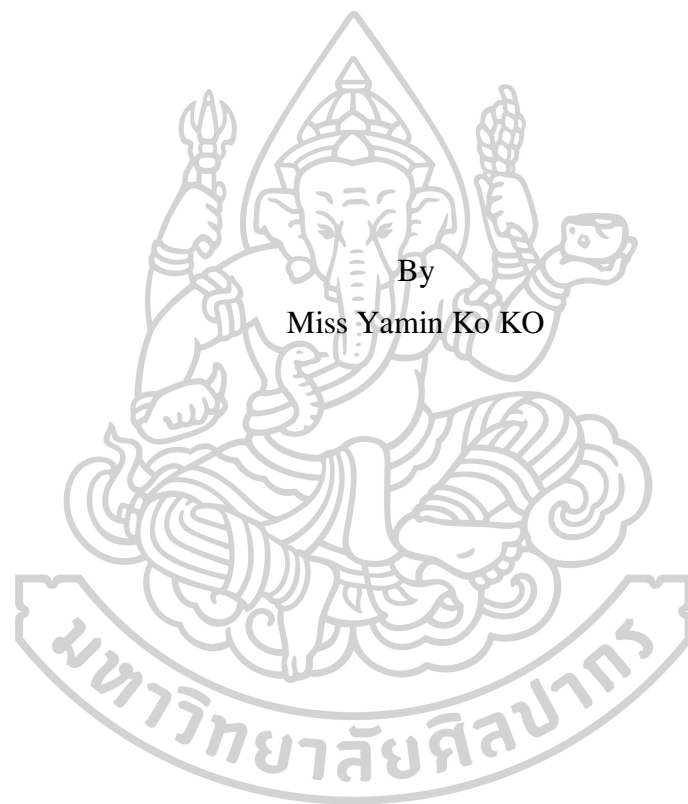
By  
Miss Yamin Ko KO

A Thesis Submitted in Partial Fulfillment of the Requirements  
for Doctor of Philosophy (PHARMACEUTICAL SCIENCES)  
Graduate School, Silpakorn University  
Academic Year 2018  
Copyright of Graduate School, Silpakorn University



วิทยานิพนธ์นี้เป็นส่วนหนึ่งของการศึกษาดำเนินการตามหลักสูตรปริญญาตรีบัณฑิต  
สาขาวิชาวิทยาการทางเภสัชศาสตร์ แบบ 1.1 ปริญญาตรีบัณฑิต  
บัณฑิตวิทยาลัย มหาวิทยาลัยศิลปากร  
ปีการศึกษา 2561  
ลิขสิทธิ์ของบัณฑิตวิทยาลัย มหาวิทยาลัยศิลปากร

MOLECULAR CHARACTERIZATION AND *IN SILICO* EPITOPE  
PREDICTIONS OF NSP2-HV7, GP5, AND NP OF PORCINE  
REPRODUCTIVE AND RESPIRATORY SYNDROME VIRUS FROM  
MYANMAR



By  
Miss Yamin Ko KO

A Thesis Submitted in Partial Fulfillment of the Requirements  
for Doctor of Philosophy (PHARMACEUTICAL SCIENCES)  
Graduate School, Silpakorn University  
Academic Year 2018  
Copyright of Graduate School, Silpakorn University

Title MOLECULAR CHARACTERIZATION AND *IN SILICO* EPITOPE PREDICTIONS OF NSP2-HVII, GP5, AND NP OF PORCINE REPRODUCTIVE AND RESPIRATORY SYNDROME VIRUS FROM MYANMAR

By Yamin Ko KO

Field of Study (PHARMACEUTICAL SCIENCES)

Advisor Busaba Powthongchin

---

Graduate School Silpakorn University in Partial Fulfillment of the Requirements for the Doctor of Philosophy

..... Dean of graduate school  
(Associate Professor Jurairat Nunthanid, Ph.D.)

Approved by

..... Chair person  
(Assistant Professor Sunee Techaarpornkul , Ph.D.)

..... Advisor  
(Assistant Professor Busaba Powthongchin , Ph.D.)

..... Co Advisor  
(Assistant Professor Suang Rungpragayphan , Ph.D.)

..... External Examiner  
(Associate Professor Meena Sarikaputi , Ph.D.)



57356805 : Major (PHARMACEUTICAL SCIENCES)

Keyword : Porcine Reproductive and Respiratory Syndrome Virus, Nsp2-VII, GP5, NP, Molecular Characterization, In Silico Epitope Predictions

MISS YAMIN KO KO : MOLECULAR CHARACTERIZATION AND *IN SILICO* EPITOPE PREDICTIONS OF NSP2-HVII, GP5, AND NP OF PORCINE REPRODUCTIVE AND RESPIRATORY SYNDROME VIRUS FROM MYANMAR THESIS ADVISOR : ASSISTANT PROFESSOR BUSABA POWTHONGCHIN, Ph.D.

Porcine reproductive and respiratory syndrome, a severe reproductive and respiratory disease in pigs, continues to cause a problem in pig production worldwide including Myanmar. In this study, six PRRSV-infected clinical samples collected from five regions of Myanmar during outbreaks in 2011 were investigated, and genetic characteristics and phylogenetic relationship of Myanmar PRRSVs were determined based on *Nsp2-HVII*, ORF5, and ORF7 gene regions. Sequence analyses revealed that all Myanmar PRRSVs shared 96.8-100% nucleotide and 94.9-100% amino acid identities of all three genes to each other, and 69.5-94.4% nucleotide and 61.4-96.7% amino acid sequence identities with VR-2332, the NA prototype, implying their source of derivation. The 30 discontinuous amino acid deletions at position 481 and 533-561 were found in the Nsp2-HVII of all Myanmar PRRSVs, indicated that they were highly pathogenic (HP)-PRRSV. The nucleotide and amino acid sequence identities of each gene were highly similar to HP-PRRSV strains, especially from Thailand, Laos, and Cambodia. From phylogenetic analyses, Myanmar PRRSVs were clustered into the same subtype 3 of NA-genotypic group as other Southeast Asian HP-PRRSV strains from Thailand, Laos, and Cambodia, suggesting their close relationships. The unique amino acid mutations found only in Myanmar PRRSVs were L292F, P431S, and V621M in Nsp2-HVII and E170G in GP5, which may be useful as a marker for monitoring genetic diversity of newly emerging HP-PRRSV strains. In order to propose a reverse vaccinology approach for the development of novel PRRS vaccine design, B-cell and T-cell epitopes from three PRRSV proteins were predicted. By using different *in silico* bioinformatics tools, a total of 44 linear B-cell epitopes, 17 MHC I binding T-cell and 97 MHC II binding T-cell epitopes were predicted from Nsp2-HVII, GP5, and NP of Myanmar PRRSV (HP/MYANMAR/2303AM/2011). Of which, SB3 of Nsp2-HVII, GB5 of GP5, and NB6 of NP were selected as first-line linear B-cell potential candidates. Furthermore, S1T5, and S2T32, G1T2, and G2T39, N1T2, and N2T10 were selected as MHC I and MHC II binding T-cell potential candidates of Nsp2-HVII, GP5, and NP, respectively. The immunogenicity of these potential PRRSV epitope vaccine candidates needs to be further verified through *in vivo* testing. This study provides basic information for monitoring newly diverging strains, future epidemiological investigation, and development of effective strategies to control PRRS in Myanmar.

## ACKNOWLEDGEMENTS

My deepest gratitude goes to my advisor, Assistant Professor Busaba Powthongchin, Ph.D. and co-advisors Assistant Professor Suang Rungpragayphan, Ph.D. and Assistant Professor Perayot Pamonsinlapatham, Ph.D. for their great guidance, support, and encouragement. I am also grateful to Associate Professor Meena Sarikaputi and Assistant Professor Sunee Techaarpornkul for their invaluable advice.

My deepest thanks go to Associate Professor Tanasait Ngawhirunpat, Ph.D., Dean, and Associate Professor Jurairat Nunthanid, Ph.D., Former Dean, Professor Pornsak Sriamornsak, Ph.D. and Lecturer Waranee Bunchuailua, Ph.D., Faculty of Pharmacy, who help me to get an opportunity for studying at Faculty of Pharmacy, Silpakorn University.

My very special thanks go to Dr. Aung Myint for the kind support of PRRSV-infected clinical samples. I also wish to thank Dr. Aung Zaw Latt, Kaythi Aye and Kay Khine Soe for their great help in DNA sequencing in Myanmar.

My special thanks are extended to Professor Dr. Zaw Than Htun, Director General, Dr. Kyaw Zin Thant, Former Director General, and Board of Directors and Head of Quality Control Division, Department of Medical Research, Myanmar for their kind help and permission to carry out this research work. My special thanks go to Dr. Marlar Myint, Former Rector of University of Pharmacy, Yangon, for her valuable advice and encouragement.

I would like to sincerely thanks to all teachers, students, researchers, staff, and all my friends in the Faculty of Pharmacy, Silpakorn University, for giving me the place, knowledge, and friendship.

I am so grateful to the Graduate School, Silpakorn University, Research and Development Institute, Silpakorn University, and Research and Creative Fund, Faculty of Pharmacy, Silpakorn University for financial support.

Lastly, and most importantly, I would like to thank my family for their love, understanding, encouragement, and providing unconditional support and wise advice in several circumstances.

Yamin Ko KO

## TABLE OF CONTENTS

	<b>Page</b>
ABSTRACT .....	D
ACKNOWLEDGEMENTS .....	E
TABLE OF CONTENTS.....	F
LIST OF TABLES .....	I
LIST OF FIGURES .....	K
LIST OF ABBREVIATIONS.....	N
CHAPTR 1 INTRODUCTION.....	1
1.1. Statement and Significance of the Problems .....	1
1.2. Objectives.....	3
1.3. Hypothesis to be tested .....	3
CHAPTER 2 LITERATURE REVIEW .....	4
2.1. Porcine Reproductive and Respiratory Syndrome (PRRS).....	4
2.1.1. General Characteristics and Economic Impacts of PRRS.....	4
2.1.2. Prevalence of PRRS in Asia.....	4
2.1.3. Prevalence of PRRS in Myanmar .....	5
2.2. Porcine Reproductive and Respiratory Syndrome Virus (PRRSV) .....	8
2.2.1. Biology and Structure of PRRSV .....	8
2.2.2. Molecular Biology of PRRSV .....	9
2.2.2.1. Non-structural Proteins.....	9
2.2.2.2. Structural proteins .....	10
2.2.3. Route of Transmission, Pathogenesis and Clinical Manifestation .....	12
2.2.3.1. Route of Transmission.....	13
2.2.3.2. Pathogenesis and Clinical Manifestation.....	13
2.2.4. Host Immunological Response to PRRSV Infection.....	14
2.2.5. Genetic Variability of PRRSV .....	16



2.2.6. Diagnosis, Control and Prevention of PRRSV infection .....	16
2.2.7. PRRS Vaccine Development.....	18
2.3. <i>In Silico</i> Bioinformatics Tools.....	19
2.3.1. Bioinformatics Tools in Genetic Analysis .....	19
2.3.2. Bioinformatics Tools in Reverse Vaccinology.....	20
CHAPTER 3 MATERIALS AND METHODS.....	24
3.1. MATERIALS .....	24
3.1.1. Reagents and Equipments .....	24
3.1.2. Primers .....	25
3.1.3. Clinical Samples.....	25
3.2. METHODS.....	28
3.2.1. Molecular Characterization .....	28
3.2.1.1. RNA Isolation .....	28
3.2.1.2. Amplification of DNA by Reverse Transcription Polymerase Chain Reaction .....	28
3.2.1.2.1. Amplification of DNA for Spleen Sample .....	31
3.2.1.2.2. Amplification of DNA for Serum Samples .....	32
3.2.1.3. Agarose Gel Electrophoresis.....	32
3.2.1.4. DNA Sequencing .....	34
3.2.1.5. Sequence Alignments and Sequence Analyses .....	34
3.2.1.5.1. Pairwise Sequence Alignments.....	34
3.2.1.5.2. Multiple Sequence Alignments.....	35
3.2.1.6. Prediction of Signal Peptide, Transmembrane Topology, and N- Glycosylation .....	35
3.2.2. Phylogenetic Tree Construction .....	35
3.2.3. <i>In silico</i> Epitope Prediction using Bioinformatics Tools .....	38
3.2.3.1. Antigenicity Prediction.....	38
3.2.3.2. Epitope Prediction .....	38
3.2.3.2.1. Prediction of Linear B- cell Epitopes.....	38
3.2.3.2.2. Prediction of MHC I binding T-cell Epitopes .....	39

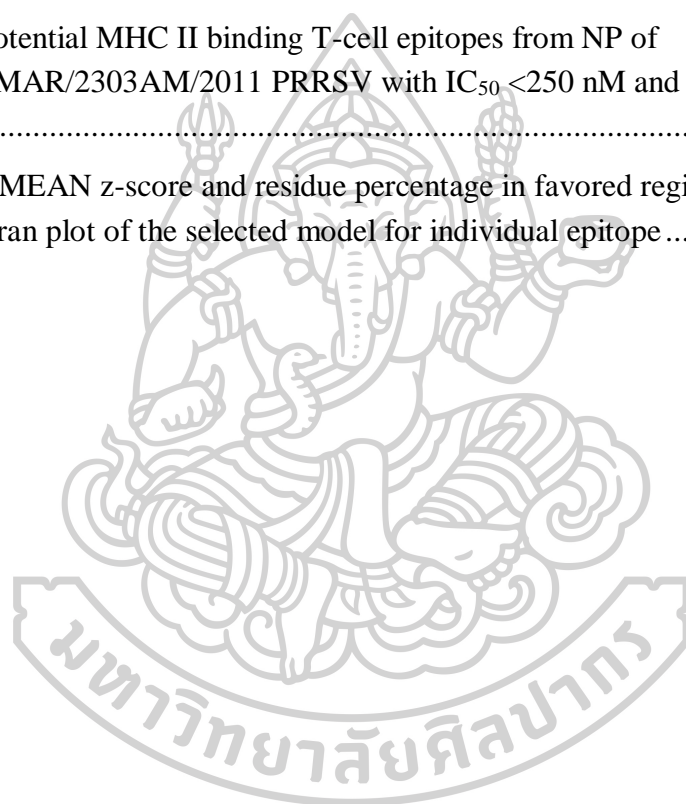


3.2.3.2.3. Prediction of MHC II binding T-cell Epitopes.....	39
3.2.3.3. Epitope Conservancy Prediction .....	40
3.2.3.4. Protein Model Prediction and Validation .....	40
CHAPTER 4 RESULTS .....	42
4.1. Molecular Characterization .....	42
4.1.1. RNA Isolation, PCR Amplification, and DNA Sequencing .....	42
4.1.2. Pairwise Sequence Alignments of <i>Nsp2-HVII</i> , ORF5, and ORF7 .....	44
4.1.3. Amino Acid Sequence Analyses .....	48
4.1.3.1. The middle hypervariable region of non-structural protein-2 (Nsp2-HVII).....	48
4.1.3.2. The major envelope protein, glycoprotein 5 (GP5) .....	53
4.1.3.3. The nucleocapsid protein (NP) .....	56
4.2. Phylogenetic Analyses .....	59
4.3. <i>In silico</i> Epitope Prediction using Bioinformatics Tools .....	63
4.3.1. Antigenicity Prediction of the Nsp2-HVII, GP5, and NP .....	63
4.3.2. Prediction of Linear B-cell epitopes .....	64
4.3.3. Prediction of T-cell epitopes .....	70
4.3.3.1. Prediction of MHC I binding T-cell epitopes .....	70
4.3.3.2. Prediction of MHC II binding T-cell epitopes .....	76
4.3.4. Epitope Conservancy Prediction .....	90
4.3.5. Protein Model Prediction and Validation.....	90
CHAPTER 5 DISCUSSION .....	96
5.1. Genetic Characterizations and Phylogenetic Analyses.....	97
5.2. <i>In silico</i> Epitope Prediction using Bioinformatics Tools .....	100
CHAPTER 6 CONCLUSION.....	105
REFERENCES .....	106
APPENDIX.....	119
VITA.....	133

## LIST OF TABLES

	<b>Page</b>
Table 1. The primers used for amplification of Nsp2-HVII, ORF5, and ORF7 genes	25
Table 2. Background information on PRRSV-infected clinical samples from pig farms in Myanmar during 2011 .....	27
Table 3. PRRSV reference strains used in the study .....	37
Table 4. GenBank accession number of Nsp2-HVII, ORF5, and ORF7 of Myanmar PRRSVs analyzed in the study.....	44
Table 5. Pairwise comparisons of the nucleotide (nt) and amino acid (aa) sequences of Nsp2-HVII, ORF5, and ORF7 between six Myanmar PRRSVs .....	45
Table 6. Pairwise comparisons of the nucleotide (nt) and amino acid (aa) sequences of Nsp2-HVII, ORF5, and ORF7 between six Myanmar PRRSVs, NA prototype (VR-2332) and EU prototype (Lelystad).....	46
Table 7. Pairwise comparisons of the nucleotide (nt) and amino acid (aa) sequences of Nsp2-HVII, ORF5, and ORF7 between six Myanmar PRRSVs and Asian reference PRRSV strains.....	47
Table 8. The antigenicity score of Nsp2-HVII, GP5, and NP of six Myanmar PRRSVs .....	63
Table 9. Potential linear B-cell epitopes predicted from Nsp2-HVII of HP/MYANMAR/2303AM/2011 PRRSV with BCPred and APP score (>0.75) and VaxiJen antigenicity score (>0.5).....	66
Table 10. Potential linear B-cell epitopes predicted from GP5 of HP/MYANMAR/2303AM/2011 PRRSV with BCPred and APP score (>0.75) and VaxiJen antigenicity score (>0.5).....	68
Table 11. Potential linear B-cell epitopes predicted from NP of HP/MYANMAR/2303AM/2011 PRRSV with BCPred and APP score (>0.75) and VaxiJen antigenicity score (>0.5).....	69
Table 12. Potential MHC I binding T-cell epitopes from Nsp2-HVII of HP/MYANMAR/2303AM/2011 PRRSV with total processing score and IC <sub>50</sub> for specific SLA MHC I alleles .....	72
Table 13. Potential MHC I binding T-cell epitopes from GP5 of HP/MYANMAR/2303AM/2011 PRRSV with total processing score and IC <sub>50</sub> for specific SLA MHC I alleles .....	73

Table 14. Potential MHC I binding T-cell epitopes from NP of HP/MYANMAR/2303AM/2011 PRRSV with total processing score and IC <sub>50</sub> for specific SLA MHC I alleles .....	75
Table 15. Potential MHC II binding T-cell epitopes from Nsp2-HVII of HP/MYANMAR/2303AM/2011 PRRSV with IC <sub>50</sub> <250 nM and VaxiJen antigenicity score > 0.5 .....	78
Table 16. Potential MHC II binding T-cell epitopes from GP5 of HP/MYANMAR/2303AM/2011 PRRSV with IC <sub>50</sub> <250 nM and VaxiJen antigenicity score > 0.5 .....	82
Table 17. Potential MHC II binding T-cell epitopes from NP of HP/MYANMAR/2303AM/2011 PRRSV with IC <sub>50</sub> <250 nM and VaxiJen antigenicity score > 0.5 .....	88
Table 18. QMEAN z-score and residue percentage in favored region of Ramachandran plot of the selected model for individual epitope .....	93



## LIST OF FIGURES

	<b>Page</b>
Figure 1. Distribution map of PRRS outbreaks in Myanmar during 2011 .....	7
Figure 2. Schematic representation of PRRSV particle showing the location of structural proteins GP2a, GP2b (E), GP3, GP4, GP5, GP5a, M and N.....	8
Figure 3. Schematic representation of the PRRSV genome organization.....	9
Figure 4. Schematic representation of the Nsp2 .....	10
Figure 5. Schematic representation of the GP5.....	11
Figure 6. Schematic representation of the NP.....	12
Figure 7. Illustration of the immune response in pig after infection with the porcine reproductive and respiratory syndrome (74).....	14
Figure 8. Schematic representation of the vaccine development by conventional approach and reverse vaccinology (13).....	22
Figure 9. Myanmar map showing the location of collected clinical samples .....	26
Figure 10. Flow diagram of RNA extraction from spleen sample using GeneJET viral DNA and RNA purification kit (Thermo Fisher Scientific) .....	29
Figure 11. Flow diagram of RNA Extraction from serum samples using QIAamp viral RNA purification kit (Qiagen) .....	30
Figure 12. Flow diagram of purification of gel cuts using Gel/PCR DNA fragments extraction kit (Nucleospin) .....	33
Figure 13. Flow diagram summarizing the linear B-cell epitopes, MHC I binding and MHC II binding T-cell epitope predictions .....	41
Figure 14. Gel electrophoresis (2% agarose) of PCR products of (A) Nsp2-HVII, bands at about 1000 bp (B) ORF5, bands at about 600 bp and (C) ORF7, bands at about 400 bp.....	43
Figure 15. Multiple amino acid sequence alignment of Nsp2-HVII (residues 265 – 628) between six Myanmar PRRSVs and the corresponding region of VR-2332 and its vaccine strain, RespPRRS, LP-PRRSVs (Chinese CH1a and its vaccine strain, CH1R), and HP-PRRSVs (Chinese JXA1 and its vaccine strain, JXA1R), Vietnamese 07QN, Thai HP/THAILAND/19500LL/2010, Laotian BH58/10, and Cambodian 10CAM46/2010) .....	52

Figure 16. Multiple amino acid sequence alignment of GP5 (200 residues) between six Myanmar PRRSVs, VR-2332 and its vaccine strain, RespPRRS, LP-PRRSVs (Chinese CH1a and its vaccine strain, CH1R), and HP-PRRSVs (Chinese JXA1 and its vaccine strain, JXA1R), Vietnamese 07QN, Thai HP/THAILAND/19500LL/2010, Laotian BH58/10, and Cambodian NA/CAMC044/2010) .....	55
Figure 17. Multiple amino acid sequence alignment of NP (123 residues) between six Myanmar PRRSVs, VR-2332 and its vaccine strain, RespPRRS, LP-PRRSVs (Chinese CH1a and its vaccine strain, CH1R), and HP-PRRSVs (Chinese JXA1 and its vaccine strain, JXA1R), Vietnamese 07QN, Thai HP/THAILAND/ 19500LL/2010, and Laotian BH58/10) .....	58
Figure 18. Phylogenetic tree of PRRSVs based on nucleotide sequences of Nsp2-HVII gene.....	60
Figure 19. Phylogenetic tree of PRRSVs based on nucleotide sequences of ORF5 gene.....	61
Figure 20. Phylogenetic tree of PRRSVs based on nucleotide sequences of ORF7 gene.....	62
Figure 21. The diagram summarizing linear B-cell epitope prediction.....	65
Figure 22. The diagram summarizing MHC I binding T-cell epitope prediction .....	71
Figure 23. The diagram summarizing MHC II binding T-cell epitope prediction.....	77
Figure 24. (A) Modelled 3D structure of NP of Myanmar PRRSVs (B) 3D structure of NP, showing selected MHC I T-cell epitope, N1T2 (LSDSGRISY) in $\beta$ -sheet region (C) Ramachandran plot of modelled structural template for NP showing 99.1% residues in favored region.....	92
Figure 25. Modelled peptide structure of predicted linear B-cell, MHC I and MHC II binding T-cell epitopes .....	94
Figure 26. Schematic diagram showing analogous or different mutations between Nsp2-HVII (left, black line) and GP5 (right, red line) of Southeast Asian HP-PRRSVs .....	99

**LIST OF ABBREVIATIONS**

°C	Degree Celsius
μL	Microliter
aa	Amino Acid
CD4 <sup>+</sup>	Cluster of Differentiation 4
CD8 <sup>+</sup>	Cluster of Differentiation 8
cDNA	Complementary Deoxyribonucleic Acid
cm	Centimeter
CTL	Cytotoxic T lymphocyte
DNA	Deoxyribonucleic Acid
EDTA	Ethylenediaminetetraacetic Acid
e.g.	exempli gratia (Latin); for example
EtOH	Ethanol
EU	European
mg	Milligram
g	Relative Centrifugal Force
GP	Glycoprotein
h	Hour
HLA	Human Leucocyte Antigen
HP	Highly Pathogenic
i.e.	id est (Latin); that is
IEDB-AR	Immune Epitope Database – Analysis Resources
IFN-γ	Interferon gamma
L	Liter
LP	Low pathogenic
M	Mole
MHC	Major Histocompatibility Complex
min	Minute
MLV	Modified Live Vaccine
mL	Milliliter
mM	Millimole

NP	Nucleocapsid Protein
NA	North American
nM	Nanomole
Nsp	Non-structural Protein
nt	Nucleotide
ORF	Open Reading Frame
PCR	Polymerase Chain Reaction
pH	Power of Hydrogen
pmol	Picomole
®	Registered Trademark
RNA	Ribonucleic Acid
rpm	Revolution per Minute
RT	Room Temperature
RT-PCR	Reverse Transcription Polymerase Chain Reaction
s	Second
SLA	Swine Leucocyte Antigen
TAE	Tris-Acetate buffer
TE	Tris-EDTA buffer





## CHAPTR 1

### INTRODUCTION

#### 1.1. Statement and Significance of the Problems

Porcine reproductive and respiratory syndrome (PRRS) is a major threat to swine production worldwide that causes massive economic losses (1, 2). It is characterized by severe reproductive failure in pregnant sows (e.g. high rate of abortion, premature birth, stillbirth, and mummified fetuses) and respiratory problems in pigs of any age especially piglets (3, 4). The PRRS was first reported almost simultaneously in North America and Western Europe in the late 1980s, and after that globally distributed (5). Genetic hypervariability and host-immune escape ability of PRRS virus (PRRSV) are the major problems in controlling PRRS (6, 7). In 2006, the emergence of highly pathogenic (HP) PRRSV in China, which caused significant high morbidity and mortality rate showed the impact of genetic hypervariability and heterogeneity of PRRSV and recently HP-PRRSV is the prevalent strain in Asian countries (8, 9). Thus, the genetic hypervariation has to be taken into account for vaccination strategy of PRRSV since currently available PRRSV vaccines fail to provide substantial effect against the heterologous virus, and genetic recombination between vaccine and field strains can lead to the emergence of more virulent strains (7). Therefore, novel field strains of PRRSV are being continuously isolated and genetic characteristics and phylogenetic relationships of the PRRSV are periodically analyzed in all affected countries, to investigate the source of infection, genetic evolution of PRRSV and the choice of PRRSV vaccine. On the other hands, several approaches for the development of new PRRSV vaccines such as modified live vaccines (MLV), inactivated vaccines and recombinant subunit vaccines have been studied (10). In spite of extensive efforts, little progress has been made to improve the protective efficacy of PRRSV vaccines and heterogeneity of virus makes it difficult to design the effective vaccine based on single strain (7, 10). With advances in genomic sequencing and bioinformatics, vaccine development comes into a new era where it is feasible to access the entire antigenic repertoire of a pathogen and an approach is designated as reverse vaccinology (11, 12). The development of the MenB vaccine against *Neisseria meningitidis* serogroup B is the first successful

application of reverse vaccinology approach and it has been successfully applied to various pathogens (13). Together with advanced *in silico* bioinformatics tools, this approach significantly improves the process of vaccine candidates identification by prediction of epitopes (B-cell and T-cell epitopes) which are potential to be antigenic or immunogenic, from the genome sequence of specific organisms with reduced laborious screening task and less time-consuming (12). Hence, *in silico* prediction of vaccine targets from the genome sequences of circulating PRRSV strains becomes a novel approach to develop a new vaccine for rapidly diverging PRRS virus.

Among the PRRSV proteins, there are three proteins of high research interest: non-structural protein 2 (Nsp2), glycoprotein 5 (GP5), and nucleocapsid protein (NP), which are regarded as the genetic markers for characterization of PRRSV. The Nsp2 is the largest non-structural protein involved in viral replication. It is the highest diverse protein, especially in the middle hypervariable region (Nsp2-HVII), and shares only less than 40% amino acid identity among genotypes (5). The GP5 is a major envelope protein with variable numbers of N-glycans that plays important roles in virus neutralization. It is the most variable structural protein and there is 45-48% amino acid sequence difference between two genotypes. The NP, the most abundant and highly antigenic, is an important target for serological detection (14-17).

In Myanmar, the first PRRS outbreak emerged in Mandalay in February 2011, and later on, several outbreaks occurred during that year (18, 19). The PRRS caused death to a large number of pigs with approximately 34% of the pig population died during the first outbreak in Mandalay. High mortality and morbidity rate of the disease caused significant loss in Myanmar pig population. The Livestock Breeding and Veterinary Department allowed to use North America type modified live vaccine at the end of 2017 and Ingelvac PRRS MLV, Boehringer Ingelheim, Germany is currently being used in Myanmar (20). The PRRS cases are still being reported in the Myanmar pig farms but, there is limited information about molecular characteristics and epidemiology of the PRRSV circulated in Myanmar. In this study, with the intention of examining the genetic characteristics of PRRSVs spread during the outbreaks in Myanmar in 2011, the sequences of the middle hypervariable region of Nsp2 encoding gene (denoted as *Nsp2-HVII*), ORF5, and ORF7 of Myanmar PRRSVs were analyzed and their phylogenetic relationships with the sequences of reference

PRRSVs in GenBank database were also determined. In addition, linear B-cell, MHC I and MHC II binding T-cell epitopes from the deduced amino acid sequences of *Nsp2-HVII*, ORF5, and ORF7 were predicted using various current bioinformatics tools. This study could provide useful information for epidemiological investigations, effective vaccine selection and efficient controlling programs of PRRSV in Myanmar, and notably useful reverberations for the development of a novel vaccine and immunodiagnostic markers for PRRSV.

## 1.2. Objectives

The objectives of this study were:

- 1.2.1. To analyze the genetic characteristics of six Myanmar PRRSVs based on the nucleotide and the deduced amino sequences of *Nsp2-HVII*, ORF5, and ORF7
- 1.2.2. To construct the phylogenetic trees, based on *Nsp2-HVII*, ORF5, and ORF7 of Myanmar PRRSVs and the reference strains, published in GenBank, NCBI database
- 1.2.3. To predict the linear B-cell epitopes, and MHC I and MHC II binding T-cell epitopes from the deduced amino acid sequences of *Nsp2-HVII*, ORF5, and ORF7 of Myanmar PRRSVs using current bioinformatics tools

## 1.3. Hypothesis to be tested

- 1.3.1. Genetic and phylogenetic analyses based on *Nsp2-HVII*, ORF5, and ORF7 sequences determine genetic characteristics of Myanmar PRRSVs
- 1.3.2. Potential linear B-cell and MHC I and MHC II binding T-cell epitopes from deduced amino acid sequences of *Nsp2-HVII*, ORF5, and ORF7 of Myanmar PRRSVs are identified by using current bioinformatics tools

## **CHAPTER 2**

### **LITERATURE REVIEW**

#### **2.1. Porcine Reproductive and Respiratory Syndrome (PRRS)**

##### **2.1.1. General Characteristics and Economic Impacts of PRRS**

Porcine reproductive and respiratory syndrome (PRRS), is a persistent, highly infectious viral disease which causes reproductive failure in sows, glits and boars and respiratory distress in all ages of pigs (4). It was first recognized in North American and European swine herds in 1987 and 1990 and has since been identified throughout the pig-producing countries such as North America, South America, Europe and Asia (21, 22). Recently, PRRS is one of the most prevalent swine diseases in the world and cause the greatest economic losses in swine-production worldwide. According to the reports from PRRS Control 2015, estimated annual losses due to PRRS in the United States is approximately 560 million US dollars and in Japan is approximately 280 million US dollars, which are much higher than other important viral diseases in the swine such as classical swine fever and pseudorabies. Notably, the prevalence of atypical or highly pathogenic PRRSV strains in Asia has an extensive economic impact on that region (9). The PRRS is still uncontrollable, mainly due to the remarkable genetic variability of PRRS virus (PRRSV) and the lack of fully efficacious vaccines.

##### **2.1.2. Prevalence of PRRS in Asia**

In Asia, the first outbreak of PRRS was reported in China at the end of 1995, since then, the PRRSV has been circulating in the farms of China and regular outbreaks had occurred in different provinces (23). Chinese typical PRRSV strains, CH1a and BJ4 were isolated in Beijing province during 1996, and several divergent strains of both EU and NA genotypes from many different regions of China have been investigated throughout the extensive molecular characterizations. In June 2006, HP-PRRS disease which affected more than 2 million pigs with 400, 000 deaths, emerged in Jiangxi province of China and rapidly disseminated throughout the country.

Phylogenetic analysis on causative HP-PRRSV strain (JXA1) revealed that it might evolve from Chinese typical strain CH1a and nucleotide or amino acid deletions were found in Nsp2 gene (8, 24). Then, HP-PRRS was initially found in Hai Duong province in the northern part of Vietnam then southern provinces in 2007. Phylogenetic studies revealed that Vietnamese PRRSVs are closely related to Chinese strains (e.g. JXA1, HUB1, HUN, JX0612) from 2006 to 2007 (25). Among which, first isolated 07QN is closely related to JXA1, which was found to be widely spread to Laos, Thailand, Cambodia and the Philippines (26, 27) In Laos, HP-PRRSV appeared as severe outbreaks in Vientiane and seven districts in June 2010. The disease affected more than 13, 000 pigs and the average mortality rate was about 25% (28). In Thailand, the incidence of PRRSV was serologically evident in 1986 and the first isolate was identified as NA genotype in 1996 (29). Genetic analyses on ORF5 and complete genomes of Thailand isolates suggested that not only EU and NA genotypes but also recombinant strains of two genotypes existed in Thailand (30, 31). According to annual surveillance from 2008 to 2013, there is 13.86 % PPRS prevalence in Thailand pig population (32). In 2010, an outbreak of HP-PRRS was reported in Nong Khai, a border province, near Laos (33). However, HP-PRRSV first appeared in Thailand two years before the outbreak (34). Genetic characterization on Nsp2 gene and ORF5 confirmed that HP-PRRSV had been introduced to Thailand through illegal transport of infective pigs from Vietnam through Laos (34).

In the same year, 2010, HP-PRRS outbreaks occurred in three provinces (Battambang, Kampong Cham, and Kampot) in Cambodia, and Tabuk province in the Philippines (9). Likewise in Thailand, HP-PRRSV was introduced into Cambodia since 2008. In Myanmar, the first outbreak of HP-PRRS was reported in Mandalay region, located at the center of Myanmar in early 2011. Recently, the sequence analysis on ORF5, ORF7, and Nsp2 of PRRSV strain from the first outbreak of India confirmed that derivatives of China HP-PRRSV had appeared in India (35).

### **2.1.3. Prevalence of PRRS in Myanmar**

In Myanmar, the first outbreak of PRRS was reported in February 2011, in the central region, Mandalay (18). Since the first outbreak, the disease affected 34 townships in 12 districts in six Regions and States within five months. The disease



was spread to Naypyitaw, Sagaing, Magway, and then to southern regions, including Bago, Yangon, Ayeyarwady Regions, and Mon State (36). It was reported that some townships in Mandalay (Aungmyetharsan, Chanayetharsan, Mahaaungmye, Chanmyatharsi, Pyigyitagun, Amarapura, Madaya), where more than 1,000 infected pigs died of the PRRS. On April 2011, 100 pigs out of a total of more than 300 pigs from two pig farms in Naypyitaw Region (Pobba Thiri and Zabu Thiri Townships) was found infected with PRRS (37). The distribution of PRRS in Myanmar was shown in **Figure 1**.

According to the World Organization for Animal Health (OIE) report in 2011, six outbreaks of PRRS occurred between April and May in Mandalay and Bago. During outbreaks, a total of 1,456 pigs showed PRRS symptoms and 595 of them died (19). The same period, 294 pigs in Taungoo township in Bago Region had been infected and 79 of them died (38). The first reported outbreak was found in backyard farm which located close to the commercial farm in Mandalay. At first, the disease was spread among small farms in urban areas then to suburban areas. Within a few months, several outbreaks were documented due to the uncontrollable movement of infected pig and the high death rate was found. At that time, no PRRS vaccine was available and high mortality and morbidity caused approximately 34% reduction in pig population in the country (37, 39). However, detailed information of PRRS in Myanmar was limited and genetic characteristics of PRRS virus, circulated in Myanmar, have not been well characterized.



*Figure 1. Distribution map of PRRS outbreaks in Myanmar during 2011*

Number ① - ⑧ are the PRRS affected areas. The outbreaks were first reported in Mandalay Region and spread to Naypyitaw, Sagaing, Magway, Bago, Yangon, Ayeyarwady Regions and Mon State.



## 2.2. Porcine Reproductive and Respiratory Syndrome Virus (PRRSV)

### 2.2.1. Biology and Structure of PRRSV

The PRRSV, an etiological agent of PRRS, belongs to the family *Arteriviridae*, genus *Arterivirus*, and order *Nidovirales* (40). It is a small, round or oval-shaped, enveloped virus of 50-74 nm diameter and has a smooth outer surface with few protruding features (**Figure 2**). The virion consists of a central core containing a positive, linear, non-segmented, single-stranded RNA genome, enclosed by icosahedral nucleocapsid. The nucleocapsid (N) is covered by the lipid bilayer envelope which is composed of viral structural glycoproteins (GPs) and membrane (M) protein.

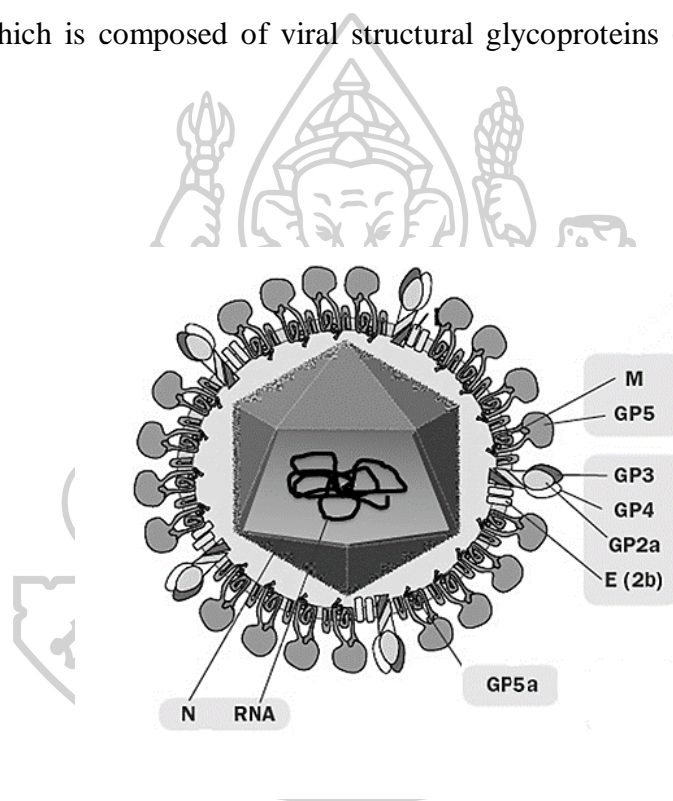


**Figure 2.** Schematic representation of PRRSV particle showing the location of structural proteins GP2a, GP2b (E), GP3, GP4, GP5, GP5a, M and N

The GP5 and M proteins are shown as heterodimeric complexes and GP2a, GP3 and GP4 are shown as heterotrimers. Single-stranded RNA is enclosed in NP (16).

### 2.2.2. Molecular Biology of PRRSV

The viral genome has approximately 14.9 - 15.5 kb in length. The genome contains at least ten overlapping open reading frames (ORFs 1a, 1b, 2, 2b, 3, 4, 5a, 5, 6, and 7) (**Figure 3**).

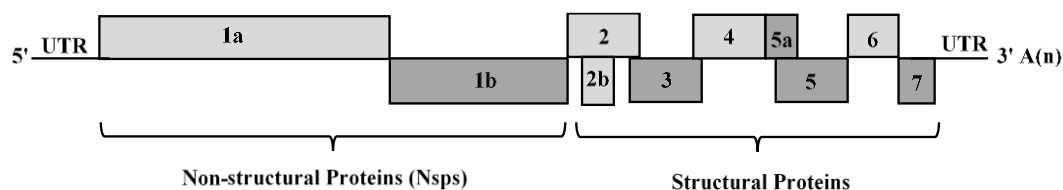


**Figure 3. Schematic representation of the PRRSV genome organization**

#### 2.2.2.1. Non-structural Proteins

The ORF1a and ORF1b of PRRSV genome encode two large replicase polyproteins (PLP) 1a and 1ab, which are further cleavage into sixteen non-structural proteins (Nsp1 $\alpha$ , Nsp1 $\beta$ , Nsp2, Nsp2N, Nsp2TF, Nsp3, Nsp4, Nsp5, Nsp6, Nsp7 $\alpha$ , Nsp7 $\beta$ , Nsp8, Nsp9, Nsp10, Nsp11, and Nsp12) by different viral proteases which are encoded within ORF1a (41-43). The Nsp1 $\alpha$  is responsible for subgenomic mRNA synthesis whereas Nsp1 $\beta$  is important for genome replication.

#### Non-structural Protein 2 (Nsp2)

Among non-structural proteins, the Nsp2 is the largest and varying in size from 1168 to 1196 residues between different PRRSV strains (5), (44, 45). It is the most variable non-structural protein with 32% identity between subtypes (45). Nsp2 has hypervariable (HV) I region and a papain-like protease domain (PLP2) at N-terminus, which is followed by a HVII region and a hydrophobic region containing four to five predicted transmembrane (TM) helices (**Figure 4**) (17, 46). Different amino acid deletions and insertions occurred in Nsp2, and discontinuous deletion of 30 amino acids in the middle HVII of Nsp2 region is initially significance characteristic of HP-PRRSV (**Figure 4**) (47, 48). Therefore, genetic studies on PRRSV strains have been done on this Nsp2 region, mostly in the HV region.

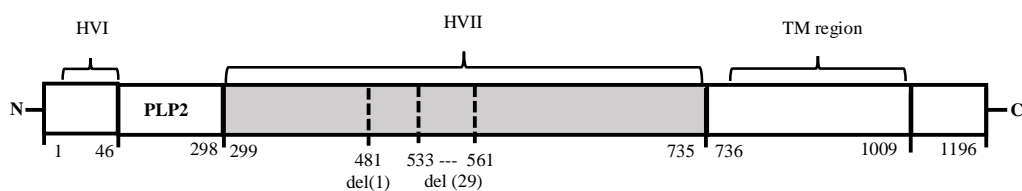


**Figure 4. Schematic representation of the Nsp2**

The Nsp2 protein contains hypervariable region I (HVI, residues 1-46), papain-like protease domain (PLP2) in the region (residues 46-298), the middle hypervariable region II (HVII, residues 299-735) and predicted transmembrane domains in the region (residues, 876-1009). When compared with VR-2332 (NA prototype), the HVII of HP-PRRSVs contains one amino acid deletion (481 residue) and 29 continuous amino acid deletion (residues 533-561), which is the significant marker of HP-PRRSV.

#### 2.2.2.2. Structural proteins

The ORFs 2 - 5 of PRRSV translate into structural glycoproteins including GP2, GP3, GP4, and GP5. The ORF6 and ORF7 encode non-glycosylated proteins, membrane (M) and nucleocapsid (N), respectively (16).

#### Glycoprotein 5 (GP5)

Among structural proteins, the 200-residue GP5 is a major structural protein and is the most variable protein, with 51-55 % sequence identity between EU and NA genotypes (14, 49). The variations are mostly found at putative N-terminus of 1-25 amino acid residues (50). Prediction by SignalP 3.0 indicates that signal peptide (1-31 amino acid residues) is located at N-terminus and followed by a hydrophilic domain, which is assumed to expose outside of the virion as ectodomain (46). The ectodomain is followed by hydrophobic region (60-125) which is supposed to span one or three times as TM helices and the endodomain constitutes a large C-terminus of residues 130-200 (16, 46) (**Figure 5**). Sequence analysis by TMHMM and HMMTOP prediction revealed the second TM between residues 63-82 and the last TM was between residues 107-125 in NA type (46). There are two to five N-glycosylation

sites in GP5 protein and the number and location of N-glycosylation sites in GP5 can change over the course of infection. Glycosylation on Asparagine (N), N44 and N51 in NA PRRSV (N46 and N53 in Lelystad PRRSV) have been found. Glycosylation on N44 in NA or N46 in EU was strongly required for both assembly and infectivity whereas, N51 or N53 glycosylation in NA and EU, respectively did not show to be important (51). In addition, the neutralizing epitopes have been identified in the ectodomain of GP5 (52-54). The small protein, GP5a has recently identified and it is essential for virus viability.

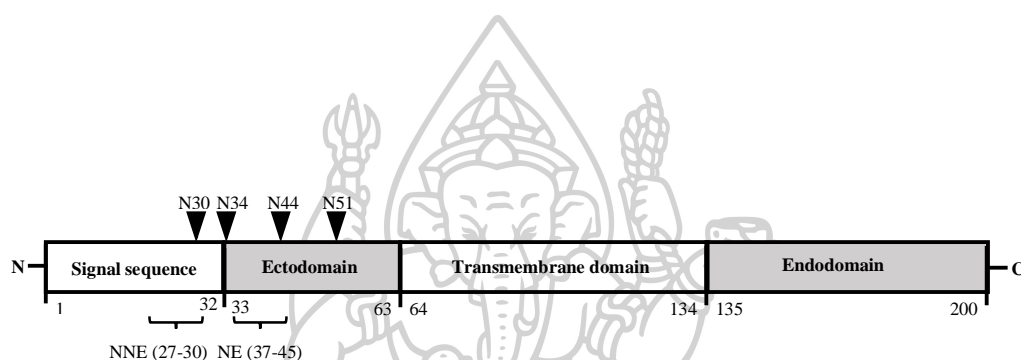


**Figure 5. Schematic representation of the GP5**

The GP5 contains a signal sequence of residues 1-32, ectodomain (residues 33-63), two to three transmembrane domains within residues 64-134 and endodomain residues 135-200. The non-neutralizing epitope (NNE, residues 27-30) and neutralizing epitope (NE, residues 37-45) located in the signal sequence and the ectodomain regions. The (▼) indicates potential N-linked glycosylation sites at residues 30, 34, 44 and 51).

### Nucleocapsid protein (NP)

The 123-amino acid NP is the sole component of the viral nucleocapsid and does not encode a transmembrane domain or an ectodomain. It exists as a homodimer and contains RNA binding domain at N-terminus thus plays a role in ribosomal biogenesis. Moreover, the nuclear and nucleolar localization sequences within the RNA-binding domain target the NP to the nucleus of infected cells (55, 56). It also involves in virus assembly in the cytoplasm (46, 55). And also, it is the most abundant protein and constitutes 20-40% of virion. The NP is highly antigenic and contains antigenic domains (**Figure 6**). Although anti-N antibodies have little or no neutralizing activity, it is served as a useful genetic marker for the diagnosis of PRRS (16, 46, 57).

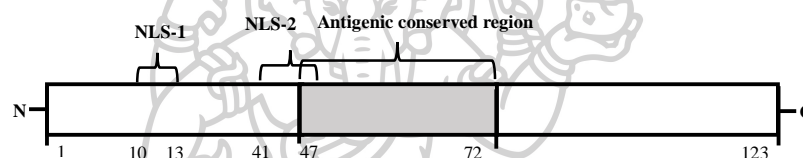


**Figure 6. Schematic representation of the NP**

Nuclear localization signal domains NLS1 (residues 10-13) and NLS 2 (residues 41-47) of NP. The NP contains antigenic conserved region at residues 47-72.

Because of significant genetic characteristics and important roles in virus infectivity and immune response, most of the genetic studies of PRRSVs had been done on ORF1a encoding Nsp2-HVII, ORF5 and ORF7 (33, 58-61).

### 2.2.3. Route of Transmission, Pathogenesis and Clinical Manifestation

The PRRS is the pandemic viral infection in pigs and the major cause of global widespread is the movement of infective pigs between or within the countries. After the introduction of PRRSV, it spreads quickly to uninfected pigs in the herds within two to three months. The virus survival is optimal in cold temperature and little sunshine (i.e. low ultra-violet light exposure), so why, the virus spread and disease outbreak increase during the winter season or in cold climate region of the country (62).

### **2.2.3.1. Route of Transmission**

Since PRRSV can persist in the host animals for a long period, the chronic persistent carrier is the critical source of PRRSV transmission (63). The virus shed in the body fluids of the infected pigs and direct contact with infected saliva, nasal secretion, urine, semen, and feces is the major route of transmission. There is an event of airborne transmission, but, it is less likely to occur and may concern only for the short distances (i.e. less than 3 km) from the infected farms and particularly in winter. Transmission via contaminated materials (e.g. cloths, boots, gloves, equipment) and insect vectors (houseflies and mosquitoes) are significant, however, rodent vector transmission is unknown (64-66).

### **2.2.3.2. Pathogenesis and Clinical Manifestation**

Pigs (*Sus scrofa*) are the natural host of PRRSV and the infection is initiated by an invasion of local macrophages then it spread rapidly to lymphoid organs and the lungs. PRRSV has restrictive tropism for monocyte lineages such as porcine alveolar macrophages (PAMs), peripheral blood monocytes and pulmonary intravascular macrophages (PIMs) where viral replication takes place. Viremia occurs in 6 to 12 hours of post infection and peak between 7 to 14 days, at which clinical signs of infection appear. Viremia generally lasts for 28 days and PRRSV may persist in tonsils and lymph nodes for about 250 days and follow by the clearance of viremia. Cellular injury induced by the virus cause organs lesions, resulting in pneumonia, myocarditis, vasculitis, encephalitis, and lymphadenopathy (3, 4, 67). Pathologic differences had been demonstrated as variation in severity of clinical signs and characterized as apathogenic, low virulent and highly virulent strains. Generally, the pathogenicity of EU types is less than that of NA types and most of the outbreaks have been caused by NA related PRRSV strains (68, 69). The most common features of PRRS are a reproductive failure in breeding gilts and sows, and respiratory problems in pigs of all ages, especially in young pigs. In the endemic stage, the first clinical signs of infection are lethargy, anorexia, fever, dyspnea and cyanosis of extremities. After that, sows begin to cause reproductive failure such as late-term abortion, premature, stillbirth, mummified fetuses for 1 to 4 months (70, 71). Atypical PRRS, caused by a highly pathogenic strain of PRRSV, produces high fever (41-42°C), severe reproductive failure in pregnant female pigs (early and late-term



abortion), severe respiratory distress with high mortality (greater than 5% in sows and boars) (8, 72). As PRRSV can suppress the host immune system, the infected pigs are prone to secondary or opportunistic infections such as porcine circovirus 2 (PCV2), *Salmonella enterica*, *Haemophilus parasuis*, *Mycoplasma spp.*, *E.coli* and *Leptospira spp.* (73).

#### 2.2.4. Host Immunological Response to PRRSV Infection

The delayed and weak protective humoral and cellular in both innate and adaptive immune responses are the important problems in PRRS infection and hence PRRSV can usually cause persistent infection in pigs. However, the PRRSV infected pigs can eliminate the infection at 3-4 months of post infection (PI) and can develop protective immunity when exposed to the same strain.

In humoral immunity, viral specific antibodies, IgM can be detected in serum at 5-7 days of PI and declines rapidly to an undetectable level after 2-3 weeks. Serum IgG can be detected at 7-10 days PI and reach peak level at 2-4 weeks PI. It remains constant for several months and decreases to a low level by 300 days PI (**Figure 7**). However, initially produced antibodies shortly after PRRSV infection does not have neutralizing activities and are mainly directed primarily towards NP and Nsp2, followed by GP5 and M protein. PRRSV-specific neutralizing antibodies (NA) that inhibit PRRSV infection can be found at about 4 weeks PI and maintained for a long period though at a low level (**Figure 7**). Neutralizing antibodies develop slowly and at a low level (67, 74).

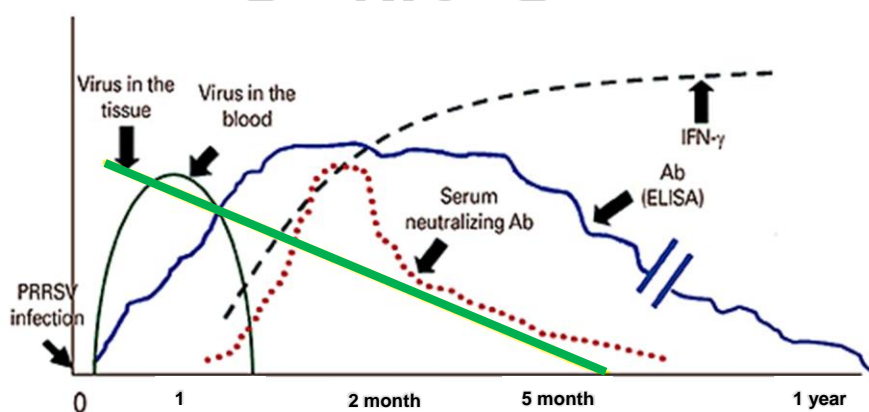


**Figure 7. Illustration of the immune response in pig after infection with the porcine reproductive and respiratory syndrome (74)**



The epitopes for neutralizing antibody production are present in GP3, GP4, GP5 and M protein (7, 53, 75). Particularly, host NA response is mainly against major enveloped proteins GP5 and M. Linear neutralizing peptide epitopes (<sup>29</sup>WSFADGN<sup>35</sup>) of Lelystad and (<sup>37</sup>SHIQLIYNL<sup>45</sup>) of VR-2332 were identified by peptide-based epitope mapping. Delayed and low level of host NA antibodies against GP5 has been attributed by many factors. Studies from Ostrowski et al. (2002), and Plagemann (2004) revealed the presence of non-neutralizing (decoy) epitope (<sup>27</sup>VLAN<sup>30</sup>) that can hinder the response of major neutralizing epitopes (52-54). It has also been postulated that the poor neutralizing antibodies titers are due to the presence of N-glycosylation in immunogenic domains in GP5 (76). Although early and abundant production of antibodies against NP does not have neutralizing activity and they are useful for serological diagnosis of PRRS infection. Besides GP5 and M, the neutralizing domains are also localized in minor enveloped protein GP4. The antibodies specific for GP4 have been shown to neutralize PRRSV, but less effectively than GP5-specific neutralizing antibodies.

In cellular-immune response, T cell responses to PRRSV are weak, transient and highly variable. The lymphocyte proliferation was not detected until 4 weeks PI. The CD<sub>4</sub><sup>+</sup>CD<sub>8</sub><sup>+</sup> porcine memory T helper cells and CD<sub>4</sub><sup>+</sup>CD<sub>8</sub><sup>+</sup> cytotoxic T cells are IFN- $\gamma$  secreting cells and their responses to PRRSV appear approximately after 4 weeks of post infection and last for 5 to 10 weeks (73, 77, 78). Interferon (IFN)- $\gamma$  has been shown to block PRRSV replication, however, the number of IFN- $\gamma$  producing T cells following infection is weak and delayed (79). It may be due to virus-mediated suppression of type I IFN and other proinflammatory cytokines such as IL-1, IL-12, tumor necrosis factor  $\alpha$  (TNF- $\alpha$ ) and up-regulation of anti-inflammatory cytokines such as IL-10 and transforming-growth factor  $\beta$  (TGF- $\beta$ ), and induction of regulatory T cell (T<sub>reg</sub>) response (80). The cellular immune response may be strain-dependent because induction of TGF- $\beta$  and T<sub>reg</sub> response were exposed in NA-genotype, but not in EU-genotype. In PRRSV infected pigs, T-cell response is directed against GP2a, GP3, GP4, GP5, M, and N proteins.

### **2.2.5. Genetic Variability of PRRSV**

The PRRSV was first isolated in the Netherlands in 1990, which was recognized as the European (EU) prototype, Lelystad virus. In the subsequent year, it was isolated in North America and characterized as the North American (NA) prototype, ATCC VR-2332 virus (81, 82). Due to the genetic differences between prototypes, two distinct genotypes, EU or genotype I and NA or genotype II had been identified (45, 50). The sequences identity of deduced amino acids between Lelystad and VR-2332 are approximately 63% in ORF 2, 60% in ORF3, 69% in ORF4, 59% in ORF5, 81% in ORF6 and 65% in ORF7 (5, 14, 83). The viral isolates within both EU and NA genotypes are also substantially divergent. The ORFs 2-4 of NA isolates have considerable sequence variation and these isolates show different pathogenicities (84). However, ORF6 and 7 of the NA isolates are highly conserved and shared 96 to 100% amino acid identity (50). However, the EU genotype has also been found in North America (United States, Canada), and in Asia (Thailand, China, South Korea, Malaysia). Likewise, NA genotype is also present in some countries of Europe through the use of NA strains-live attenuated PRRSV vaccine.

Recently, the two novel recombinant PRRSVs, GZgy17 and SCya18 which had genetic characters of HP-PRRS were isolated in Southern China. The GZgy17 strain exhibited higher pathogenicity than that of SCya18 and caused 20% death of tested piglets (85). Thus why molecular characterization or phylogenetic analyses of PRRS field strains have been conducting in PRRS infected countries to investigate the source of the infection and to determine the genetic diversity of the new strain, even though no further PRRS outbreak occurs.

### **2.2.6. Diagnosis, Control and Prevention of PRRSV infection**

Clinical signs of PRRSV infection are often unobvious, therefore any routine clinical diagnosis must be confirmed by detection of PRRSV or its specific antibodies. Serum, lungs, lymph node, tonsil, spleen section or oral fluid are widely used clinical specimens for PRRSV detection in the pig. The most commonly used diagnostic methods for PRRS are enzyme-linked immunosorbent assay (ELISA) and polymerase chain reaction (PCR). The ELISA can detect PRRSV-specific IgG antibodies against GP5 and NP in PRRSV infected pigs between 7 and 14 days PI.

The Immunoperoxidase monolayer assay (IPMA) and indirect immunofluorescence assay (IFA) can also be used. The DNA sequencing of ORF5 region is used to discriminate vaccinated and infected pig in vaccinated farms since vaccine viruses can co-exist with field strains for some period of time and no marker vaccine has been available (86, 87).

Recent control measures include the use of vaccines, the management of incoming pigs and the implementation of biosecurity protocols to reduce the risk of PRRSV spread within and between herds (88). Among which, vaccination is the major focus to control the spread of PRRSV in most countries. Injectable forms of live attenuated and killed vaccines containing different types of prevalence strains (e.g. NVDC-JXA1 in killed vaccine and VR-2332 in the live attenuated vaccine) are available in the market since 1994 (10). RespRRS/Repro<sup>®</sup> (called Ingelvac<sup>®</sup> PRRS MLV from VR-2332), first live attenuated vaccine, was approved for use in 3-18 week old pigs in the USA in 1994 and in Korea in 1996. Later on, many PRRS-MLV (Amervav<sup>®</sup> from EU-VP046 strain, Porcellis<sup>®</sup> from EU-DV strain, Foster<sup>®</sup>) and killed vaccines (Suivac<sup>®</sup>, Progressis<sup>®</sup>) containing different genotypes have been produced by different countries. PRRS MLVs from Chinese field strain (CH-1R) and HP-PRRS strain (HUN4-F112), and inactivated vaccine from Chinese field strain (CH-1a) are licensed and used in China (9). In Thailand, Ingelvac<sup>®</sup> PRRS and Foster<sup>®</sup> PRRS MLV are used to control field strain of PRRSV. Ingelvac<sup>®</sup> MLV has been allowed to use in Myanmar in 2017 (20).

Currently, PRRSV MLV and inactivated vaccine containing either EU or NA strains have been licensed for use in many swine production countries. However, their protective efficacy against heterologous strains is variable and substandard. Therefore, the efficacy of PRRSV MLVs seems to be affected by the degree of genetic similarity between the infected field strain and vaccine strain. The determination of homologous strain against vaccine protection is not clear. The GP5 is a major protein of the viral particle and it contains neutralizing epitope, therefore, genetic similarity at the GP5 was initially used to predict the protective efficacy of a vaccine.

For safety concern, vaccinated pigs can shed vaccine virus in semen, feces, and oral fluids and subsequently transmission has occurred. In addition, co-existence of

vaccine strains and field strains may lead to evolving newly strains with different antigenicity. For safety concern, vaccine virus from MLV can revert to virulence and cause disease. The use of MLV is limited in some countries, including the United Kingdom, where only permit the inactivated vaccines used for breeding animals (7).

Inactivated or killed vaccines are safer than MLVs but it provides limited efficacy. The potential use of PRRS inactivated vaccine is used as a therapeutic vaccine in PRRSV positive farms because it only helps to increase antibody and CMI responses to the infecting virus (89, 90). As a summary, current PRRS MLVs only protect clinical diseases but not able to completely prevent infection and transmission especially against heterologous strains (91-93). Hence, due to the lack of effective vaccines, PRRS is still uncontrollable and disseminated throughout the world.

### **2.2.7. PRRS Vaccine Development**

Various attempts have been done to develop novel PRRSV vaccines, which could induce a rapid and robust protective immune response, provide broad-spectrum protection with good safety. Moreover, vaccines that confer serological differentiation between natural infection and vaccination are also necessary to develop. Although often stated as providing incomplete cross-protection, MLVs are generally considered as the most effective PRRSV vaccines, many efforts are made for the development of novel PRRSV MLV. Current PRRSV MLVs are prepared using a conventional method by serial passage of different PRRSV strains in cell cultures (10).

Different approaches have been used to enhance the efficacy of the vaccine. Several types of adjuvants have been tested on protective efficacy commercially live attenuated PRRSV vaccine. Reverse genetics is used to remove the N-linked glycans in different viral proteins (e.g. GP3 and GP5) to improve neutralizing antibody production and to modify the viral genes (e.g. Nsp1 $\alpha$  and 1 $\beta$ , Nsp2, ORF7) to enhance immune responses (94-96). In order to produce broad protection, polyvalent vaccine composed of viral genes from different PRRSV strains. For example, a vector virus carrying fragments of GP5 from different heterologous PRRSV strains has been tested (97). The DNA vaccines, subunit vaccines and synthetic peptide vaccines (98). The DIVA (Differentiating Infected from Vaccinated Animals) vaccine, a serological marker vaccine which involves the elimination of one or more B-cell epitopes from

the vaccine strain had been investigated (99, 100). Although many studies on PRRSV vaccine development have been contributing meaningful information concerning the individual proteins to elicit a protective immune response, the protective efficacy of these vaccines is less than that of MLVs and cannot provide solid protection against challenge viruses.

## **2.3. *In Silico* Bioinformatics Tools**

### **2.3.1. Bioinformatics Tools in Genetic Analysis**

*In silico* bioinformatics tools are computational tools which are used to analyze the information related to molecules such as genes, genomes, and proteins (101). They are valuable in molecular biology, for example, analysis of nucleotide and protein sequences, prediction of ORFs, analysis of gene expression, designing primers, and prediction of protein secondary structure (3D structure, post-translational modifications, hydrophilicity, and hydrophobicity, potential antigenic and various domains). The genome can give billions of information by utilization of bioinformatics applications. The DNA analysis is one of the main tasks of bioinformatics and comprises two parts, 1) functional genomics which involves to determine the function of the proteins and 2) comparative genomics, related to the comparison of sequences from different strains or organisms to elucidate their functional changes and to determine ancestries or correlations with disease conditions (102). In order to conduct genetic analysis, the genetic sequence of the organism needs to obtain by DNA sequencing or retrieving from the databases. The number of genetic databases are available from the European Molecular Biology Laboratory (EMBL, <http://www.embl.org>) in Europe and GenBank from the National Institutes of Health (NIH-NCBI: <http://www.ncbi.nlm.nih.gov/>) in North America. In Japan, the databases can be searched in DNA Databank (DDBJ: <http://www.ddbj.nig.ac.jp>). The SWISSPROT, SCOP and Protein Data Bank (PDB) offers the protein databases and experimentally determined crystal structures of biological macromolecules or proteins (103, 104).

Similarity searching is a fundamental bioinformatics application for genetic characterization. This can provide various information such as genetic identification, structural motif identification, and functional association, etc. The Basic Local



Alignment and Search Tools (BLAST) is the most widely used algorithm for searching genetic sequence similarity between two DNA or protein sequences. It is an accurate program and includes different applications such as nucleotide blast, protein blast, blastx, tblastn and tblastx (103, 104).

To find out mutation events, sequence alignment algorithms which match between the sequences and search for the homologous regions are available. The frequently used programs of pairwise alignments for sequence identity and similarity are freely available and friendly user programs, EMBOSS Needle and EMBOSS Waterman from the European Molecular Biology Open Software Suite (EMBOSS) which offers over 100 applications for sequence analysis. The EMBOSS Needle is a global alignment tool while EMBOSS Waterman is a local alignment program (103, 105, 106). To compare more than two nucleotide or protein sequences, multiple sequence alignment algorithms from EMBL-EBI, such as MUSCLE, Clustal Omega, ClustalW, T-Coffee, MAFFT, etc. can be used. Of which, MUSCLE (Multiple Sequence Comparison by Log-Expectation) is the very fast program which can analyze large numbers of sequences and give the alignment data with high accuracy (107). The ExPASy is the common bioinformatics resource program which offers a number of free bioinformatics software packages. It can provide different bioinformatics tools for genomics proteomics, transcriptomics, phylogeny, system biology, population genetics, structural analysis, etc. For example, HMMTOP and TMHMM for prediction of transmembrane helices; NetNGly for prediction of N-linked glycosylation sites and QMEAN for estimation of protein model quality are the commonly used genomics and proteomics tools from ExPASy server. For phylogenetic studies, PAUP\*, RAxML, Phylml, MEGA and Phylip programs are available. Of which, Phylip is one of the most commonly used phylogenetic analysis software (108, 109). The Phylip is a package software consisting of 30 programs that cover the most aspects of phylogenetic analysis.

### **2.3.2. Bioinformatics Tools in Reverse Vaccinology**

The conventional approach of vaccine development is laborious and time-consuming, and only a few numbers of potential vaccine antigens had been identified for pathogens. The revolutionary vaccine development approach using *in silico*

bioinformatics tools has been developed for the prediction of vaccine targets or epitopes without the need for cultivation, thus known as reverse vaccinology (**Figure 8**). It starts from the genetic sequencing and, selection of the antigens that are most likely to be vaccine candidates from the gene segments by computer analysis softwares. The benefits of this approach are 1) it can be applied to both cultivable and non-cultivable microorganisms 2) all protein antigens that the pathogen can express at any time, regardless of whether they are expressed *in vivo* or *in vitro* (11). As a drawback, this approach is unable to identify non-protein antigens such as polysaccharides and glycolipids. Screening for protective immunity is the rate-limiting due to limited knowledge of vaccine immunology for good correlation of protection. However, the development of the MenB vaccine for *Neisseria meningitidis* B is the successful application of reverse vaccinology (110). The bioinformatics approach has already proven its potency in the case of human immunodeficiency virus, multiple sclerosis, tuberculosis, and malaria with desired results (111-114). It is less time-consuming and is a leading approach to develop a novel vaccine against infections that currently have a few or no control measure by improving the knowledge on the host immune response and the genetic background of the pathology (115). Therefore, this approach might be suitable for rapidly diverging pathogens and it becomes a great interest for PRRS vaccine development.

The prediction of peptides or epitopes (B-cell and T-cell epitopes) that are potentially immunogenic, by bioinformatics tools is the fundamental step of reverse vaccinology. To date, different *in silico* bioinformatics algorithms for prediction of epitopes (B-cell and T-cell epitopes) are available. The B-cell epitopes are short peptides or a region of a large structure, which bind with the antibodies. Particularly, 10-15 residue-long peptide epitope can stimulate the immune system to produce antibodies that bind to the peptide (116). The B-cells epitopes are classified as linear or continuous and conformational or discontinuous epitopes. The prediction of discontinuous epitopes based on the 3D structure of the protein is problematic because of the difficulties in defining the correct conformation of epitopes (117). Therefore, the most B-cell epitope predictions focus on linear epitopes. There are two major types of B-cell epitope prediction methods, sequence-based and structure-based methods (116). The ABCpred, BepiPred, Bcepred, BCPREDS, and B-cell epitope



prediction softwares from IEBD-AR are the commonly used sequence-based method using amino acid scales or sophisticated machine-learning techniques (118-121). Ellipro software based on 3D structure and can be used for both linear and conformational epitopes (122). The structure-based prediction tools such as CEP, Discotope, BEPro, SEPPA, and EpiSearch servers are available for the prediction of conformational epitopes (123, 124).

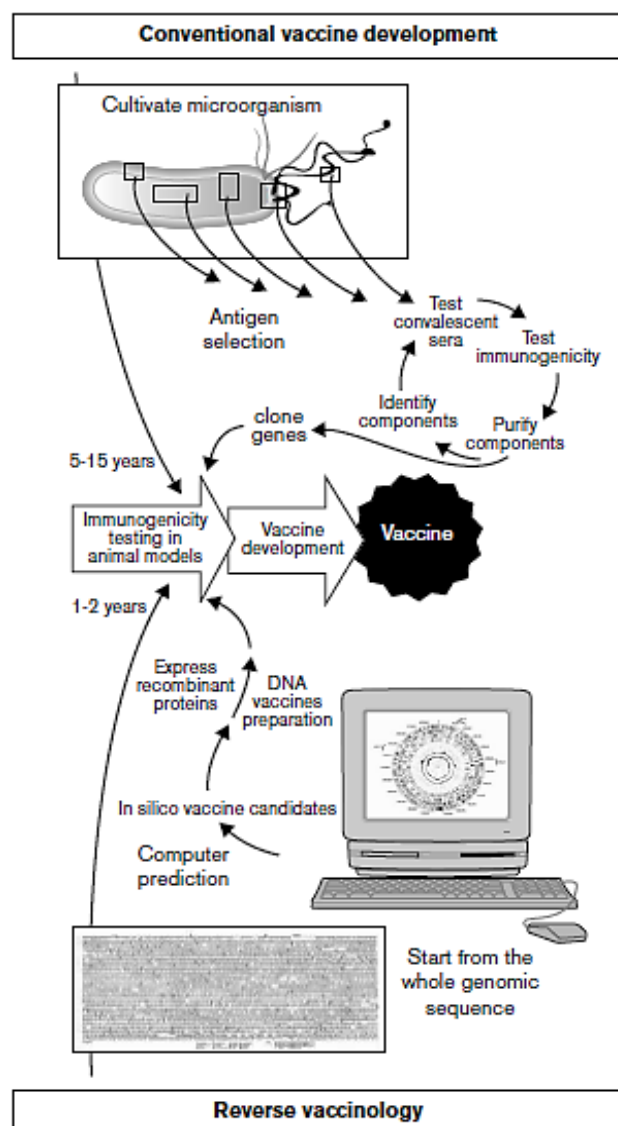


*Figure 8. Schematic representation of the vaccine development by conventional approach and reverse vaccinology (13)*

T-cell epitope prediction algorithms have been developed based on the binding of epitopes to the groove of MHC I or MHC II molecules because epitopes bound to MHC interact with T-cell receptors (TCRs) after transport to the surface of antigen presenting cell (APC). The MHC I molecule has a single closed groove where epitope with 8-15 amino acids can bind (117, 125). The MHC II binding epitopes vary in length from 12-25 amino acid, but the interaction with the groove is 9-mer length peptide (117, 126). Based on the peptide sequence, the discrimination between binders and non-binders has been done by determining the binding affinity ( $IC_{50}$ ) (117, 127). Depending on this factor, a variety of machine-learning and structure or motif-based algorithms have been established (128-133). The predictions of MHC I binding epitopes have high accuracy (134-136). The different MHC I binding prediction tools such as SYFPEITHI, ProPed1, RANKPEP, PSSM, NetMHC, etc. are available. Notably, NetMHCpan from IEDB-AR generates a prediction of binding affinity to MHC I molecules of human as well as chimpanzee, macaque, gorilla, cow, pig, and mouse (136). Moreover, MHC I processing server and WAPP server are the combinational tools which offer a prediction of proteasomal processing, TAP transport, and MHC I binding to produce the overall processing score for each epitope. However, prediction of MHC II binding T-cell epitopes has limited success by low prediction accuracy of the prediction tools. It is due to insufficient training data, difficulty on identifying binding core (9 peptides) within longer peptides used for training, and lack of consideration of the influence of flanking residues and the permissiveness of the binding groove of MHC II molecules (134, 137). The ProPred, SVMH, MHC2Pred and RANKPEP, IEDB MHC II binding prediction server can predict the epitope for a number of MHC II molecules (42-51 alleles) (115). But, most of the servers provide predictions of binding affinity to human MHC II alleles (HLA-DR, HLA-DQ, and HLA-DP).

## CHAPTER 3

### MATERIALS AND METHODS

#### 3.1. MATERIALS

##### 3.1.1. Reagents and Equipments

###### - Kits

GeneJET viral DNA and RNA purification kit	Thermo Fisher Scientific
QIAamp viral RNA purification kit	Qiagen
Revert aid first strand cDNA synthesis kit	Thermo Fisher Scientific
One-step RT-PCR kit	Qiagen
Dream Taq Green PCR master mix (2x)	Thermo Fisher Scientific
2X Taq master mix	Vivantis
Gel and PCR clean-up, Nucleospin	Macherey-Nagel

###### - Chemicals and Reagents

Gel loading dye, 6X	Vivantis
DNA ladder, 100bp plus	Vivantis
Agarose, molecular biology grade	Vivantis
Tris-HCl	Vivantis
EDTA	Sigma
Acetic acid	Sigma

All other unlisted chemicals were analytical grade and purchased from BioMed, Vivantis, Merck, and Sigma.

###### - Vaccine

PEDV and transmissible gastroenteritis virus combined inactivated vaccine, SuiShot® PT-100	Knack Kohlan Co., Ltd.
--	------------------------

###### - Equipments

Thermal cycler, GeneAmp PCR system 9700	Applied Biosystems
Multi Genius, Bio imaging system	Syngene
Nanodrop-one	ThermoFisher Scientific
Micro-centrifuge, mini	Gyrozen
Centrifuge, Biofuge	Stratos Sorvall
Water-bath	Daiki scientific Co.

pH/Ion meter, SevenCompact	Mettler Toledo
Autoclave	Rexall Industries Co. Ltd.
Analytical balance	Sartorius

### 3.1.2. Primers

The specific primers for amplification of *Nsp2-HVII*, ORF5 and ORF7 were designed based on the nucleotide sequences of six reference PRRSV strains (NA prototype: VR-2332, China low pathogenic (LP)-PRRSV: CH-1a, HP-PRRSV from China HP-PRRSV: JXA1, Thailand: HP/THAILAND/19500LL/2010, Laos: BH58/10, Vietnam: 07QN) from the GenBank databases. All primers were synthesized and purified by Sigma-Aldrich, USA. The sequences of the primers are shown in **Table 1**.

**Table 1. The primers used for amplification of *Nsp2-HVII*, ORF5, and ORF7 genes**

Primer	Primer Sequence (5'- 3')
Nsp2-1F	AAGTCTTGAGGAATGCTTGG
Nsp2-1R	GACAGGGAGCTGCTTGATGA
ORF5-F	ATGTTGGGGAAATGCTTGACC
ORF5-R	CTAGAGACGACCCATTGTTCC
ORF7-F	ATGCCAAATAACAACGGCAAG
ORF7-R	TCATGCTGAGGGTGATGCTGT

### 3.1.3. Clinical Samples

The PRRSV-infected clinical samples (1 spleen and 5 sera) were obtained from Advanced Biologicals, Myanmar. The samples were collected during necropsy from the pigs died after showing clinical signs of PRRS in the 2011 outbreaks. These clinical samples were from separate non-vaccinated backyard farms or breeding farms in five different regions of Myanmar as seen in **Figure 9**. (HP/MYANMAR/2303AM/2011 from Magway, HP/MYANMAR/0204AM1/2011 and HP/MYANMAR/0204AM2/2011 from Madaya, (HP/MYANMAR/1908AM/2011 from Insein, HP/MYANMAR/ 2510AM/2011 from Nyaungdon, and HP/MYANMAR/0411AM/2011 from Pyinmana). The detailed information of

collected PRRSV-infective samples is shown in **Table 2**. All samples were identified as positive for PRRSV by Reverse Transcription-Polymerase Chain Reaction (RT-PCR).



**Figure 9. Myanmar map showing the location of collected clinical samples**

The ● symbol indicates the townships where the PRRSV-infected clinical samples used in the study were collected chronologically as follows: HP/MYANMAR/2303AM/2011 from Magway (March), HP/MYANMAR/0204AM1/2011 and HP/MYANMAR/0204AM2/2011 from Madaya (April), HP/MYANMAR/1908AM/2011 from Insein (August), HP/MYANMAR/2510AM/2011 from Nyaungdon (October), and HP/MYANMAR/0411AM/2011 from Pyinmana (November).

**Table 2. Background information on PRRSV-infected clinical samples from pig farms in Myanmar during 2011**

No.	ID	Type	Time	Townships, Regions/ States	Background Information
1.	HP/MYANMAR/2303AM/2011	Spleen	March 2011	Magway, Magway	The sample was taken from 15-days old piglet died of severe PRRS after 3 days of infection.
2.	HP/MYANMAR/0204AM1/2011	Serum	April 2011	Madaya, Mandalay	The samples were collected from two adult pigs 2 hours after their deaths.
3.	HP/MYANMAR/0204AM2/2011	Serum	April 2011	Madaya, Mandalay	
4.	HP/MYANMAR/1908AM/2011	Serum	August 2011	Insein, Yangon	The sample was obtained from a boar died with PRRS signs in a breeding farm. The boar was brought from the farm in Hlegu, Yangon Division (in which one sow and nine suckling pigs died with PRRS signs in May 2011) a week before its death.
5.	HP/MYANMAR/2510AM/2011	Serum	October 2011	Nyaungdon, Ayeyarwady	The sample was taken from a PRRS suspected pig just after death and it was also co-infected with porcine circovirus type-2 (PCV2).
6.	HP/MYANMAR/0411AM/2011	Serum	November 2011	Pyinmana, Naypyitaw	The sample was collected from a sow, which had a high fever and severe respiratory problems before death. The <i>Haemophilus parasuis</i> was isolated from blood, lung, and brain of it.



## 3.2. METHODS

### 3.2.1. Molecular Characterization

#### 3.2.1.1. RNA Isolation

Total viral RNA from spleen were directly extracted using GeneJET viral DNA and RNA purification kit (Thermo Scientific, USA) according to the manufacturer's protocol as shown in **Figure 10**. Briefly, 20 mg of the spleen was cut into small pieces and homogenized with TE (Tris-EDTA) buffer. The 200  $\mu$ L of a lysis solution with carrier RNA (cRNA) was added to the spleen homogenate. After the addition of 20  $\mu$ L of proteinase K, the lysate was incubated at 56°C for 30 min. Then, 300  $\mu$ L of ethanol was added and the lysate mixture was incubated at room temperature (RT) for 3 min. The lysate was transferred to the spin column. After subsequent washing with wash buffer 1 and 2, the RNA was eluted with 30  $\mu$ L of 56°C preheated elution buffer.

For serum samples, QIAamp viral RNA purification kit (Qiagen, Germany) was used according to the manufacturer's protocol as shown in **Figure 11**. In brief, 140  $\mu$ L of serum was incubated with 560  $\mu$ L of AVL solution containing cRNA at RT for 10 min. Then, 560  $\mu$ L of ethanol was added and the mixture was transferred to the QIAamp mini column. The total RNA from serum was eluted with 60  $\mu$ L of AVE buffer after subsequent washing with AW1 and AW2 buffers. The total RNA extracted from spleen and serum samples were stored at -80°C.

#### 3.2.1.2. Amplification of DNA by Reverse Transcription Polymerase Chain Reaction

Reverse transcription polymerase chain reactions (RT-PCR) were performed for three gene regions *i.e.* *Nsp2-HVII*, ORF5, and ORF7. The *Nsp2-HVII* was amplified using the primers, Nsp2-1F and Nsp2-1R. The ORF5 was amplified with ORF5-F and ORF5-R, while the ORF7 was amplified with ORF7-F and ORF7-R. The sequences of the primers are shown in **Table 1**.

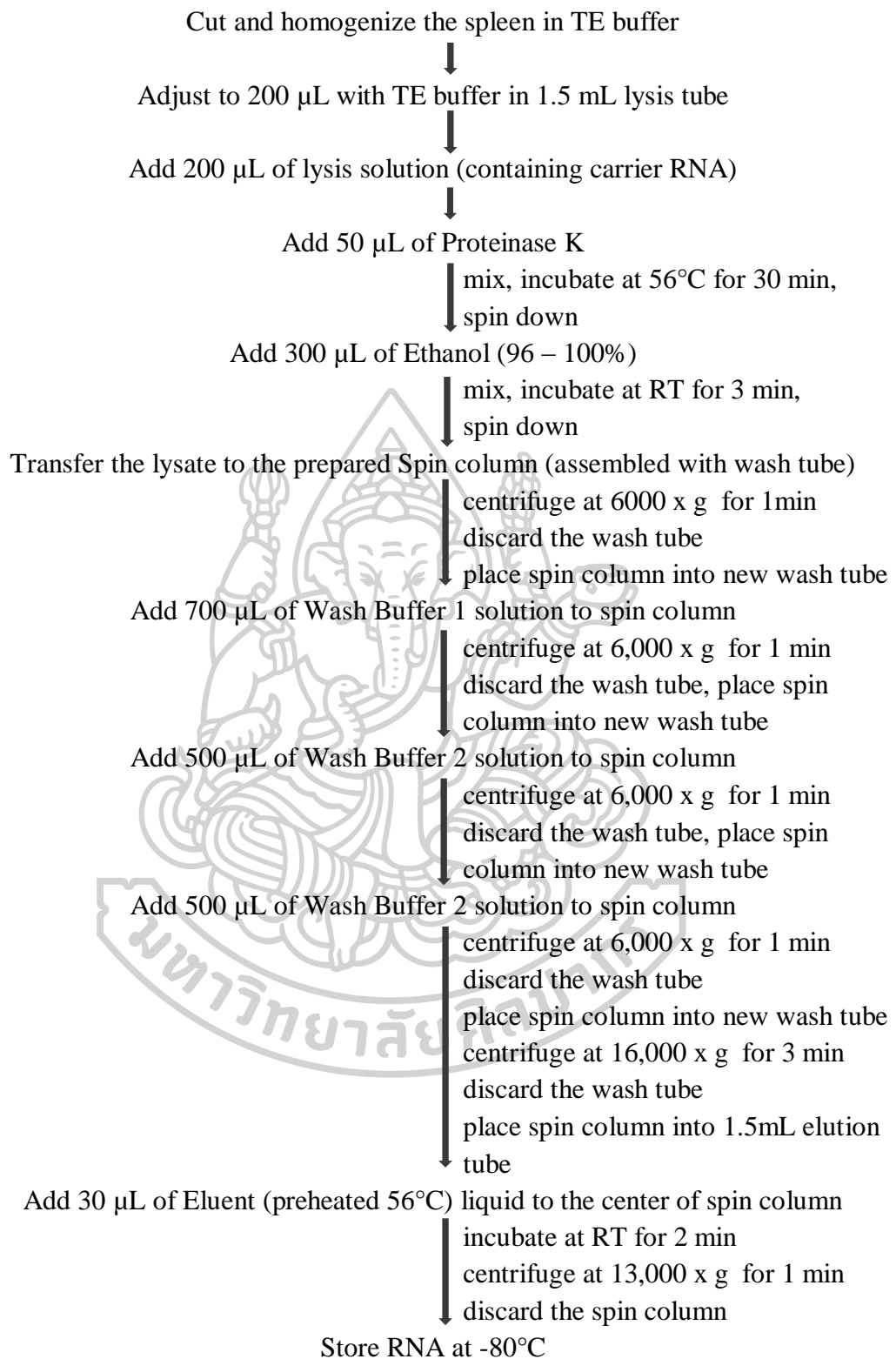


**Figure 10. Flow diagram of RNA extraction from spleen sample using GeneJET viral DNA and RNA purification kit (Thermo Fisher Scientific)**

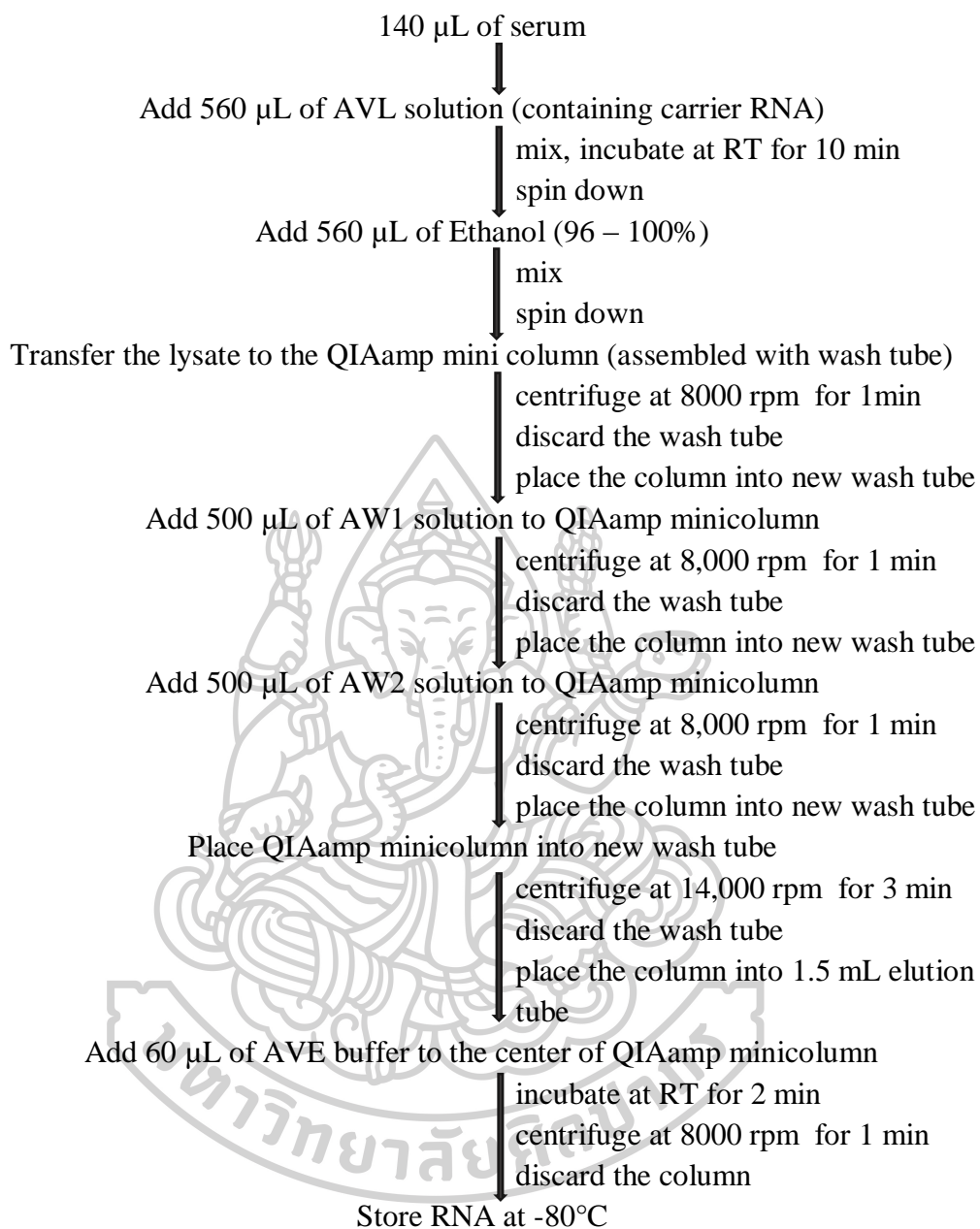


**Figure 11. Flow diagram of RNA Extraction from serum samples using QIAamp viral RNA purification kit (Qiagen)**

### 3.2.1.2.1. Amplification of DNA for Spleen Sample

For the spleen homogenate, two-step PCR method was used for amplification of DNA. The cDNA from total RNAs was synthesized using RevertAid First Strand cDNA Synthesis kit (Thermo Fisher Scientific, USA). A total of 25  $\mu$ L Reverse transcription reaction mixture contained

RNA templates	5 $\mu$ L
RiboLock RNase inhibitor	1 $\mu$ L
5 x reaction buffer	4 $\mu$ L
dNTPs mix (10 mM)	2 $\mu$ L
Reverse primer (10 $\mu$ M)	1 $\mu$ L
Nuclease-free water	12 $\mu$ L

Reverse transcription reaction was performed in a thermal cycler at 42°C for 60 min, then 70°C for 5 min. The obtained cDNAs were amplified by PCR using Dream Taq DNA polymerase kit (Thermo Fisher Scientific, USA). The 50  $\mu$ L of PCR reaction mixture was composed of

cDNA templates	10 $\mu$ L
Dream Taq master mix	25 $\mu$ L
Forward primers (10 $\mu$ M)	1 $\mu$ L
Reverse primers (10 $\mu$ M)	1 $\mu$ L
Nuclease-free water	13 $\mu$ L

The PCR reaction was done in a thermal cycler and included initial denaturation at 95°C for 3 min, 35 cycles of denaturation at 95°C for 30 sec, annealing at 60°C (for *Nsp2-HVII*) or 53°C (for ORF5 and ORF7) for 30 sec, extension at 72°C for 1 min, and final extension at 72°C for 10 min and then stored at -80°C.

### 3.2.1.2.2. Amplification of DNA for Serum Samples

For the serum samples, *Nsp2-HVII*, ORF5, and ORF7 were amplified from RNA using the One-Step RT-PCR kit (Qiagen, Germany). The 25  $\mu\text{L}$  of RT-PCR reaction mixture was composed of

RNA templates	5 $\mu\text{L}$
5x reaction buffer	5 $\mu\text{L}$
dNTPs mix(10 mM)	1 $\mu\text{L}$
Forward primers (10 $\mu\text{M}$ )	1 $\mu\text{L}$
Reverse primers (10 $\mu\text{M}$ )	1 $\mu\text{L}$
Enzyme mix	1 $\mu\text{L}$
Nuclease-free water	11 $\mu\text{L}$

The RT-PCR reaction was performed in a thermal cycler and consists of pre-PCR reaction at 50°C for 30 min, initial denaturation at 95°C for 3 min, 35 cycles of denaturation at 94°C for 45 sec, annealing at 60°C (for *Nsp2-HVII*) or 53°C (for ORF5 and ORF7) for 45 sec, extension at 72°C for 1 min then final extension at 72°C for 10 min and stored at -80°C.

In all DNA amplification, porcine epidemic diarrhea (PED) virus inactivated vaccine was used as a negative control. After the amplification reaction was completed, the PCR products were examined by agarose gel electrophoresis.

### 3.2.1.3. Agarose Gel Electrophoresis

The PCR products were verified by running gel electrophoresis. The 2 g of agarose powder was dissolved in 100 ml of 1x TAE buffer (40 mM Tris-HCl, 40mM Acetic acid, 2.5 mM EDTA, pH 8.0) and boiled until agarose powder was completely melted. After cooling down, the melted gel solution was poured into the mold and allowed to set at RT. The 2  $\mu\text{L}$  of PCR product was mixed with 2  $\mu\text{L}$  of 6x loading dye and 6  $\mu\text{L}$  of 1x TAE buffer. The mixture was loaded into the well of the gel that is submerged in the 1x TAE buffer in the electrophoresis tank. The electrophoresis reaction was performed at 50 V for 50 min. After the electrophoresis reaction was finished, the gel was stained in ethidium bromide for 5 min and destained in water for 15 min. The DNA bands were visualized by observation on a UV transilluminator.

By comparing with 100 base pair (bp) DNA ladder (VC 100plus, Vivantis, USA), the PCR products at specified bp (*Nsp2-HVII*: about 1000 bp, ORF5: about 600 bp, ORF7: about 400 bp) were excised from the gel. These gel cuts were purified using a Gel/PCR DNA fragments extraction kit (Nucleospin, Germany) according to the manufacturer's protocol as shown in **Figure 12**.

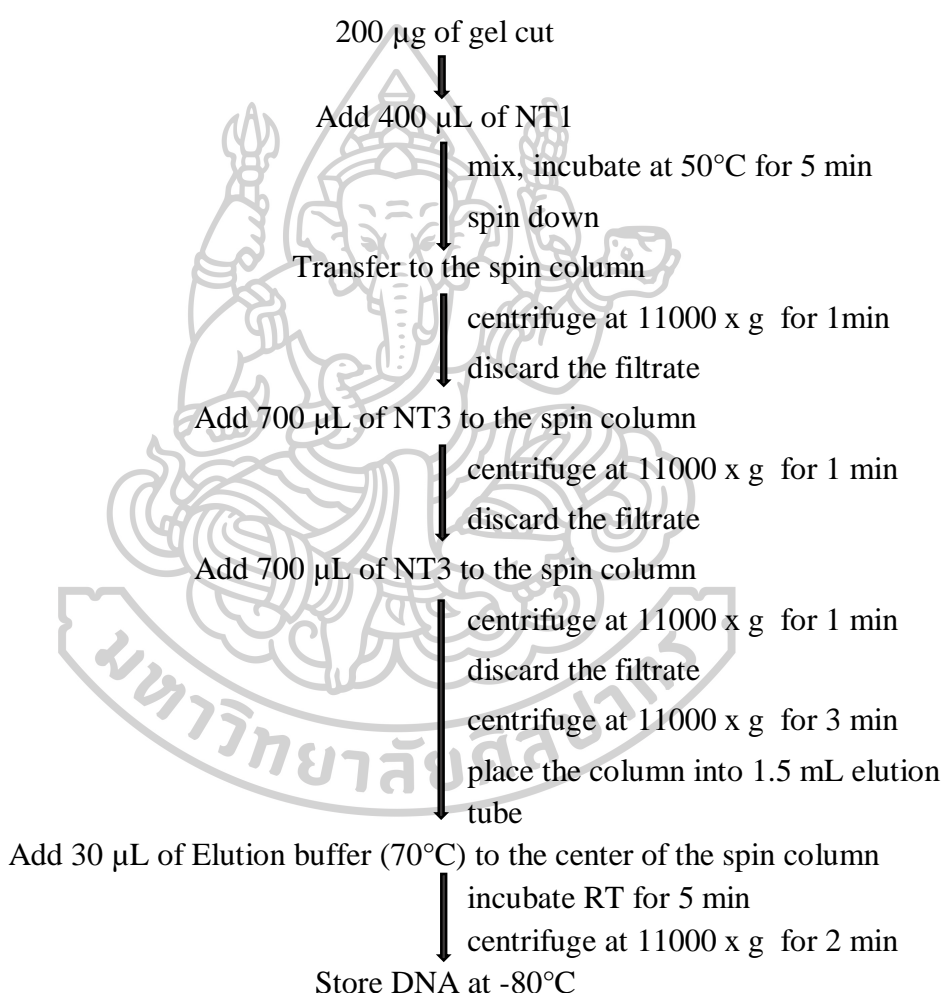


**Figure 12.** Flow diagram of purification of gel cuts using Gel/PCR DNA fragments extraction kit (Nucleospin)



#### 3.2.1.4. DNA Sequencing

The DNA concentrations of PCR products from each isolate were determined by NanoDrop One (Thermo Fisher Scientific) and the PCR products containing more than 20 ng/μL of DNA concentration were sent for DNA sequencing.

The sequencings of both strands of purified PCR amplicons were carried out with specific primers using Sangers' DNA Sequencing by Sol Gent, Co., South Korea. For DNA sequencing of *Nsp2-HVII*, two sets of sequencing primers *i.e.* Nsp2-2F(5'-ACCCCCTCCACCAAGAGTT-3') and Nsp2-2R (5'-CCGACCCACTCAAAGG TGTC-3') and Nsp2-3F (5'-GTCCTCACAGACGGAATATG-3') and Nsp2-3R (5'-TTAGCAGATCCTCCTCCATC-3') were additionally used to analyze the overlapping regions within targeted regions of *Nsp2-HVII*. The obtaining nucleotide sequences of *Nsp2-HVII*, ORF5, and ORF7 of six Myanmar PRRSVs were edited and manually fine-tuned using BioEdit Sequence Alignment Editor (version 7.2.5) (138). The verified sequences of *Nsp2-HVII*, ORF5, and ORF7 of six Myanmar isolates were deposited in GenBank, NCBI database.

#### 3.2.1.5. Sequence Alignments and Sequence Analyses

##### 3.2.1.5.1. Pairwise Sequence Alignments

To determine sequence identity, pairwise sequence alignments of nucleotides and deduced amino acids of each gene segment (*Nsp2-HVII*, ORF5, and ORF7) of six Myanmar PRRSVs with the corresponding reference sequences of EU prototype (Lelystad, Genbank ID: M96262), NA prototype (VR-2332, Genbank ID: U87392) and its vaccine strain RespPRRS (Ingelvac MLV, Genbank ID: AF066183), low-pathogenic PRRSV strains from China (CH1a, Genbank ID: AY032636 and its vaccine strain CH1R, Genbank ID: EU807840), and highly- pathogenic PRRSV strains in Asia (Chinese JXA1, Genbank ID: EF112445 and its vaccine strain JXA1R, Genbank ID: JQ804986; Vietnamese 07QN, Genbank ID: FJ394029; Thai HP/THAILAND/19500LL/2010, Genbank ID: KF735060; and Laotian BH58/10, Genbank ID: JN626287; Cambodian 10CAM46/2010 for *Nsp2-HVII*, Genbank ID: KF995276; NA/CAM/C044/2010 for GP5, Genbank ID:KF698642) were done using the EMBOSS needle program version 6.5.7 (105). The sequence data of ORF7 of Cambodian PRRSV strain was not available in the GenBank database.

### 3.2.1.5.2. Multiple Sequence Alignments

Multiple sequence alignments of the deduced amino acids of each gene segment of six Myanmar PRRSVs with the representative strains mentioned in 3.2.1.5.1 (except Lelystad) were performed with MUSCLE version 3.8.31(107) to analyze the changes within the functional domains.

### 3.2.1.6. Prediction of Signal Peptide, Transmembrane Topology, and N-Glycosylation

The presence of signal sequence within Nsp2-HVII, GP5, and NP of six Myanmar PRRSVs was determined by using SignalP 4.1, from ExPASy server and default cut-off set at 0.450 (139). The HMMTOP 2.0 software was used to predict the localization of proteins (intracellular or surface proteins or the presence of transmembrane domains (TM)) (140).

The presence of potential N-glycosylation sites was predicted by using NetNGlyc 1.0 server. It has a prediction accuracy of 76% and the prediction based on the presence of consensus sequence Asn-Xaa-Ser/Thr, where Asn is asparagine, Xaa is any amino acid except Proline, Ser is serine and Thr is threonine, because asparagine in this sequence is usually glycosylated in proteins produced by eukaryotes, archaea and rarely bacteria (141). Default 0.5 was considered as a threshold potential.

To perform the prediction of signal sequences, membrane topology, and N-glycosylation sites, the amino acid sequences of Nsp2-HVII, GP5, and NP of six Myanmar PRRSVs were subjected into the corresponding servers.

### 3.2.2. Phylogenetic Tree Construction

To investigate the genetic relationship between Myanmar PRRSVs and reference PRRSV strains, phylogenetic analyses based on the nucleotide and amino acid sequences of each gene segment (*Nsp2-HVII*, ORF5, and ORF7) of six Myanmar PRRSVs and the reference sequences from GenBank database (**Table 3**) were independently generated via the Neighbor-Joining method and Maximum Likelihood methods using the PHYLIP computer package program version 3.695 (142). The reliability of the branching order and robustness of the phylogenetic analysis were

evaluated by means of the bootstraps method with 1000 replicates. Graphic outputs of phylogenetic trees were generated by TreeView version 1.6.6 (143).

Firstly, multiple sequence alignments of the deduced amino acids of those three gene segments with the representative strains mentioned in **Table 3** were performed with MUSCLE software from EMBL-EBI tools for phylogenetic tree construction (107). Then, the phylogenetic trees were generated as mentioned above.



**Table 3. PRRSV reference strains used in the study**

Strain ID	Place	Year	GenBank Accession no.
HP/THAILAND/19500LL/2010	Thailand	2010	KF735060
01NP1	Thailand	2001	DQ056373
01CB1	Thailand	2001	DQ864705
10CAM46/2010 ( <i>Nsp2-HVII</i> )	Cambodia	2010	KF995276
NA/CAM/C044/2010 (ORF5)	Cambodia	2010	KF698642
07QN	Vietnam	2007	FJ394029
BH58/10	Laos	2010	JN626287
VR-2332	USA	1990	U87392
Lelystad	Netherlands	1991	M96262
CH1a	China	1996	AY032626
BJ4	China	2000	AF331831
HB-2(sh)2002	China	2002	AY262352
HN1	China	2003	AY457635
NB/04	China	2004	FJ536165
GD3	China	2005	GU269541
JXA1	China	2006	EF112445
WUH1	China	2006	EU187484
HUN4	China	2006	EF635006
07HEN	China	2007	FJ393457
CH1R	China	2008	EU807840
KP	China	2008	GU232735
JXA1R	China	2009	JQ804986
09HUB7	China	2009	GU168567
DC	China	2010	JF748718
YN/2011	China	2011	JX857698
PL97-1	South Korea	1997	AY585241
PA8	Canada	2000	AF176348
DK-2004-17-PI	Denmark	2004	KC862578
SP	Singapore	1998	AF184212
EDRD1 ( <i>Nsp2-HVII</i> )	Japan	1992	AB288356
EDRD1 (ORF5, ORF7)	Japan	1992	D45852
RespPRRS (Ingelvac MLV)	Vaccine strain		AF066183
AMERVAC	Vaccine strain		GU067771

### 3.2.3. *In silico* Epitope Prediction using Bioinformatics Tools

Some bioinformatics tools for the porcine genome have yet not been developed. Pig has similarity in size and physiology to human, and is genetically closely related to that of human, especially for immune gene families, thus, the bioinformatics tools using human genome were used in some parts of prediction (i.e. MHC II binding T-cell epitope prediction) in this study (144-146). The bioinformatics tools were selected based on their free accessibility, and on prediction characteristics and efficiency of the tools.

#### 3.2.3.1. Antigenicity Prediction

Antigenicity of Nsp2-HVII, GP5, and NP from six Myanmar PRRSVs were determined using VaxiJen v2.0 server with a default threshold value of 0.4 (147).

#### 3.2.3.2. Epitope Prediction

According to the high amino acid identities i.e. 95 - 100% between six Myanmar PRRSVs, HP/MYANMAR/2303AM/2011 was used as the representative for *in silico* predictions of linear B-cell and MHC I and MHC II binding T-cell epitopes of Nsp2-HVII, GP5, and NP. The flowchart describing the methodology for *in silico* prediction of epitopes was shown in **Figure 13**.

##### 3.2.3.2.1. Prediction of Linear B- cell Epitopes

The linear B-cell epitopes were predicted by BCPRED server for Nsp2-HVII, GP5, and NP of HP/MYANMAR/2303AM/2011 Myanmar PRRSV using BCPred and APP methods. The primary sequences of each protein in the plain format were put into the prediction. Prediction peptide length was set at 14 - 16 amino acids and specificity was set at 75%. The predicted epitopes with BCpred and APP scores of greater than 0.75 were selected and the repeated sequences were filtered out. The selected epitopes were further subjected to antigenicity prediction by using VaxiJen v2.0 server (147). The epitopes with VaxiJen antigenicity score of greater than 0.5 were chosen as potential linear B-cell epitopes.

### 3.2.3.2.2. Prediction of MHC I binding T-cell Epitopes

The MHC I processing prediction server and MHC I binding prediction server from IEDB-AR were used to predict the probable MHC I binding T-cell epitopes. MHC I processing prediction server contains combined algorithm of proteasomal C terminal cleavage prediction, transporter of antigenic peptide (TAP) transport efficiency, and MHC class I binding efficiency, and the predictions were carried out through NetMHCpan2.0 method (135, 139). The threshold value was set at 0.5 for obtaining sensitivity and specificity of 0.89 and 0.94, respectively. The length of epitopes was set as nine amino acid residues before prediction. The total score for each epitope was computed by summing up the values of cleavage by proteasomal C, the efficiency of TAP and binding of the given peptide to MHC I alleles. The epitopes were selected based on the total scores of above zero. Furthermore, the binding affinity of the peptide with swine leukocyte antigen (SLA) MHC I alleles, was also determined as half-maximal inhibitory concentration ( $IC_{50}$ ) by using MHC I binding T-cell prediction server using NetMHCpan2.0 algorithm which can predict the binding to a broad range of MHC class I SLA alleles (45 SLA alleles) (135, 148, 149). The epitopes with  $IC_{50}$  less than 250 nM were selected as potential MHC I binding T- cell epitopes.

### 3.2.3.2.3. Prediction of MHC II binding T-cell Epitopes

The MHC II binding T-cell epitope prediction server for SLA MHC II molecules has not been available. Due to the high genetic similarity between human and porcine immunomes and major histocompatibility complex, prediction of MHC II binding T- cell epitopes for HLA MHC II alleles were used. The MHC II binding T-cell epitope prediction server from IEDB-AR using NetMHCIIpan2.0 method was employed to predict the  $IC_{50}$  of epitope at specific MHC II alleles (150). The NetMHCIIpan2.0 method found out MHC II binding epitopes that can interact with 27 HLA-DP, HLA-DQ and HLA-DR alleles (144-146, 151, 152). The core peptides (nine amino acid length) having  $IC_{50}$  less than 250 nM were selected. Then, the antigenicity of the selected epitopes from each protein was determined with VaxiJen v2.0 server and the epitopes with VaxiJen antigenicity score greater than 0.5 were chosen as potential MHC II binding T-cell epitopes (147).



### 3.2.3.3. Epitope Conservancy Prediction

The epitope conservancy of predicted linear B-cell epitopes, MHC I or MHC II binding T- cell epitopes was examined using Epitope Conservancy Analysis Tool developed by IEDB-AR (153). The percentage of the conservancy of each epitope was measured within 15 Asian HP-PRRSV reference strains retrieved from the GenBank database.

### 3.2.3.4. Protein Model Prediction and Validation

The 3D structure of three proteins was designed by a template-based method using the Swiss-Model server. Swiss-Model searches the potential model templates from the template library (SMTL and PDB) with BLAST and HHBlits, and the models were designed based on target-template alignment (154, 155). The protein templates which have sequence identity of above 50% were filtered. Of which, the template with the highest sequence identity had been chosen for model evaluation and validation. The 3D structures of the first-line predicted epitopes were designed by using PEP-FOLD3, *de novo* peptide structure prediction server at the RPBS mobile portal (156, 157). The PEP-FOLD3 *de novo* software was used to predict potential protein structure and generates the best five models for peptides containing 5 to 50 amino acid residues.

The quality of the model structure was validated using z-score determined by Qualitative Model Energy Analysis (QMEAN) server from ExPASy Bioinformatics Resource Portal. The QMEAN offers an estimate of the degree of nativeness of the structural features observed on a global scale and QMEAN z-score around zero indicates good agreement between the model structure and experimental structure. The z-score -4.0 or below shows the model with low quality (158). Ramachandran plot generated from RAMPAGE server was used to check the maximum proteins residues were in the favored or allowed regions of Ramachandran plots except glycine (159). In PEP-FOLD3 *de novo* prediction, the model with highest QMEAN z-score and >75% of residues in favored regions of Ramachandran plots had been chosen as the best model. Mapping of predicted epitopes on protein templates was done using Swiss-Pdb viewer 4.1.0 (160).

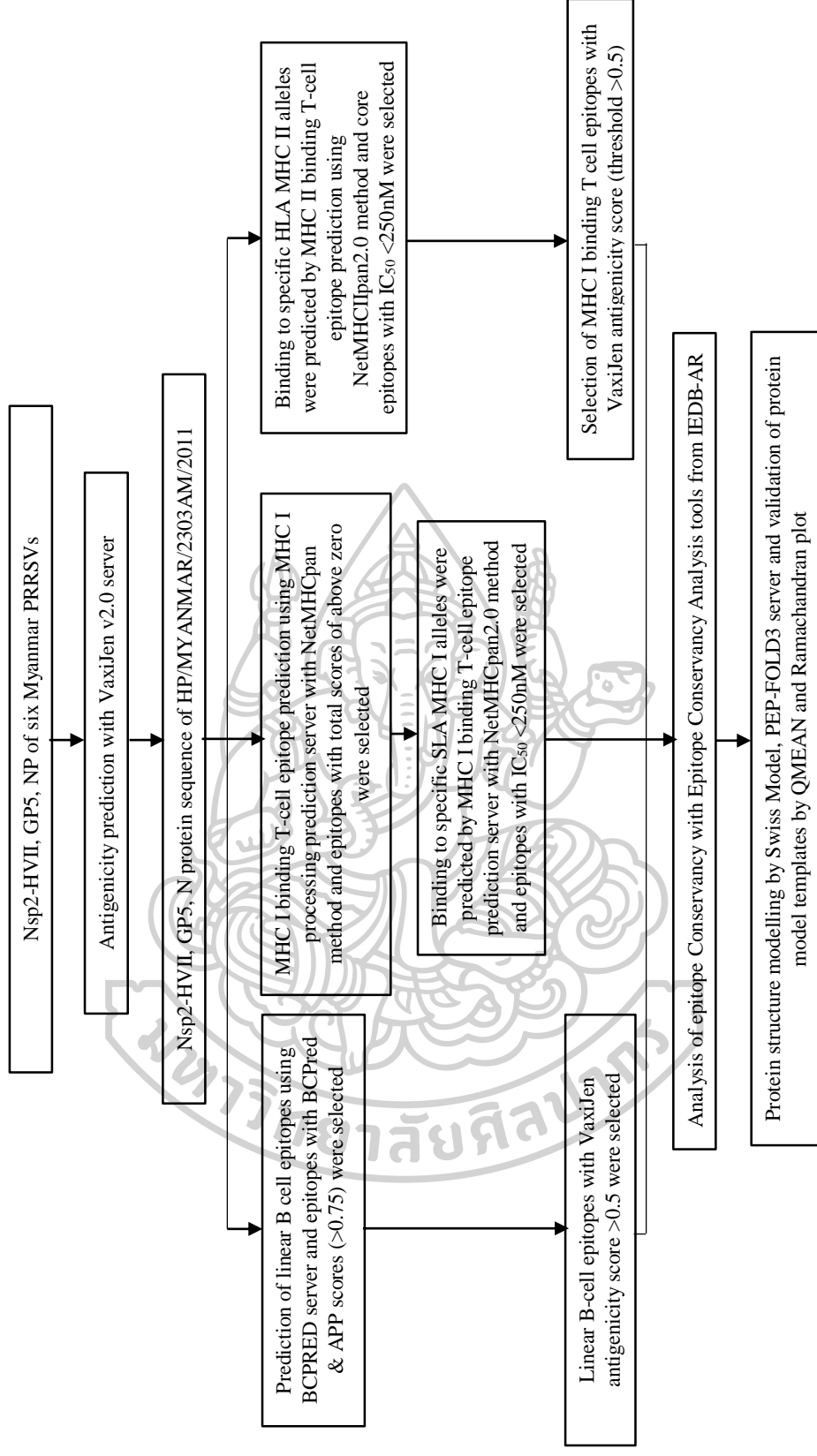


Figure 13. Flow diagram summarizing the linear B-cell epitopes, MHC I binding and MHC II binding T-cell epitope predictions

## CHAPTER 4

### RESULTS

#### 4.1. Molecular Characterization

##### 4.1.1. RNA Isolation, PCR Amplification, and DNA Sequencing

Total RNA could be directly extracted from each clinical sample. The *Nsp2-HVII*, ORF5, and ORF7 from all six RNA samples were successfully amplified. The PCR products of cDNA are shown in **Figure 14 A, B** and **C**. The purified PCR products were sequenced and the nucleotide sequences of all PCR products were verified as respective gene regions of PRRSV by BLAST search. The forward and reverse nucleotide sequences of each gene region were analyzed and edited using BioEdit software, and the complete sequences of *Nsp2-HVII* [1002 bp (334 aa)], ORF5 [603 bp (200 aa)], and ORF7 [372 bp (123 aa)] of all six Myanmar PRRSVs were obtained. The nucleotide sequences of *Nsp2-HVII*, ORF5, and ORF7 of six Myanmar PRRSVs have been submitted to GenBank, NCBI database under the accession numbers shown in **Table 4**. Sequencing chromatograms for three gene regions are shown in **Appendix I**.



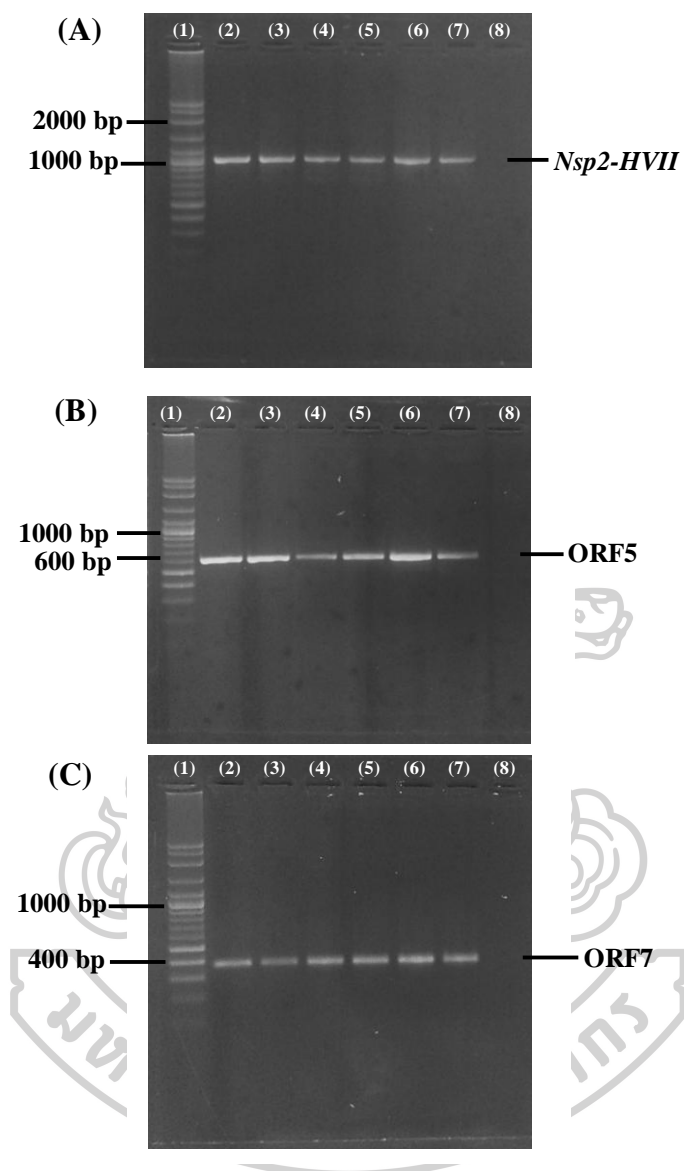


**Figure 14. Gel electrophoresis (2% agarose) of PCR products of (A) *Nsp2-HVII*, bands at about 1000 bp (B) *ORF5*, bands at about 600 bp and (C) *ORF7*, bands at about 400 bp**

Lane (1): DNA ladder, VC 100 bp plus

Lane (2): HP/MYANMAR/2303AM/2011

Lane (3): HP/MYANMAR/1908AM/2011

Lane (4): HP/MYANMAR/0204AM1/2011

Lane (5): HP/MYANMAR/0204AM2/2011

Lane (6): HP/MYANMAR/2510AM/2011

Lane (7): HP/MYANMAR/0411AM/2011

Lane (8): Negative Control (PCR product of PED inactivated vaccine)

**Table 4. GenBank accession number of *Nsp2-HVII*, *ORF5*, and *ORF7* of Myanmar PRRSVs analyzed in the study**

PRRSV ID	GenBank Accession no.		
	<i>Nsp2-HVII</i>	<i>ORF5</i>	<i>ORF7</i>
HP/MYANMAR/2303AM/2011	MF991914	MF991920	MF991926
HP/MYANMAR/0204AM1/2011	MF991915	MF991921	MF991927
HP/MYANMAR/0204AM2/2011	MF991916	MF991922	MF991928
HP/MYANMAR/1908AM/2011	MF991917	MF991923	MF991929
HP/MYANMAR/2510AM/2011	MF991918	MF991924	MF991930
HP/MYANMAR/0411AM/2011	MF991919	MF991925	MF991931

#### 4.1.2. Pairwise Sequence Alignments of *Nsp2-HVII*, *ORF5*, and *ORF7*

Pairwise sequence alignments of each gene segment using EMBOSS Needle program showed that nucleotide sequence identities of *Nsp2-HVII*, *ORF5*, and *ORF7* between the six Myanmar PRRSVs were 96.8-100%, 98.8-100%, and 97.8-100%, respectively, with 94.9-100%, 98-100%, and 100% identities of their corresponding deduced amino acid sequences (**Table 5**). Among these strains, the HP/MYANMAR/2510AM/2011 from Nyaungdon showed the least identity to others especially for *Nsp2-HVII* (96.8-97.1% nucleotide and 94.9-95.2 % amino acid sequence identities). Remarkably, HP/MYANMAR/0204AM1/2011 and HP/MYANMAR/0204AM2/2011 from Madaya were identical at both nucleotide and amino acid levels.

When compared to the NA prototype (VR-2332), Myanmar PRRSVs showed 69.5-70.2%, 89.1-89.2%, and 93.5-94.4% nucleotide sequence identities of *Nsp2-HVII*, *ORF5*, and *ORF7*, respectively (**Table 6**). However, they showed only 47.6 - 48.3 %, 62.8 - 63.3 %, and 60.1-60.5% identities of those three gene segments in that order to the EU prototype (Lelystad). Similarly, higher identities with the NA prototype than with the EU prototype were also found at the amino acid level (**Table 6**). These results suggested that all Myanmar PRRSV sequences were close to that of the NA genotype. Therefore, further sequence comparisons with Asian reference strains were performed with the NA-derived PRRSV.

All Myanmar PRRSVs showed higher nucleotide and amino acid identities to HP-PRRSVs (JXA1 and JXA1R, 07QN, HP/Thailand/19500LL/2010, B58/10, 10CAM46/2010 and NA/CAMC044/2010) than to LP-PRRSVs (CH1a and CH1R) as shown in **Table 7**. The highest nucleotide sequence identities of all three genes were found with HP/Thailand/19500LL/2010 (95.4-99.2 %) and BH58/10 (96.0-99.3 %).

**Table 5. Pairwise comparisons of the nucleotide (nt) and amino acid (aa) sequences of Nsp2-HVII, ORF5, and ORF7 between six Myanmar PRRSVs**

**1** = HP/MYANMAR/2303AM/2011, **2** = HP/MYANMAR/0204AM1/2011

**3** = HP/MYANMAR/0204AM2/2011, **4** = HP/MYANMAR/1908AM/2011

**5** = HP/MYANMAR/2510AM/2011, **6** = HP/MYANMAR/0411AM/2011

<i>Nsp2-HVII</i>	<b>1</b>		<b>2</b>		<b>3</b>		<b>4</b>		<b>5</b>		<b>6</b>	
	<b>nt</b>	<b>aa</b>	<b>nt</b>	<b>aa</b>	<b>nt</b>	<b>aa</b>	<b>nt</b>	<b>aa</b>	<b>nt</b>	<b>aa</b>	<b>nt</b>	<b>aa</b>
<b>1</b>	-	-	99.5	99.1	99.5	99.1	99.8	100	97.0	95.2	99.4	99.4
<b>2</b>	99.5	99.1	-	-	100	100	99.3	99.1	97.1	94.9	99.4	99.4
<b>3</b>	99.5	99.1	100	100	-	-	99.3	99.1	97.1	94.9	99.5	99.1
<b>4</b>	99.8	100	99.3	99.1	99.3	99.1	-	-	96.8	95.2	99.5	99.1
<b>5</b>	97.0	95.2	97.1	94.9	97.1	94.9	96.8	95.2	-	-	97	95.2
<b>6</b>	99.4	99.4	99.5	99.1	99.5	99.1	99.4	99.4	97	95.2	-	-
<b>ORF5</b>												
<b>1</b>	-	-	100	100	100	100	99.8	100	99	98	100	99
<b>2</b>	100	100	-	-	100	100	99.8	100	99	98	100	100
<b>3</b>	100	100	100	100	-	-	99.8	100	99	98	100	100
<b>4</b>	99.8	100	99.8	100	99.8	100	-	-	99.8	98	99.8	98
<b>5</b>	99	98	99	98	99	98	99.8	98	-	-	99	98
<b>6</b>	100	100	100	100	100	100	99.8	98	99	98	-	-
<b>ORF7</b>												
<b>1</b>	-	-	99.7	100	99.7	100	99.7	100	98.1	100	99.7	100
<b>2</b>	99.7	100	-	-	100	100	99.5	100	97.8	100	99.5	100
<b>3</b>	99.7	100	100	100	-	-	99.5	100	97.8	100	99.5	100
<b>4</b>	99.7	100	99.5	100	99.5	100	-	-	97.8	100	99.5	100
<b>5</b>	98.1	100	97.8	100	97.8	100	97.8	100	-	-	97.8	100
<b>6</b>	99.7	100	99.5	100	99.5	100	99.5	100	97.8	100	-	-



**Table 6. Pairwise comparisons of the nucleotide (nt) and amino acid (aa) sequences of Nsp2-HVII, ORF5, and ORF7 between six Myanmar PRRSVs, NA prototype (VR-2332) and EU prototype (Lelystad)**

<i>Nsp2-VII</i>	<b>Lelystad</b>		<b>VR-2332</b>	
	<b>nt</b>	<b>aa</b>	<b>nt</b>	<b>aa</b>
HP/MYANMAR/2303AM/2011	48.3	42.1	70.1	61.7
HP/MYANMAR/0204AM1/2011	48.3	42.3	70.1	62.3
HP/MYANMAR/0204AM2/2011	48.2	42.3	70.2	62.3
HP/MYANMAR/1908AM/2011	48.2	42.2	70.2	61.7
HP/MYANMAR/2510AM/2011	47.9	40.3	70.0	62.3
HP/MYANMAR/0411AM/2011	47.6	42.4	69.5	61.4
<b>ORF5</b>				
HP/MYANMAR/2303AM/2011	63.1	56.6	89.2	88.5
HP/MYANMAR/0204AM1/2011	63.3	56.6	89.1	88.5
HP/MYANMAR/0204AM2/2011	63.1	56.6	89.2	88.5
HP/MYANMAR/1908AM/2011	63.1	56.6	89.2	88.5
HP/MYANMAR/2510AM/2011	63.1	55.6	89.2	88.5
HP/MYANMAR/0411AM/2011	62.8	56.6	89.2	88.5
<b>ORF7</b>				
HP/MYANMAR/2303AM/2011	60.5	62.8	94.4	96.7
HP/MYANMAR/0204AM1/2011	60.5	62.8	94.4	96.7
HP/MYANMAR/0204AM2/2011	60.1	62.8	94.1	96.7
HP/MYANMAR/1908AM/2011	60.1	62.8	94.1	96.7
HP/MYANMAR/2510AM/2011	60.5	62.8	94.0	96.7
HP/MYANMAR/0411AM/2011	60.1	62.8	93.5	96.7

**Table 7. Pairwise comparisons of the nucleotide (nt) and amino acid (aa) sequences of Nsp2-HVII, ORF5, and ORF7 between six Myanmar PRRSVs and Asian reference PRRSV strains**

**1** = HP/MYANMAR/2303AM/2011, **2** = HP/MYANMAR/0204AM1/2011, **3** = HP/MYANMAR/0204AM2/2011, **4** = HP/MYANMAR/1908AM/2011, **5** = HP/MYANMAR/2510AM/2011, **6** = HP/MYANMAR/0411AM/2011

	RespPRRS		CH-1a		CH-IR		JXA1		JXAIR		HPThailand		07QN		BH58/10		10CAM46		
	nt	aa	nt	aa	nt	aa	nt	aa	nt	aa	nt	aa	nt	aa	nt	aa	nt	aa	
<b>Nsp2-VII</b>																			
<b>1</b>	70.0	61.2	82.6	79.1	82.7	79.3	97.0	95.2	96.1	93.1	97.6	97.3	96.5	94.9	97.8	97.3	98.1	97.8	
<b>2</b>	70.0	61.7	82.7	78.5	82.8	78.8	97.1	94.9	96.4	93.4	97.7	97.0	96.6	94.6	97.9	97.0	97.9	97.6	
<b>3</b>	70.0	61.7	82.7	78.5	82.8	78.8	97.1	94.9	96.4	93.4	97.7	97.0	96.6	94.6	97.9	97.0	98.2	97.6	
<b>4</b>	70.0	61.2	82.4	79.1	82.5	79.3	96.8	95.2	95.9	93.1	97.4	97.3	96.3	94.9	97.6	97.3	98.2	97.9	
<b>5</b>	69.3	61.7	82.2	78.2	82.3	78.5	95.8	93.4	94.9	91.3	96.6	95.5	95.3	93.1	96.8	95.5	97.1	96.1	
<b>6</b>	69.8	60.9	82.6	78.5	82.7	79.1	97.0	95.2	96.1	93.1	97.6	97.3	96.5	94.9	97.8	97.3	98.1	97.9	
<b>ORF5</b>																			
<b>1</b>	88.9	87.5	94.5	92.0	93.7	90.5	98.5	98.0	97.8	96.0	99.2	99.5	98.3	98.5	99.3	99.5	98.0	99.0	
<b>2</b>	88.9	87.5	94.5	92.0	93.7	90.5	98.5	98.0	97.8	96.0	99.2	99.5	98.3	98.5	99.3	99.5	98.8	99.0	
<b>3</b>	88.9	87.5	94.5	92.0	93.7	90.5	98.5	98.0	97.8	96.0	99.2	99.5	98.3	98.5	99.3	99.5	98.8	99.0	
<b>4</b>	88.7	87.5	94.5	92.0	93.5	90.5	98.5	98.0	97.8	96.0	99.0	99.5	98.3	98.5	99.2	99.5	98.7	99.0	
<b>5</b>	88.8	87.5	94.4	92.0	93.7	90.5	97.8	96.0	97.0	94.5	98.5	97.5	97.7	96.5	98.7	97.5	98.2	97.0	
<b>6</b>	88.9	87.5	94.5	92.0	93.7	90.5	98.5	98.0	97.8	96.0	99.2	99.5	98.3	98.5	99.3	99.5	98.8	99.0	
<b>ORF7</b>																			
<b>1</b>	94.4	96.7	96.0	95.1	96.0	95.9	98.7	98.4	97.9	98.4	96.8	97.6	97.9	97.6	97.3	98.4	-	-	
<b>2</b>	94.1	96.7	96.0	95.1	95.7	95.9	98.4	98.4	97.9	98.4	96.5	97.6	97.9	97.6	97.0	98.4	-	-	
<b>3</b>	94.1	96.7	96.0	95.1	95.7	95.9	98.4	98.4	97.9	98.4	96.5	97.6	97.9	97.6	97.0	98.4	-	-	
<b>4</b>	94.1	96.7	96.0	95.1	96.0	95.9	98.4	98.4	97.9	98.4	96.5	97.6	97.9	97.6	97.0	98.4	-	-	
<b>5</b>	93.5	96.7	94.6	95.1	94.6	95.9	97.3	98.4	97.9	98.4	95.4	97.6	97.9	97.6	96.0	98.4	-	-	
<b>6</b>	94.1	96.7	96.0	95.1	95.7	95.9	98.4	98.4	97.9	98.4	96.5	97.6	97.9	97.6	97.0	98.4	-	-	

### 4.1.3. Amino Acid Sequence Analyses

Multiple amino acid sequence alignment of all Myanmar PRRSVs were performed with Genbank sequences of the representative PRRSV reference strains including VR-2332, RespPRRS (Ingelvac MLV), LP-PRRSVs (Chinese CH1a and CH1R), and Asian HP-PRRSVs [Chinese JXA1 and JXA1R, Vietnamese 07QN, Thai HP/Thailand/19500LL/2010, Laotian BH58/10, and Cambodian 10CAM46/2010 (*Nsp2-HVII*), and NA/CAMC044/2010 (GP5)]. The amino acid positions were based on the genome sequence of the VR-2332.

#### 4.1.3.1. The middle hypervariable region of non-structural protein-2 (Nsp2-HVII)

There were extensive mutations found in the Nsp2-HVII (residues 265 to 628) of the Myanmar PRRSVs as shown in **Figure 15**. The data showed that their sequences were more similar to HP-PRRSVs especially with HP/THAILAND/19500LL/2010, BH58/10 and 10CAM46/2010 (95.5-99.0% amino acid sequence identity), in which they shared eight identical substitutions; R280G, W410R, T428A, R450D, P495L, C510F, S519I, and E582K. It was observed that those mutations were not occurred in JXA1, JXA1R, and 07QN. These three strains had the same R280S, R450G, and C510R mutations, implying their close relationship.

The L292F, P431S, and V621M were uniquely found in five Myanmar PRRSVs except the HP/MYANMAR/2510AM/2011 from Nyaungdon. Moreover, the HP/MYANMAR/2510AM/2011 strain contained extra nine amino acid mutations at A297V, L313Q, R347Y, T419I, V453I, P492S, S532I, V594T, and K617D which were not found in other Myanmar PRRSVs and HP-PRRSVs.

It was noticeable that Nsp2-HVII of all six Myanmar PRRSVs had discontinuous 30 amino acid deletions at residues 481 and 533-561 (**Figure 15**), which regarded as the typical feature of HP-PRRSV. These deletions were in accordance with those seen in the reference HP-PRRSV strains including JXA1, JXA1R, 07QN, HP/THAILAND/19500LL/ 2010, BH58/10, and 10CAM46/2010 but not in the LP-PRRSV strains (CH1a and CH1R). No further deletion in Nsp2-HVII was found among Myanmar PRRSVs. When compared to the vaccine strains, the Nsp2-HVII of Myanmar PRRSVs were closer to JXA1R than RespPRRS (Ingelvac MLV) and CH1R. (**Figure 15**).



370 ..... 380 ..... 390 ..... 400 ..... 410 ..... 420 ..... 430 ..... 440 ..... 450  
 KVVREYGLM PTFEGPRTL PRGLDELKQ MEEDLLKLAN AGTSDMMAW AVEQVDLKTW VKNYPRTWTPP PPFKVOPRK TKPVKSLPER  
 G.L. .... S.GL. .... V. S. .... A.E. .... A. .... A. .... S. .... R. .... R. .... S. .... N  
 G.L. .... S.GL. .... V. SS. .... A.E. .... A. .... A. .... S. .... R. .... R. .... S. .... N  
 E.L. .... S.GL. .... V. S. .... T.A.E. .... A. .... A. .... S. .... R. .... R. .... S. .... G  
 E.L. .... S.GL. .... V. S. .... E.T. .... T.A.E. .... A. .... A. .... S. .... R. .... R. .... S. .... G  
 E.L. .... S.GL. .... V. SR. .... T.A.E. .... A. .... A. .... S. .... R. .... R. .... S. .... G  
 E.L. .... S.GL. .... V. S. .... T.A.E. .... R.A. .... A. .... G. .... A.S. .... R. .... R. .... S. .... D  
 E.L. .... S.GL. .... V. S. .... T.A.E. .... R.A. .... A. .... G. .... A. .... R. .... R. .... S. .... D  
 E.L. .... S.GL. .... V. S. .... T.A.E. .... R.A. .... A. .... S. .... A. .... R. .... R. .... S. .... D  
 E.L. .... S.GL. .... V. S. .... T.A.E. .... R.A. .... A. .... S. .... A. .... S. .... R. .... R. .... S. .... D  
 E.L. .... S.GL. .... V. S. .... T.A.E. .... R.A. .... A. .... S. .... A. .... S. .... R. .... R. .... S. .... D  
 E.L. .... S.GL. .... V. S. .... T.A.E. .... R.A. .... A. .... S. .... A. .... S. .... R. .... R. .... S. .... D  
 E.L. .... S.GL. .... V. S. .... T.A.E. .... R.A. .... A. .... S. .... A. .... S. .... R. .... R. .... S. .... D  
 E.L. .... S.GL. .... V. S. .... T.A.E. .... R.A. .... A. .... S. .... A. .... S. .... R. .... R. .... S. .... D  
 E.L. .... S.C. .... V. S. .... T.A.E. .... R.A. .... A. .... S. .... A. .... S. .... R. .... R. .... S. .... D

VR-2332  
 RespRRS (Ingelvac MLV)  
 CHINA CH1a  
 CHINA CH1R  
 CHINA JXAI  
 CHINA JXAIR  
 VIETNAM 07QN  
 HP/THAILAND/19500ILL/2010  
 LAOS BH58/10  
 CAMBODIA 10CAMC46/2010  
 HP/MYANMAR/2303AM/2011  
 HP/MYANMAR/1908AM/2011  
 HP/MYANMAR/0204AM1/2011  
 HP/MYANMAR/0204AM2/2011  
 HP/MYANMAR/0411AM/2011  
 HP/MYANMAR/2510AM/2011







#### 4.1.3.2. The major envelope protein, glycoprotein 5 (GP5)

The GP5 of all six Myanmar PRRSVs contained 200 amino acid residues as those of VR-2332 and other reference PRRSVs (**Figure 16**). The GP5 of all six Myanmar PRRSVs were likely to contain short signal peptide at N-terminal residues (1-31 amino acids), which was predicted with high confidence (Discrimination 'D' score of 0.84). The HMMTOP prediction in CCTOP server predicted that GP5 of all Myanmar PRRSVs possessed three TM helices: TMI (67-84) and TMII (87-104) and TMIII (107-125). Ten mutations were conserved among the Myanmar PRRSVs and the reference HP-PRRSVs. Most of them occurred in the N-terminal signal sequence (G9C, S16F, C24Y, and F25L) and the ectodomain (S35N, L39I, and N58Q). However, the S35N in the ectodomain hypervariable region I (HVI) was absent in HP/MYANMAR/2510AM/2011. Unlike other Myanmar PRRSVs and HP-PRRSVs, this HP/MYANMAR/2510AM/2011 strain did not have T121A mutation in TM III, but rather it had an added V124A mutation. Additionally, just D34S mutation was conserved between all Myanmar PRRSVs, HP/THAILAND/19500LL/2010, BH58/10 and NA/CAMC044/2010. Interestingly, E170G in the endodomain was a unique mutation conserved only across all Myanmar PRRSVs but not seen in other HP-PRRSVs, and was the single mutation different from HP/THAILAND/19500LL/2010, BH58/10, and NA/CAMC044/2010. Hence, E170G could be a distinct genetic maker of Myanmar PRRSVs.

The decoy epitope <sup>27</sup>VLAN<sup>30</sup> was conserved among all Myanmar PRRSVs, VR-2332, and HP-PRRSVs from Thailand (HP/THAILAND/19500LL/2010), Laos (BH58/10), Vietnam (07QN), and Cambodia (NA/CAMC044/2010) but was different from Chinese isolates (CH1a, CH1R, JXA1, and JXA1R) that contained an A29V substitution. In the primary neutralizing epitope (PNE), S<sup>37</sup>HL<sup>39</sup>QLIYNL<sup>45</sup>, all Myanmar PRRSVs, and HP-PRRSVs had isoleucine (I) replacement at position 39 in the (S<sup>37</sup>HL<sup>39</sup>QLIYNL<sup>45</sup>) PNE. There were five potential N-linked glycosylation sites (positions 30, 33, 35, 44, and 51) located in the ectodomain of GP5. They were conserved among HP/THAILAND/19500LL/2010, BH58/10, NA/CAMC044/2010 and five Myanmar PRRSVs. Notably, HP/MYANMAR/2510AM/2011 had Serine (S) at 33 and 35 amino acid residues so that N33 and N35 glycosylation sites were abolished. An additional N-glycosylation site, D34N in HVI, was observed only in JXA1, JXA1R, and 07QN (**Figure 16**).





#### 4.1.3.3. The nucleocapsid protein (NP)

The NP of all Myanmar PRRSVs in this study were 100% identical. They had the same size of 123 amino acids as those of the VR-2332 prototype and other reference strains. Three amino acid substitutions, K46R, H109Q, and V117A, were conserved in all Myanmar PRRSVs and HP-PRRSVs. R11K and T91A mutations presented in HP-PRRSVs were not found in all Myanmar PRRSVs as shown in **Figure 17**.









## 4.2. Phylogenetic Analyses

In order to draw the genetic relationship between Myanmar PRRSVs in this study and other 31 reference strains, phylogenetic trees based on the nucleotide or deduced amino acid sequences of *Nsp2-HVII*, ORF5, and ORF7 were independently generated using the Neighbor-Joining and Maximum Likelihood methods. Each phylogenetic tree showed a similar pattern of genetic relationship, particularly those that based on *Nsp2-HVII* and ORF5 sequences. The phylogenetic tree based on ORF7 had the lowest bootstrap values, suggesting that this tree was less instructive to determine the genetic relationship.

From all phylogenetic trees (Figures 18, 19, and 20 shown as the examples, the other phylogenetic trees were shown in **Appendix II**), it was seen that the relationship of PRRSV sequences under studied could be separated into two major groups, the NA and EU genotypic groups. The NA genotypic group could be further divided into three subtypes. Subtype 1 included the VR-2332, its attenuated vaccine strain RespPRRS, and other NA-like strains. Subtype 2 included the Chinese LP-PRRSV, CH1a and its vaccine strain, CH1R. The HP-PRRSV strains [e.g. Chinese JXA1 and its vaccine strain JXA1R, Vietnamese 07QN, Thai HP/THAILAND/19500LL/2010, Laotian BH58/10, Cambodian 10CAM46/2010 (*Nsp2-HVII*), and NA/CAMC044/2010 (GP5)] were belonged to subtype 3. All Myanmar PRRSVs in this study were enclosed in the subtype 3 of the NA genotype as with other HP-PRRSV strains. They were relatively close to the HP-PRRSV strains from Thailand (HP/Thailand/19500LL/2010), Laos (BH58/10), and Cambodia (10CAM46/2010 and NA/CAMC044/2010) based on the *Nsp2-HVII* and ORF5 sequences (**Figures 18 and 19**).

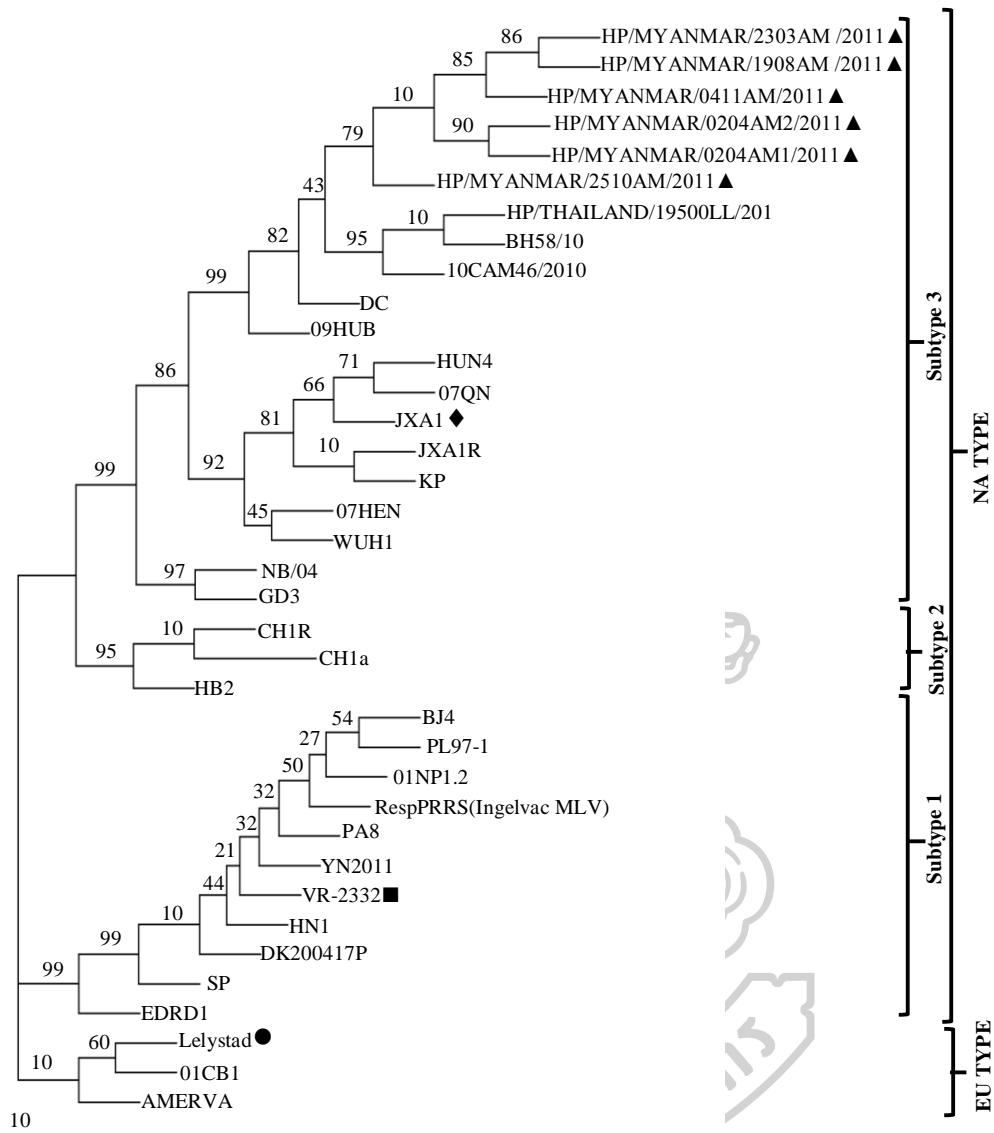


**Figure 18. Phylogenetic tree of PRRSVs based on nucleotide sequences of Nsp2-HVII gene**

The phylogenetic tree was constructed by Neighbor-joining method using Kimura 2-parameter model with 1000 bootstrapping. The (▲) indicates Myanmar PRRSVs, (◆) indicates Chinese HP-PRRSV, JXA1, (●) indicates EU prototype, Lelystad and (■) indicates NA prototype, VR-2332.

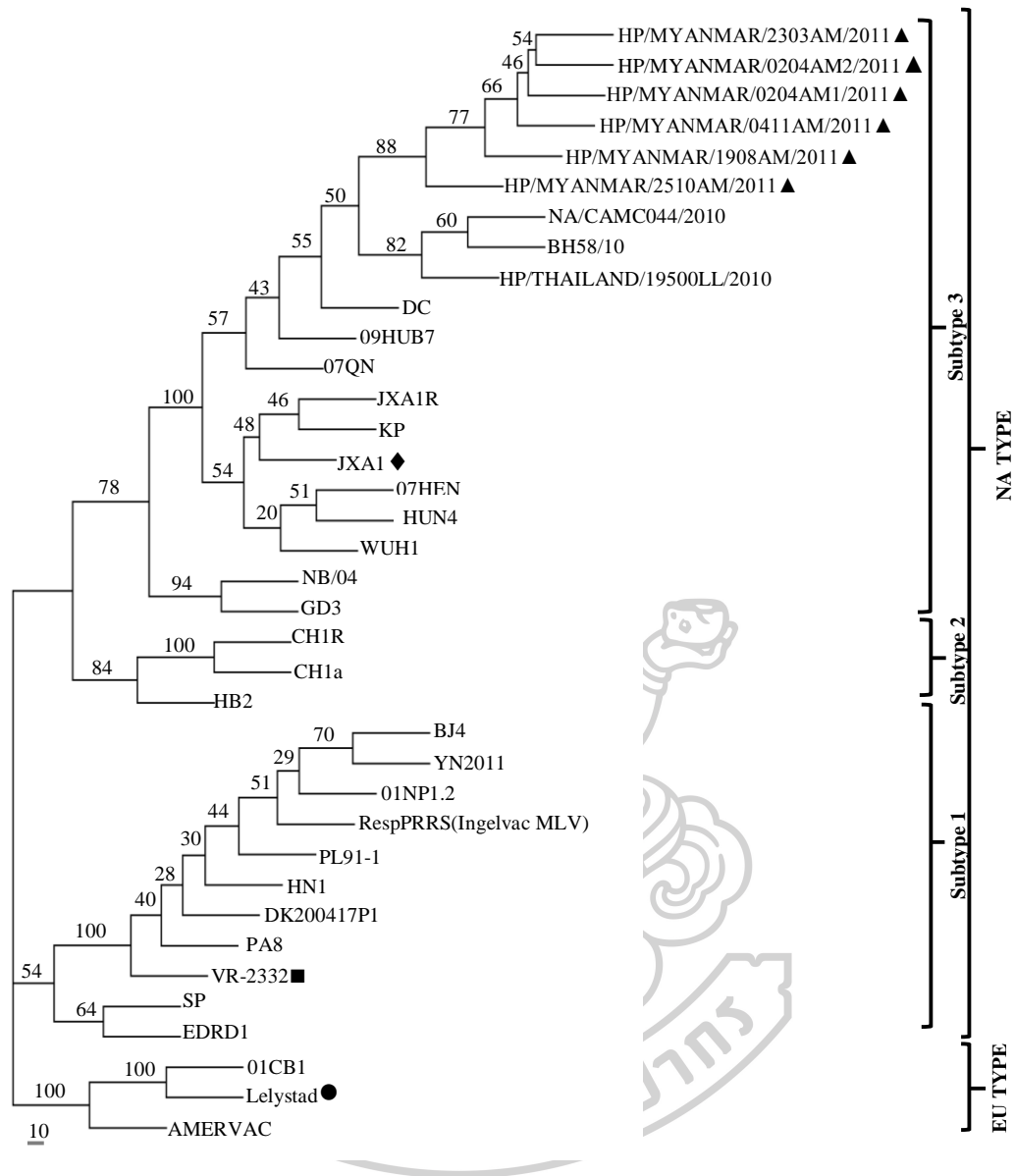


**Figure 19. Phylogenetic tree of PRRSVs based on nucleotide sequences of ORF5 gene**

The phylogenetic tree was constructed by Neighbor-joining method using Kimura 2-parameter model with 1000 bootstrapping. The (▲) indicates Myanmar PRRSVs, (◆) indicates Chinese HP-PRRSV, JXA1, (●) indicates EU prototype, Lelystad and (■) indicates NA prototype, VR-2332.

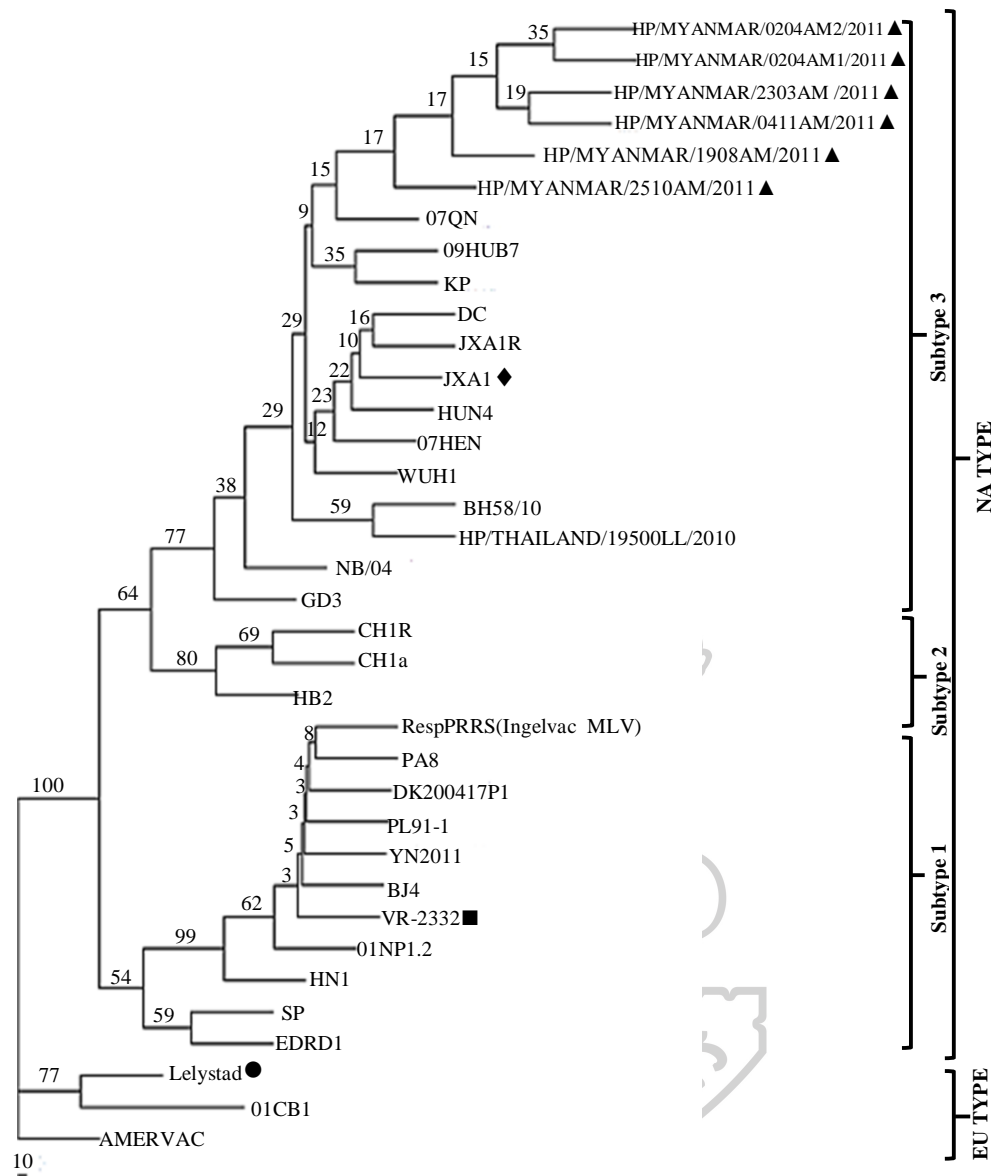


**Figure 20. Phylogenetic tree of PRRSVs based on nucleotide sequences of ORF7 gene**

The phylogenetic tree was constructed by Neighbor-Joining method using Kimura 2-parameter model with 1000 bootstrapping. The (▲) indicates Myanmar PRRSVs, (◆) indicates Chinese HP-PRRSV, JXA1, (●) indicates EU prototype, Lelystad and (■) indicates NA prototype, VR-2332.

### 4.3. *In silico* Epitope Prediction using Bioinformatics Tools

#### 4.3.1. Antigenicity Prediction of the Nsp2-HVII, GP5, and NP

VaxiJen v2.0 antigenicity prediction server was used to analyze the probable antigenicity of Nsp2-HVII, GP5, and NP of six Myanmar PRRSVs at a threshold value of 0.4. As shown in **Table 8**, the antigenicity score of Nsp2-HVII, GP5, and NP of all Myanmar PRRSVs were above 0.4, suggesting that all three proteins were antigenic.

**Table 8.** *The antigenicity score of Nsp2-HVII, GP5, and NP of six Myanmar PRRSVs*

PRRSV ID	Antigenicity score of the proteins		
	Nsp2-HVII	GP5	NP
HP/MYANMAR/2303AM/2011	0.4972	0.4705	0.5881
HP/MYANMAR/0204AM1/2011	0.4912	0.4705	0.5881
HP/MYANMAR/0204AM2/2011	0.4912	0.4705	0.5881
HP/MYANMAR/1908AM/2011	0.4713	0.4705	0.5881
HP/MYANMAR/2510AM/2011	0.4532	0.4724	0.5881
HP/MYANMAR/0411AM/2011	0.4798	0.4705	0.5881

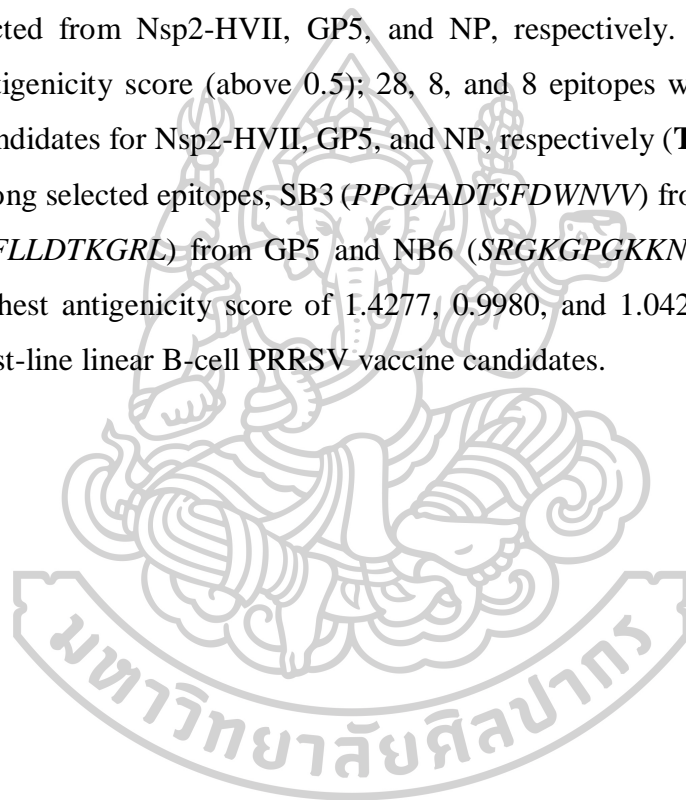


#### 4.3.2. Prediction of Linear B-cell epitopes

The prediction of linear B-cell epitopes from Nsp2-HVII, GP5, and NP of HP/MYANMAR/2303AM/2011 were performed using BCPred and AAP method from BCPRED server and the antigenicity of each predicted epitope was analyzed by VaxiJen v2.0 antigenicity prediction server. The linear B-cell epitope prediction for all three proteins was summarized in **Figure 21**.

The epitopes containing 14 and 16 amino acids were selected by the BCPred and APP score of above 0.75 at specificity 75%. The total of 49, 14, and 13 epitopes were predicted from Nsp2-HVII, GP5, and NP, respectively. By considering the VaxiJen antigenicity score (above 0.5); 28, 8, and 8 epitopes were then selected as potential candidates for Nsp2-HVII, GP5, and NP, respectively (**Table 9-11**).

Among selected epitopes, SB3 (*PPGAADTSFDWNVV*) from Nsp2-HVII, GB5 (*SCTRYTNFLDITKGRL*) from GP5 and NB6 (*SRGKGPGKKNRKKNPE*) from NP had the highest antigenicity score of 1.4277, 0.9980, and 1.0428, respectively, and were the first-line linear B-cell PRRSV vaccine candidates.



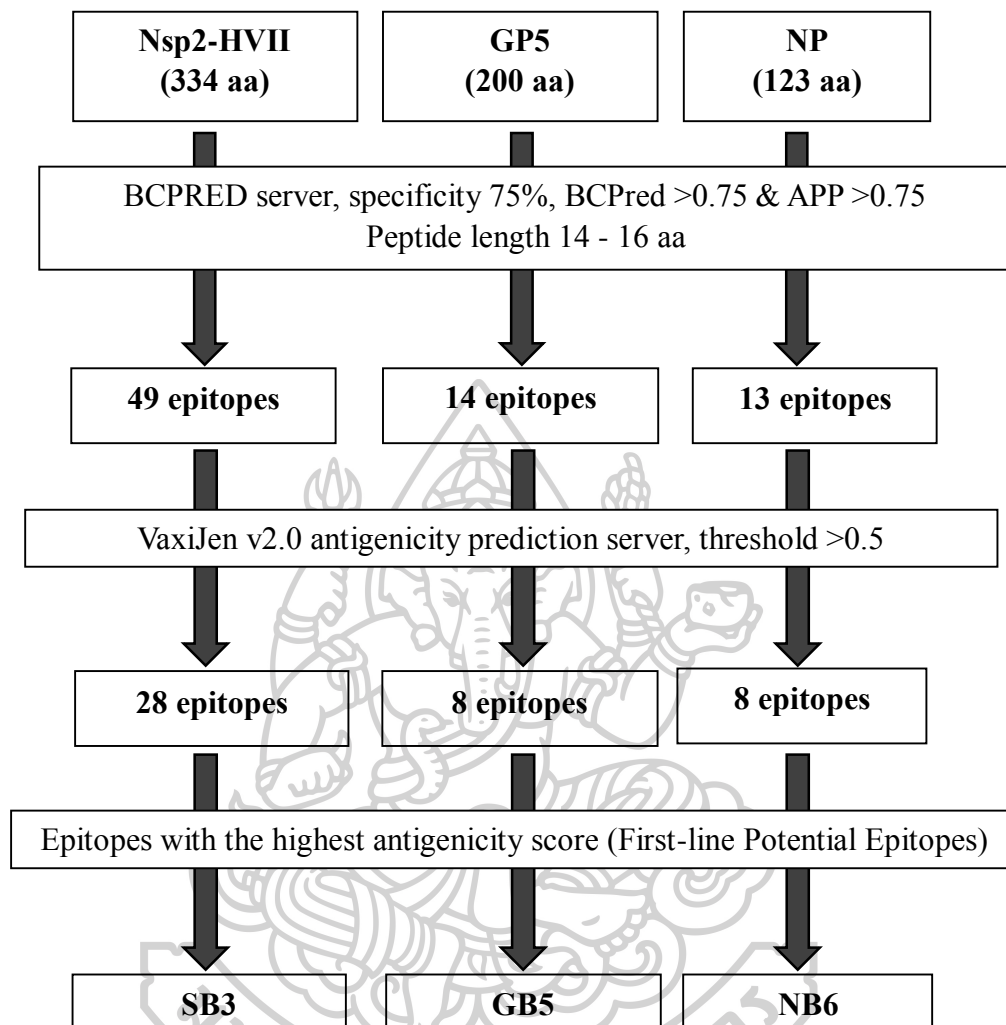


*Figure 21. The diagram summarizing linear B-cell epitope prediction*

**Table 9. Potential linear B-cell epitopes predicted from Nsp2-HVII of HP/MYANMAR/2303AM/2011 PRRSV with BCPred and APP score (>0.75) and VaxiJen antigenicity score (>0.5)**

ID	Epitope	Position	BCPred Score	APP Score	Length	VaxiJen Antigenicity Score	Conservancy (%) within 15 HP-PRRSVs
SB1	AKLERVSPPGAADT	271 – 284	-	1.000	14	0.6146	47
SB2	RVSPPGAADTSFDWNV	275 – 290	0.992	-	16	1.0130	40
<b>SB3</b>	<b>PPGAADTSFDWNV *</b>	278 – 291	0.988	-	14	<b>1.4277</b>	40
SB4	PGAADTSFDWNVVFPG	279 – 294	-	1.000	16	1.1355	0
SB5	VVFPGVEAANQTTE	290 – 303	-	1.000	14	0.8730	0
SB6	PGVEAANQTTEQPH	293 – 306	0.944	-	14	0.8696	53
SB7	SVPLTAFSLNCYYPA	326 – 77	-	1.000	16	0.5143	87
SB8	SLSNCYYPAQGDEVH	333 – 341	0.994	-	16	0.5038	73
SB9	YYP AQDEVHHRER	338 – 351	-	1.000	14	0.9358	73
SB10	PAQDEVHHRERLN	340 – 353	0.994	-	14	0.7473	73
SB11	MSTGLGPRPVLPSG	370 – 383	0.913	-	14	0.8492	73
SB12	MSTGLGPRPVLPSGLD	370 – 385	0.913	-	16	0.9219	73
SB13	ATSEMMARAAEQVD	403 – 416	0.770	-	14	0.6513	73
SB14	PRWAPPPPRVQPRR	425 – 440	-	1.000	16	0.9844	0

\* The epitope with the highest VaxiJen antigenicity score

**Table 9. Potential linear B-cell epitopes predicted from Nsp2-HVII of HP/MYANMAR/2303AM/2011 PRRSV with BCPred and APP score (>0.75) and VaxiJen antigenicity score (>0.5) (Continued.)**

ID	Epitope	Position	BCPred Score	APP Score	Length	VaxiJen Antigenicity Score	Conservancy (%) within 15 HP-PRRSVs
SB15	RWAPPSPPRVQPRRT	426 – 441	-	1.000	16	0.9666	0
SB16	APSPPRVQPRRT	428 – 441	-	1.000	14	0.9784	0
SB17	RVQPRRTKSVKSLP	435 – 448	-	1.000	14	0.5979	87
SB18	SLPEDKVPAPRRKVR	446 – 461	-	1.000	16	0.7001	53
SB19	PEDKVPAPRRKVR	448 – 461	0.992	-	14	1.1123	53
SB20	VPAPRRKVRSDCGS	453 – 466	-	1.000	14	0.7601	80
SB21	GLSAPVPAPRRVT <sup>del29</sup>	520 – 534	0.999	-	14	0.5716	0
SB22	GLSAPVPAPRRVT <sup>del29</sup> TTL	520 – 536	-	1.000	16	0.5317	0
SB23	QTEYKAFPLAPSQN	578 – 591	0.866	-	14	1.1438	33
SB24	TEYKAFPLAPSQNM	579 – 592	-	1.000	14	1.1426	33
SB25	ILEAGGQEAEEVLS	594 – 607	-	1.000	14	0.6320	40
SB26	SDILNDTNPAPMSS	610 – 623	-	1.000	14	0.8196	0
SB27	DILNDTNPAPMSSSSS	611 – 626	0.998	-	16	0.7643	0
SB28	LNDTNPAPMSSSSS	613 – 626	0.871	-	14	0.9780	0

\* The epitope with the highest VaxiJen antigenicity score

<sup>del29</sup> The epitope in 29 continuous amino acid deletion region of HP-PRRS when compared with VR-2332

**Table 10. Potential linear B-cell epitopes predicted from GP5 of HP/MYANMMAR/2303AM/2011 PRRSV with BCPred and APP score (>0.75) and VaxiJen antigenicity score (>0.5)**

ID	Epitope	Position	BCPred Score	APP Score	Length	VaxiJen Antigenicity Score	Conservancy (%) within 15 HP-PRRSVs
GB1	AVLANASNSSSHQQL <sup>‡</sup>	26 – 41	0.959	-	16	0.5241	27
GB2	ANASNSSSHQQLI <sup>‡</sup> ▲	29 – 42	0.920	-	14	0.5759	27
GB3	FVIRLAKNCMSWRY	123 – 136	-	1.000	14	0.6381	87
GB4	RLAKNCMSWRYSCT	126 – 139	0.752	-	14	0.7113	93
<b>GB5</b>	<b>SCTRYTNFLDITKGRLL*</b>	137 – 152	-	1.000	16	<b>0.9980</b>	93
GB6	RWRSPVIVEKGGKVEV	154 – 169	-	1.000	16	0.5688	80
GB7	SPVIVEKGGKVEVGGH	157 – 172	0.996	-	16	0.6480	0
GB8	PVIVEKGGKVEVGG	158 – 171	-	1.000	14	0.5844	0

<sup>‡</sup> Partial sequence of predicted epitope was shown to be immunogenic in previous studies (52, 53)

▲ The epitopes selected for antibody testing in mice

\* The epitope with the highest VaxiJen antigenicity score

*Table 11. Potential linear B-cell epitopes predicted from NP of HP/MYANMAR/2303AM/2011 PRRSV with BCPred and APP score (>0.75) and VaxiJen antigenicity score (>0.5)*

ID	Epitope	Position	BCPred Score	APP Score	Length	VaxiJen Antigenicity Score	Conservancy (%) within 15 HP-PRRSVs
NB1	GKQQKRRKKGGNGQPVNQ	6 – 19	-	1.000	14	0.5553	0
NB2	KQQKRRKKGGNGQPVN	7 – 20	0.998	-	14	0.8325	0
NB3	KQQKRRKKGGNGQPVNQL	7 – 22	0.995	-	16	0.6078	0
NB4	KRKKGGNGQPVNQLC	10 – 23	-	1.000	14	0.6414	0
NB5	QQNQRSRGKPGGKKN	32 – 46	-	1.000	14	0.6927	86
<b>NB6</b>	<b>SRGKGPGKKNRKKNPE *</b>	35 – 50	0.999	-	16	<b>1.0428</b>	71
NB7	QSRGKPGGKKNRKK	36 – 49	-	1.000	14	0.9075	76
NB8	RKKNPEKPHFLATED	46 – 61	0.920	-	16	0.5131	71

\* The epitope with the highest VaxiJen antigenicity score



### 4.3.3. Prediction of T-cell epitopes

#### 4.3.3.1. Prediction of MHC I binding T-cell epitopes

MHC I binding T-cell epitopes from three proteins of HP/MYANMAR/2303/2011 Myanmar PRRSV were predicted by using two bioinformatics tools from IEDB-AR. MHC I processing prediction server generates an overall total score for each epitope according to their combined efficiency of proteasomal cleavage, TAP transport, and MHC-I binding. This score represents the potentiality of the peptides for presentation, and the higher the score, the better they are. Six epitopes from Nsp2-HVII, 11 epitopes from GP5 and 2 epitopes from NP had been the selected based on the total score of above zero.

By using IEDB MHC I binding prediction server with NetMHCpan2.0 method, the  $IC_{50}$  of previously selected epitopes were predicted on 45 SLA MHC I alleles. To ensure the high affinity binding to specific MHC I alleles, the epitope with  $IC_{50}$  less than 250 nM were selected. Five epitopes from Nsp2-HVII, 10 epitopes from GP5 and 2 epitopes from NP were selected as potential MHC I binding T-cell epitopes. The prediction of MHC I binding T-cell epitopes was summarized in **Figure 22**. The selected epitopes from all three proteins were shown in **Table 12, 13** and **14**.

Notably, the epitope S1T4 was in one amino acid deletion region of HP-PRRSV when compared to NA prototype, VR-2332. The epitopes in transmembrane domains were less accessible for the immune responses. The G1T4, G1T5, G1T6, and G1T7 were in TMI and TMII domains of GP5 and they had less probability for a vaccine candidate. Since epitope recognized by the higher number of MHC alleles possess the higher potentiality to initiate a strong immune response, the selected epitopes from each respective protein regions, which had an affinity for the highest number of SLA MHC II alleles were filtered. The S1T5 (*LSASSQTEY*) from Nsp2-HV-II binds five SLA MHC I alleles, and N1T2 (*LSDSGRISY*) from NP possessed an affinity for nine SLA MHC I alleles as seen in **Table 12 and 14**. However, G1T6 (*ATVSTAGYY*) from GP5 showed an affinity for 8 SLA MHC I alleles but it is in the transmembrane region (TMIII). Therefore, G1T2 (*GTDWLAQKF*) which binds to 4 alleles, was selected for GP5 (**Table 13**).

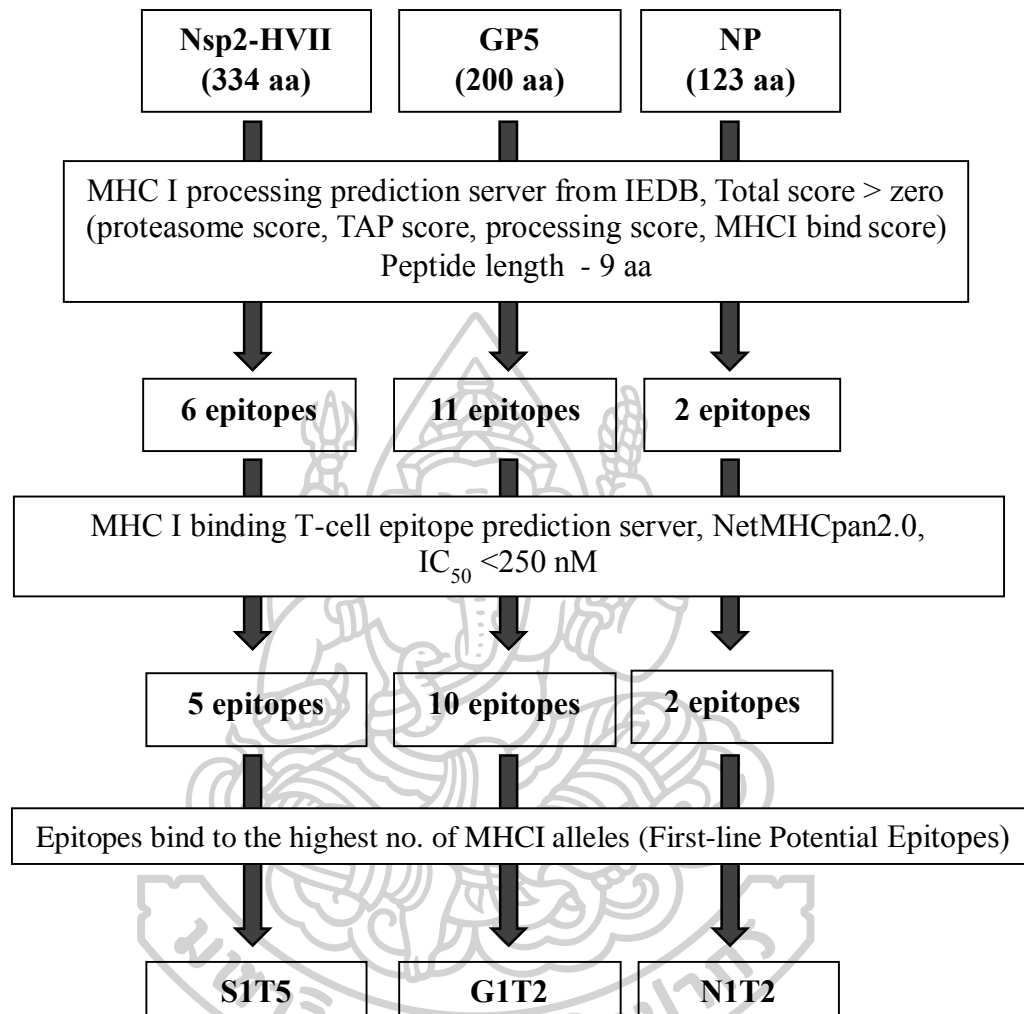


*Figure 22. The diagram summarizing MHC I binding T-cell epitope prediction*

**Table 12. Potential MHC I binding T-cell epitopes from Nsp2-HVII of HP/MYANMAR/2303AM/2011 PRRSV with total processing score and IC<sub>50</sub> for specific SLA MHC I alleles**

ID	Epitope (nonamer)	Position	Total score		MHCI Alleles	IC <sub>50</sub>	Conservancy (%) within 15 HP-PRRSVs
			(proteasome score, TAP score, processing score, MHC I bind score)				
SIT1	TSFDWNVVF	284 – 292	0.46		SLA-2*1002	162.5	0
SIT2	TAFSLSNCY	330 – 338	1.05		SLA-1-LWH	42.6	93
			1.22		SLA-1*0701	38.7	
			1.22		SLA-1*0702	38.7	
			1.08		SLA-1-LWH	53.6	
SIT3	AFSLSNCY	331 – 339	0.32		SLA-2*0102	214.4	93
SIT4	ETVGCPLNF <sup>del1</sup>	480 – 489	0.05		SLA-1-LWH	179.9	0
SIT5	LSASSQTEY*	573 – 581	0.27		SLA-2*1002	186.2	67
			0.24		SLA-1*0401	201.1	
			0.24		SLA-1-YDL01	201.1	
			0.24		SLA-2-YDL02	201.1	
			0.96		SLA-1-LWH	37.6	

\* The epitope bind to the highest number of SLA MHC I alleles

<sup>del1</sup> The epitope in one amino acid deletion region of HP-PRRSV when compared with VR-2332

**Table 13. Potential MHC I binding T-cell epitopes from GP5 of HP/MYANMAR/2303AM/2011 PRRSV with total processing score and IC<sub>50</sub> for specific SLA MHC I alleles**

ID	Epitope (nonamer)	Position	Total score		MHCI Alleles	IC <sub>50</sub>	Conservancy (%) within 15 HP-PRRSVs
			(proteasome score, TAP score, processing score, MHC I bind score)				
GIT1	NSSHIQLIY	35 – 43	0.6	174.6	SLA-2*1002	87	
			0.52	213.2	SLA-1*0701		
			1.07	58.9	SLA-1-LWH		
			0.49	62.9	SLA-1*0401	53	
			0.49	62.9	SLA-1-YDL01		
GIT2	GTDWLAQKF	52 – 60	0.49	62.9	SLA-2-YDL02		
			0.02	184	SLA-2*1002		
			0.34	222.8	SLA-1-YTH	67	
			0.44	178.9	SLA-1*1301		
			0.35	96	SLA-1-LWH	100	
GIT3	KFDWAVETF	59 – 67	0.4	182.3	SLA-1*0701	93	
			0.98	48.1	SLA-1-LWH		
GIT4	YGALTTSHF <sup>#</sup>	79 – 87	0.29	236	SLA-2*1002		
GIT5	LATVSTAGY <sup>#</sup>	93 – 101					

<sup>#</sup>The epitope contains in the transmembrane region

**Table 13. Potential MHC I binding T-cell epitopes from GP5 of HP/MYANMAR/2303AM/2011 PRRSV with total processing score and IC<sub>50</sub> for specific SLA MHC I alleles (Continued.)**

ID	Epitope (nonamer)	Position	Total score		MHC I Alleles	IC <sub>50</sub>	Conservancy (%) within 15 HP-PRRSVs
			(proteasome score, TAP score, processing score, MHC I bind score)				
GIT6	ATVSTAGYY**	94 – 102	0.36		SLA-1*0201	135.5	93
			0.36		SLA-1*0202	135.5	
			0.45		SLA-1*0401	109.9	
			0.49		SLA-1*0801	101.9	
			0.89		SLA-1-LWH	40.2	
			0.45		SLA-1-YDL01	109.9	
			0.45		SLA-2-YDL02	109.9	
			0.69		SLA-2*I002	63.9	
GIT7	TAGYYHGGRY #	98 – 106	0.15		SLA-1-LWH	216.7	67
GIT8	MSWRYSCTR	132 – 140	0.04		SLA-2*0102	123.9	93
GIT9	YAVCALAAL	112 – 120	0.03		SLA-1-TPK	47.6	93
GIT10	LLDTKGRLY	145 – 153	0.7		SLA-1*0401	58.9	100

# The epitope included in the transmembrane region

\*The epitope binds to the highest number of SLA MHC I alleles

**Table 14. Potential MHC I binding T-cell epitopes from NP of HP/MYANMAR/2303AM/2011 PRRSV with total processing score and IC<sub>50</sub> for specific SLA MHC I alleles**

ID	Epitope (nonamer)	Position	Total score			MHCI Alleles	IC <sub>50</sub>	Conservancy (%) within 15 HP-PRRSVs
			(proteasome score, TAP score, processing score, MHC I bind score)					
NIT1	CLSSIQTAF	75 – 83	0.18	SLA-2*1002	206.5	100		
			0.56	SLA-1*0801	87.0			
NIT2	LSDSGRISY*	92 – 100	0.23	SLA-1*0201	234.2	100		
			0.23	SLA-1*0202	234.2			
			1.00	SLA-1*0401	39.8			
			0.20	SLA-1*0701	246.5			
			0.20	SLA-1*0702	246.5			
			0.66	SLA-1-LWH	86.3			
		1.00	SLA-1-YDL01	39.8				
		1.00	SLA-2-YDL02	39.8				
		0.43	SLA-2*1002	146.3				

\*The epitope binds to the highest number of SLA MHC I alleles



#### 4.3.3.2. Prediction of MHC II binding T-cell epitopes

Hence, prediction of epitopes binding to MHC class II molecules was performed for human MHC II alleles such as HLA-DR, HLA-DP, HLA-DQ alleles. MHC II binding T-cell epitopes prediction tools from IEDB was used for each protein and NetMHCIIpan method was utilized to calculate IC<sub>50</sub> for MHC II alleles. The MHC II binding T-cell epitope prediction is summarized in **Figure 23**.

Total of 69, 95, and 27 epitopes from Nsp2-HVII, GP5, and NP, respectively, were selected according to IC<sub>50</sub> (less than 250nM) at specific HLA MHC II alleles. The antigenicity of the selected epitopes were analyzed by VaxiJen v2.0 antigenicity prediction tool at 0.5 threshold. Based on antigenicity score, 38, 48, and 11 epitopes from Nsp2-HVII, GP5, and NP, respectively, were selected as potential vaccine candidates. The predicted epitopes are shown in **Table 15, 16** and **17**.

As shown in **Table 16**, 17 out of 48 epitopes from GP5 spanned within TM domains and they were less likely to be good vaccine candidates. It had been estimated that epitope recognized by the higher number of MHC alleles possess a higher potentiality to induce a strong immune response. The epitope S2T32 (*YKAFPLAPS*) from Nsp2-HV-II, G2T39 (*FLLDTKGRL*) from GP5, and N2T10 (*LIRATASPS*) from NP had an affinity for the highest number of HLA MHC II alleles of 11, 11, and 10 alleles, respectively, and were considered as the first-line potential MHC II binding T-cell epitopes.

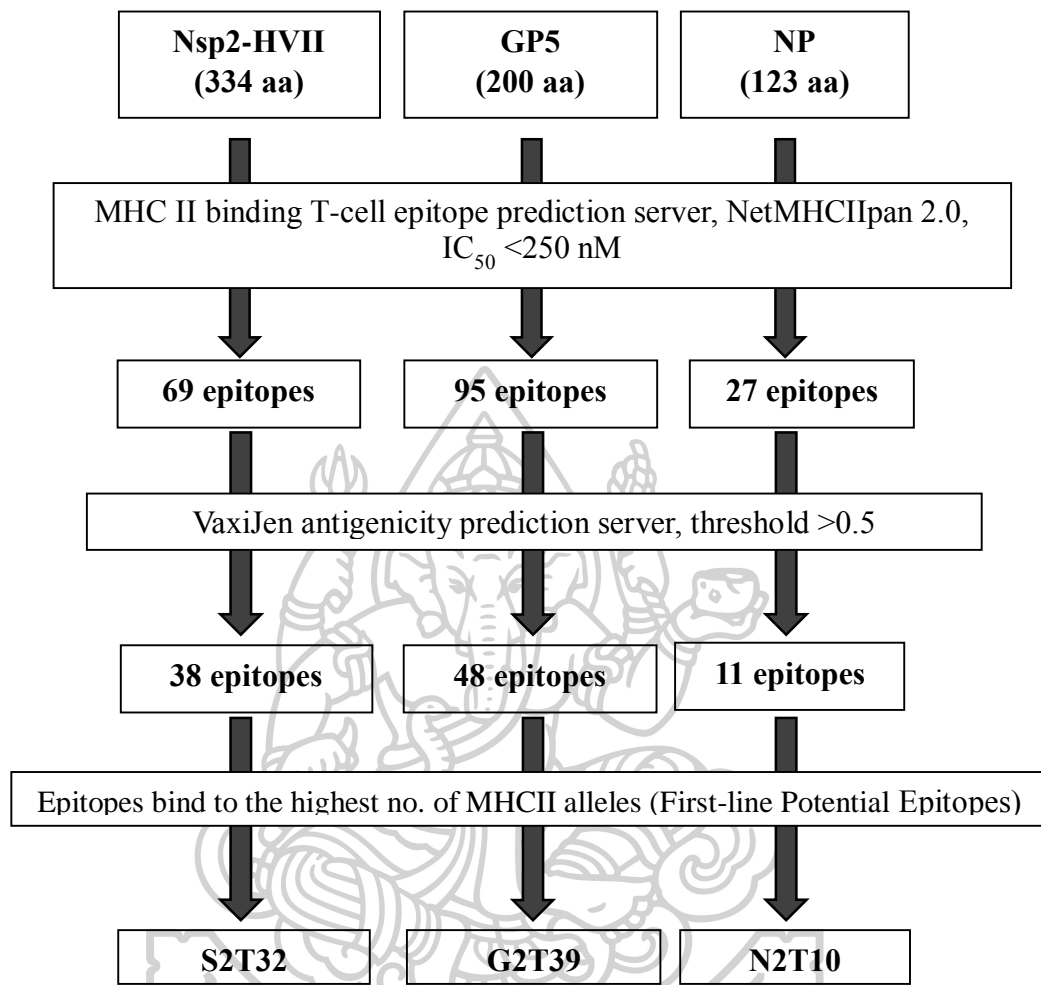


*Figure 23. The diagram summarizing MHC II binding T-cell epitope prediction*

**Table 15. Potential MHC II binding T-cell epitopes from Nsp2-HVII of HP/MYANMAR/2303AM/2011 PRRSV with IC<sub>50</sub> <250 nM and VaxiJen antigenicity score > 0.5**

ID	Core Peptide	Position	MHC II Alleles	VaxiJen Antigenicity Score	Conservancy (%) within 15 HP-PRRSVs
S2T1	LAKLERVSP	270 – 278	HLA-DRB1*12:01	1.117	87
S2T2	LERVSPPGA	273 – 281	HLA-DRB1*01:01	0.9232	47
S2T3	ERVSPPGA	274 – 282	HLA-DQA1*05:01/DQB1*03:01	0.9133	47
S2T4	NVVFPGVEA	289 – 297	HLA-DRB1*01:01	0.5838	0
S2T5	VVFPGVEAA	290 – 298	HLA-DQA1*05:01/DQB1*03:01	0.8442	0
S2T6	VFPGVEAAN	291 – 299	HLA-DQA1*05:01/DQB1*03:01	1.0084	0
S2T7	FPGVEAANQ	292 – 300	HLA-DQA1*05:01/DQB1*03:01	0.9919	0
S2T8	PGVEAANQT	293 – 301	HLA-DQA1*05:01/DQB1*03:01	1.2788	60
S2T9	SVPLTAFSL	326 – 334	HLA-DRB1*01:01	0.6921	100
S2T10	SVLSKLEEV	354 – 362	HLA-DPA1*02:01/DPB1*01:01	0.602	73
S2T11	VLEEYGLMS	363 – 371	HLA-DPA1*02:01/DPB1*14:01 HLA-DRB1*01:01 HLA-DRB1*12:01	0.5862	80
S2T12	YGLMSTGLG	367 – 375	HLA-DPA1*02:01/DPB1*01:01	1.0396	87
S2T13	GLMSTGLGP	368 – 376	HLA-DPA1*02:01/DPB1*14:01	1.2054	80
S2T14	LMSTGLGPR	369 – 377	HLA-DRB1*12:01	1.7718	80
S2T15	MSTGLGPRP	370 – 378	HLA-DQA1*05:01/DQB1*03:01	1.7870	80
S2T16	STGLGPRPV	371 – 379	HLA-DQA1*05:01/DQB1*03:01	1.8855	80
S2T17	GLGPRPVLP	373 – 381	HLA-DQA1*05:01/DQB1*03:01	0.8507	80

**Table 15. Potential MHC II binding T-cell epitopes from Nsp2-HVII of HP/MYANMAR/2303AM/2011 PRRSV with  $IC_{50} < 250$  nM and VaxiJen antigenicity score  $> 0.5$  (Continued.)**

ID	Core Peptide	Position	MHC II Alleles	VaxiJen Antigenicity Score	Conservancy (%) within 15 HP-PRRSVs
S2T18	LLKLANTQA	395 – 403	HLA-DRB1*01:01 HLA-DRB1*04:01 HLA-DRB1*04:05 HLA-DRB1*12:01	0.9662	80
S2T19	LKLANTQAT	396 – 404	HLA-DRB1*01:01 HLA-DRB1*04:01 HLA-DQA1*01:02/DQB1*06:02 HLA-DPA1*02:01/DPB1*14:01 HLA-DQA1*05:01/DQB1*03:01	0.7453	80
S2T20	LANTQATSE	398 – 406	HLA-DPA1*02:01/DPB1*14:01	0.6349	80
S2T21	ATSEMMARA	403 – 411	HLA-DQA1*01:02/DQB1*06:02 HLA-DQA1*05:01/DQB1*03:01	0.5044	33
S2T22	TSEMMARAA	404 – 412	HLA-DQA1*05:01/DQB1*03:01	0.5036	33
S2T23	EMMARAAEQ	406 – 414	HLA-DQA1*03:01/DQB1*03:02 HLA-DQA1*01:02/DQB1*06:02	0.5106	33
S2T24	MARAAEQVD	408 – 416	HLA-DQA1*05:01/DQB1*02:01	0.9578	33
S2T25	WVKSYPRWA	420 – 428	HLA-DRB1*01:01 HLA-DRB1*09:01 HLA-DRB1*11:01 HLA-DRB1*15:01 HLA-DRB5*01:01	0.7008	13
S2T26	VKSYPRWAP	421 – 429	HLA-DRB1*12:01	0.9574	13
S2T27	DCGSPVLMG	463 – 471	HLA-DQA1*05:01/DQB1*03:01	0.5667	53

**Table 15. Potential MHC II binding T-cell epitopes from Nsp2-HVII of HP/MYANMAR/2303AM/2011 PRRSV with  $IC_{50} < 250$  nM and VaxiJen antigenicity score  $> 0.5$  (Continued.)**

ID	Core Peptide	Position	MHC II Alleles	VaxiJen Antigenicity Score	Conservancy (%) within 15 HP-PRRSVs
S2T28	SEPVLPAS	500 – 508	HLA-DQA1*05:01/DQB1*03:01	0.5226	47
S2T29	PLIGLAPVP	517 – 525	HLA-DQA1*05:01/DQB1*03:01	1.1432	0
S2T30	LIGLAPVPA	518 – 526	HLA-DRB1*09:01	1.4978	0
			HLA-DRB1*01:01		
			HLA-DRB1*04:01		
			HLA-DRB1*04:05		
			HLA-DRB1*12:01		
			HLA-DPA1*02:01/DPB1*14:01		
			HLA-DQA1*05:01/DQB1*03:01		
S2T31	LAPVPAPRR	521 – 529	HLA-DRB1*01:01, HLA-DRB1*09:01	0.615	0
			HLA-DRB1*11:01		
			HLA-DRB1*12:01		
			HLA-DRB5*01:01		
S2T32	YKAFFLAPS*	581 – 589	HLA-DRB1*01:01	1.2816	33
			HLA-DRB1*04:01		
			HLA-DRB1*04:05		
			HLA-DRB1*07:01		
			HLA-DRB1*09:01		
			HLA-DRB1*11:01		
			HLA-DRB1*12:01		
			HLA-DRB1*15:01		
			HLA-DRB5*01:01		
			HLA-DQA1*05:01/DQB1*03:01		
			HLA-DPA1*02:01/DPB1*14:01		

**Table 15. Potential MHC II binding T-cell epitopes from Nsp2-HVII of HP/MYANMAR/2303AM/2011 PRRSV with  $IC_{50} < 250$  nM and VaxiJen antigenicity score  $> 0.5$  (Continued.)**

ID	Core Peptide	Position	MHC II Alleles	VaxiJen Antigenicity Score	Conservancy (%) within 15 HP-PRRSVs
S2T33	FPLAPSQNM	584 – 592	HLA-DRB1*01:01 HLA-DRB1*07:01	0.8244	80
S2T34	SQNMGILEA	589 – 597	HLA-DPA1*02:01/DPB1*14:01 HLA-DQA1*01:02/DQB1*06:02	0.9490	80
S2T35	ILEAGGQEA	594 – 602	HLA-DQA1*05:01/DQB1*03:01	0.6784	40
S2T36	AGGQEAEEV	597 – 605	HLA-DQA1*05:01/DQB1*03:01 HLA-DQA1*03:01/DQB1*03:02 HLA-DQA1*04:01/DQB1*04:02	1.0172	40
S2T37	EAGGQEAEE	596 – 604	HLA-DQA1*03:01/DQB1*03:02	0.8478	40
S2T38	TNPAPMSSS	616 – 625	HLA-DQA1*05:01/DQB1*03:01	1.1412	0

\*The epitope binds to the highest number of HLA MHC II alleles



**Table 16. Potential MHC II binding T-cell epitopes from GP5 of HP/MYANMAR/2303AM/2011 PRRSV with  $IC_{50} < 250$  nM and VaxiJen antigenicity score  $> 0.5$**

ID	Core Peptide	Position	MHC II Alleles	VaxiJen Antigenicity Score	Conservancy (%) within 15 HP-PRRSVs
G2T1	LFLWCIVPF	15 – 23	HLA-DPA1*02:01/DPB1*01:01	0.7604	80
			HLA-DPA1*01:03/DPB1*02:01		
			HLA-DPA1*01:03/DPB1*04:01		
			HLA-DPA1*03:01/DPB1*04:02		
			HLA-DPA1*02:01/DPB1*14:01		
G2T2	LWCIVPFYL	17 – 27	HLA-DRB1*01:01	1.5679	93
			HLA-DRB1*12:01		
G2T3	WCIVPFYLA	18 – 26	HLA-DPA1*01:03/DPB1*02:01	1.0778	93
			HLA-DPA1*01:03/DPB1*04:01		
			HLA-DPA1*02:01/DPB1*14:01		
G2T4	CIVPFYLAV	19 – 27	HLA-DPA1*02:01/DPB1*01:01	0.9174	93
			HLA-DPA1*01:03/DPB1*02:01		
			HLA-DPA1*01:03/DPB1*04:01		
			HLA-DPA1*03:01/DPB1*04:02		
			HLA-DPA1*02:01/DPB1*14:01		
G2T5	IVPFYLAVL	20 – 28	HLA-DPA1*02:01/DPB1*14:01	0.8802	93
G2T6	HIQLIYNLT	38 – 46	HLA-DRB1*12:01	0.6565	87
			HLA-DRB1*01:01		
G2T7	IYNLTLCLEL	42 – 50	HLA-DRB1*12:01	0.6573	100
			HLA-DPA1*02:01/DPB1*14:01		
			HLA-DPA1*02:01/DPB1*01:01		
			HLA-DPA1*03:01/DPB1*04:02		
			HLA-DPA1*02:01/DPB1*14:01		

**Table 16. Potential MHC II binding T-cell epitopes from GP5 of HP/MYANMAR/2303AM/2011 PRRSV with  $IC_{50} < 250$  nM and VaxiJen antigenicity score  $> 0.5$  (Continued.)**

No.	Core Peptide	Position	MHC II Alleles	VaxiJen Antigenicity Score	Conservancy (%) within 15 HP-PRRSVs
G2T8	YNLTLCELN	43 – 51	HLA-DPA1*02:01/DPB1*01:01 HLA-DPA1*01:03/DPB1*02:01 HLA-DPA1*01:03/DPB1*04:01 HLA-DPA1*03:01/DPB1*04:02 HLA-DPA1*02:01/DPB1*14:01 HLA-DPA1*02:01/DPB1*14:01 HLA-DQA1*01:01/DQB1*05:01 HLA-DPA1*02:01/DPB1*01:01 HLA-DPA1*01:03/DPB1*02:01 HLA-DPA1*01:03/DPB1*04:01 HLA-DQA1*03:01/DPB1*04:02 HLA-DQA1*05:01/DQB1*03:01	0.8128	100
G2T9	WLAQKFDWA	55 – 63		1.7446	53
G2T10	AQKFDWAVE	57 – 65		1.5892	53
G2T11	VIFPVLTHI <sup>#</sup>	68 – 76		0.5187	100
G2T12	HIVSYGALT <sup>#</sup>	75 – 83		0.8224	
G2T13	IVSYGALTT <sup>#</sup>	76 – 84		1.2431	100
G2T14	VSYGALTT <sup>#</sup>	77 – 85	HLA-DPA1*02:01/DPB1*14:01 HLA-DQA1*05:01/DQB1*03:01 HLA-DPA1*02:01/DPB1*14:01 HLA-DQA1*05:01/DQB1*03:01	0.9108	100
G2T15	SYGALTTSH <sup>#</sup>	78 – 86	HLA-DQA1*05:01/DQB1*03:01 HLA-DRB1*01:01, HLA-DRB1*04:01 HLA-DRB1*04:05, HLA-DRB1*07:01 HLA-DRB1*09:01, HLA-DRB1*11:01 HLA-DRB1*12:01, HLA-DRB1*15:01 HLA-DRB5*01:01	0.9326 0.9313	100 100
G2T16	YGALTTSHF <sup>#</sup>	79 – 87		0.9313	100

**Table 16. Potential MHC II binding T-cell epitopes from GP5 of HP/MYANMAR/2303AM/2011 PRRSV with  $IC_{50} < 250$  nM and VaxiJen antigenicity score  $> 0.5$  (Continued.)**

No.	Core Peptide	Position	MHC II Alleles	VaxiJen Antigenicity Score	Conservancy (%) within 15 HP-PRRSVs
G2T17	GALTTSHFL <sup>#</sup>	80 – 88	HLA-DPA1*02:01/DPB1*14:01	0.6305	100
G2T18	LTTSHFLDT <sup>#</sup>	82 – 90	HLA-DPA1*02:01/DPB1*01:01 HLA-DPA1*01:03/DPB1*02:01 HLA-DPA1*01:03/DPB1*04:01 HLA-DPA1*03:01/DPB1*04:02 HLA-DPA1*02:01/DPB1*14:01	0.6097	100
G2T19	SHFLDVTGL <sup>#</sup>	85 – 93	HLA-DRB1*01:01	0.6615	93
G2T20	DTVGLATVS <sup>#</sup>	89 – 97	HLA-DQA1*05:01/DQB1*03:01	1.1540	93
G2T21	TVGLATVST <sup>#</sup>	90 – 98	HLA-DRB1*01:01	1.1728	93
G2T22	VGLATVSTA <sup>#</sup>	91 – 99	HLA-DQA1*05:01/DQB1*03:01 HLA-DQA1*01:02/DQB1*06:02	0.8234	93
G2T23	GLATVSTAG <sup>#</sup>	92 – 100	HLA-DQA1*05:01/DQB1*03:01	0.5675	93
G2T24	ATVSTAGYY <sup>#</sup>	94 – 102	HLA-DQA1*05:01/DQB1*03:01	0.5038	93
G2T25	IYAVCALAA <sup>#</sup>	111 – 119	HLA-DRB1*01:01 HLA-DRB1*04:05 HLA-DRB1*07:01 HLA-DRB1*12:01 HLA-DRB1*15:01	0.5948	93
G2T26	YAVCALAAL <sup>#</sup>	112 – 120	HLA-DQA1*05:01/DQB1*03:01 HLA-DQA1*01:02/DQB1*06:02		
G2T27	CALAALICF <sup>#</sup>	115 – 123	HLA-DPA1*02:01/DPB1*14:01 HLA-DPA1*02:01/DPB1*14:01	0.6016 0.7960	93 80
G2T28	LICFVIRLA	120 – 128	HLA-DRB1*12:01	1.7938	80

**Table 16. Potential MHC II binding T-cell epitopes from GP5 of HP/MYANMAR/2303AM/2011 PRRSV with  $IC_{50} < 250$  nM and VaxiJen antigenicity score  $> 0.5$  (Continued.)**

No.	Core Peptide	Position	MHC II Alleles	VaxiJen Antigenicity Score	Conservancy (%) within 15 HP-PRRSVs
G2T29	ICFVIRLAK	121 – 129	HLA-DRB1*08:02 HLA-DRB1*11:01 HLA-DRB1*12:01 HLA-DRB1*15:01	0.7179	80
G2T30	FVIRLAKNC	123 – 131	HLA-DRB1*01:01 HLA-DPA1*02:01/DPB1*01:01 HLA-DPA1*03:01/DPB1*04:02 HLA-DPA1*02:01/DPB1*14:01	0.6772	87
G2T31	VIRLAKNCM	124 – 133	HLA-DRB1*12:01	0.8839	100
G2T32	AKNCMSWRY	128 – 136	HLA-DRB5*01:01	0.7072	100
G2T33	NCMSWRYSC	130 – 138	HLA-DRB1*12:01	2.1531	93
G2T34	RYSCTRYTN	135 – 143	HLA-DRB1*11:01	0.8514	93
G2T35	YSCTRYTNF	136 – 144	HLA-DRB1*07:01 HLA-DRB5*01:01 HLA-DPA1*02:01/DPB1*01:01 HLA-DPA1*01:03/DPB1*02:01 HLA-DPA1*01:03/DPB1*04:01 HLA-DPA1*03:01/DPB1*04:02 HLA-DPA1*02:01/DPB1*05:01 HLA-DPA1*02:01/DPB1*14:01	1.4115	93
G2T36	CTRYTNFLL	138 – 146	HLA-DRB1*12:01 HLA-DRB1*15:01	1.2753	100
G2T37	YTNFLDGTK	141 – 149	HLA-DRB5*01:01	1.0584	100

**Table 16. Potential MHC II binding T-cell epitopes from GP5 of HP/MYANMAR/2303AM/2011 PRRSV with  $IC_{50} < 250$  nM and VaxiJen antigenicity score  $> 0.5$  (Continued.)**

Core Peptide	Position	MHC II Alleles	VaxiJen Antigenicity Score	Conservancy (%) within 15 HP-PRRSVs
G2T38 TRYTNFLLD	139 – 147	HLA-DPA1*02:01/DPB1*01:01 HLA-DPA1*01:03/DPB1*02:01 HLA-DPA1*01:03/DPB1*04:01	1.0159	100
G2T39 FLDDTKGRL*	144 – 152	HLA-DRB1*01:01 HLA-DRB1*03:01 HLA-DRB1*11:01 HLA-DRB1*12:01 HLA-DRB1*13:02 HLA-DRB1*15:01 HLA-DRB3*01:01 HLA-DRB3*02:02 HLA-DRB4*01:01 HLA-DRB5*01:01 HLA-DPA1*02:01/DPB1*14:01	0.9062	100
G2T40 LLDDTKGRLY	145 - 153	HLA-DRB1*01:01 HLA-DRB1*07:01 HLA-DPA1*02:01/DPB1*01:01 HLA-DPA1*01:03/DPB1*02:01 HLA-DPA1*01:03/DPB1*04:01 HLA-DPA1*02:01/DPB1*14:01	0.5566	100
G2T41 LYRWRSPI	152 – 160	HLA-DRB1*01:01, HLA-DRB1*04:05 HLA-DRB1*07:01, HLA-DRB1*12:01 HLA-DRB1*15:01, HLA-DRB5*01:01	0.5946	100

**Table 16. Potential MHC II binding T-cell epitopes from GP5 of HP/MYANMAR/2303AM/2011 PRRSV with  $IC_{50} < 250$  nM and VaxiJen antigenicity score  $> 0.5$  (Continued.)**

No.	Core Peptide	Position	MHC II Alleles	VaxiJen Antigenicity Score	Conservancy (%) within 15 HP-PRRSVs
G2T42	YRWRSPIV	153 – 161	HLA-DRB1*01:01 HLA-DRB1*07:01 HLA-DRB1*09:01 HLA-DRB3*02:02 HLA-DRB5*01:01 HLA-DPA1*02:01/DPB1*14:01	0.6094	93
G2T43	VIVEKGGKV	159 – 167	HLA-DRB1*12:01	0.6865	80
G2T44	EKGKVEVG	163 – 171	HLA-DQA1*05:01/DQB1*03:01	0.7122	7
G2T45	HLIDLKRVV	172 – 180	HLA-DRB1*12:01	1.1426	100
G2T46	LIDLKRVVL	173 – 181	HLA-DRB1*12:01 HLA-DPA1*02:01/DPB1*14:01	1.0981	100
G2T47	SAATPLTRV	184 – 192	HLA-DQA1*05:01/DQB1*03:01 HLA-DQA1*01:02/DQB1*06:02	0.6054	80
G2T48	YRWRSPIV	153 – 161	HLA-DRB1*01:01 HLA-DRB1*07:01 HLA-DRB1*09:01 HLA-DRB3*02:02 HLA-DRB5*01:01	0.6094	93

\*The epitope binds to the highest number of HLA MHC II alleles

# The epitope contains in transmembrane regions



**Table 17. Potential MHC II binding T-cell epitopes from NP of HP/MYANMAR/2303AM/2011 PRRSV with  $IC_{50} < 250$  nM and VaxiJen antigenicity score  $> 0.5$**

ID	Core Peptide	Position	MHC II Alleles	VaxiJen Antigenicity Score	Conservancy (%) within 15 HP-PRRSVs
N2T1	VNQLCQMLG	19 – 27	HLA-DRB1*12:01 HLA-DRB4*01:01	0.5232	100
N2T2	LCQMLGKII	22 – 30	HLA-DRB1*01:01 HLA-DRB1*11:01 HLA-DRB1*12:01 HLA-DRB1*15:01 HLA-DRB4*01:01 HLA-DRB5*01:01 HLA-DPA1*02:01/DPB1*14:01	0.8545	100
N2T3	QLCLSSIQT	73 – 81	HLA-DRB1*01:01	1.0648	100
N2T4	LCLSSIQTA	74 – 82	HLA-DRB1*12:01 HLA-DRB4*01:01 HLA-DQA1*01:02/DQB1*06:02 HLA-DPA1*02:01/DPB1*01:01	0.8559	100
N2T5	FNQGAGTCT	83 – 91	HLA-DPA1*02:01/DPB1*14:01 HLA-DRB1*01:01	0.7458	21
N2T6	SDSGRISYT	93 – 101	HLA-DQA1*05:01/DQB1*03:01 HLA-DQA1*05:01/DQB1*03:01	1.2698	100

**Table 17. Potential MHC II binding T-cell epitopes from NP of HP/MYANMAR/2303AM/2011 PRRSV with  $IC_{50} < 250$  nM and VaxiJen antigenicity score  $> 0.5$  (Continued.)**

ID	Core Peptide	Position	MHC II Alleles	VaxiJen Antigenicity Score	Conservancy (%) within 15 HP-PRRSVs
N2T7	ISYTVFSL	99 – 107	HLA-DRB1*12:01	1.0184	100
N2T8	TVEFSLPTQ	101 – 109	HLA-DPA1*02:01/DPB1*14:01	0.6400	79
N2T9	VEFSLPTQH	102 – 110	HLA-DPA1*02:01/DPB1*14:01	0.5091	79
N2T10	LIRATASPS*	114 – 122	HLA-DRB1*12:01 HLA-DRB1*04:01 HLA-DRB1*04:05 HLA-DRB1*07:01 HLA-DRB1*08:02 HLA-DRB1*09:01 HLA-DRB1*13:02 HLA-DRB1*15:01 HLA-DRB3*02:02 HLA-DRB5*01:01	1.0075	86
N2T11	IRATASPSA	115 – 123	HLA-DQA1*05:01/DQB1*03:01 HLA-DQA1*05:01/DQB1*03:01	0.7968	86

\*The epitope bind to the highest number of HLA MHC II alleles

#### 4.3.4. Epitope Conservancy Prediction

Percentage conservancy of the predicted epitopes from Nsp2-HVII, GP5, and NP of HP/MYANMAR/2303/2011 PRRSV was determined using Epitopes Conservancy Analysis from IEDB. Because of high sequence identity, the selected epitopes had relatively higher percentage conservancy within six Myanmar PRRSVs.

The conservancy of each epitope within a set of 15 reference HP-PRRSV strains in Asia at 100% sequence identity threshold level are shown in **Table 9 - 17**. The first-line linear B-cell epitopes, GB5 of GP5 and NB6 of NP had the higher conservancy level of 93% and 71%, respectively, while SB3 of Nsp2-HVII had only 40%. Since, Nsp2-HVII is the highly variable regions, 10 predicted linear B-cell epitopes from Nsp2-HVII had no conservancy within 15 HP-PRRSV. Except GB1, GB2, GB7, and GB8, all predicted linear B-cell epitopes from GP5 had conservancy of above 50%. From NP, all predicted linear B-cell epitopes had conservancy within a range of 71- 86%, but 4 predicted linear B-cell epitopes, NB1, NB2, NB3, and NB4 had no conservancy within reference HP-PRRSVs.

The selected MHC I binding T-cell epitopes, S1T5 of Nsp2-HVII, G1T2 of GP5 and N1T2 of NP had 67%, 53% and 100% conservancy, respectively. All predicted MHC I binding T-cell epitopes from GP5 had conservancy within a range of 67-100%, while epitopes from NP had 100% conservancy. However, S1T1 and S1T4 of Nsp2-HVII had no conservancy within 15 HP-PRRSVs.

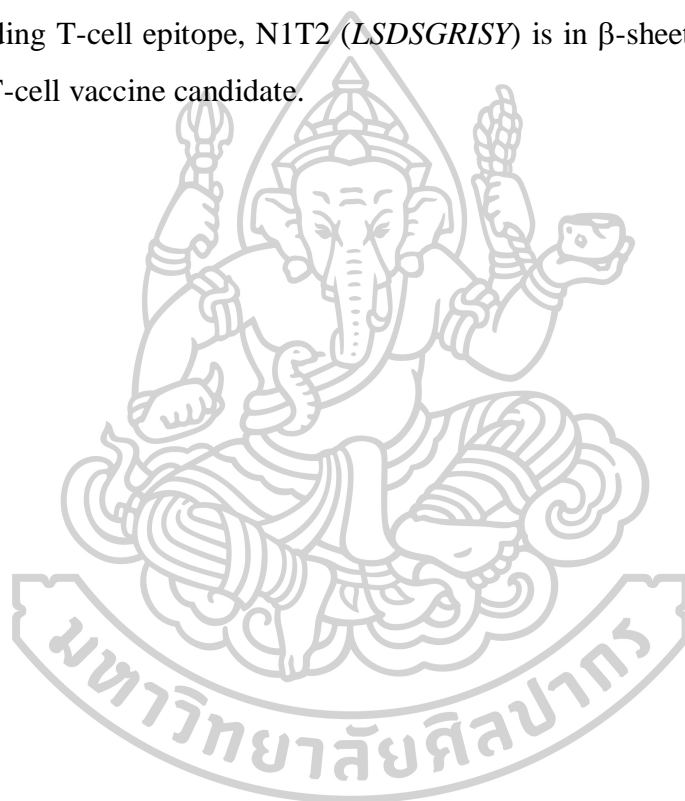
The selected MHC II binding T-cell epitopes, G2T39 of GP5 and N2T10 had 100% and 86% conservancy, respectively, but S2T39 of Nsp2-HVII had 33%. Eight predicted epitopes from Nsp2-HVII had no conservancy. All predicted MHC II binding T-cell epitopes were above 50% conservancy except G2T43 of GP5 and N2T5 of NP.

#### 4.3.5. Protein Model Prediction and Validation

Based on sequence identity, the top seven templates (out of 14 templates) were filtered for Nsp2-HVII, 2zfz.1.A, 2zfz.1.B, 4a4a.1.A, 2vcb.1.A, 1ptf.1.A, 1fu0.1.A and 1fu0.1.B. Of which, the model 2zfz.1.A and 2zfz.1.B had the highest sequence identity of 23% with low coverage of 0.09. Similarly for GP5, six templates were filtered out of 16 templates, 4m6t.1.A, 2v4.1.B, 2v4.1.C, 2v4.1.E, 2v4.1.L and 2v4.1.M. A

template 4m6t.1 had the highest sequence identities (17%) with low coverage. Therefore, they were not the best fit protein models for Nsp2-HVII and GP5 protein.

For NP, among the top 6 filtered models, the template 1p65.1A, had 97% sequence identity and had 3D structure in PDB (161). Moreover, the quality of the model template was determined as QMEAN z-score of 1.23 and Ramachandran plot showed residue in favored region was 99.1%. Therefore, the template 1p65.1A from PDB was good quality protein model, for NP of Myanmar PRRSVs (**Figure 24A, 24C**). As shown in **Figure 24B**, epitope mapping by Swiss.pdb software, showed that MHC I binding T-cell epitope, N1T2 (*LSDSGRISY*) is in  $\beta$ -sheet region and it might be a novel T-cell vaccine candidate.



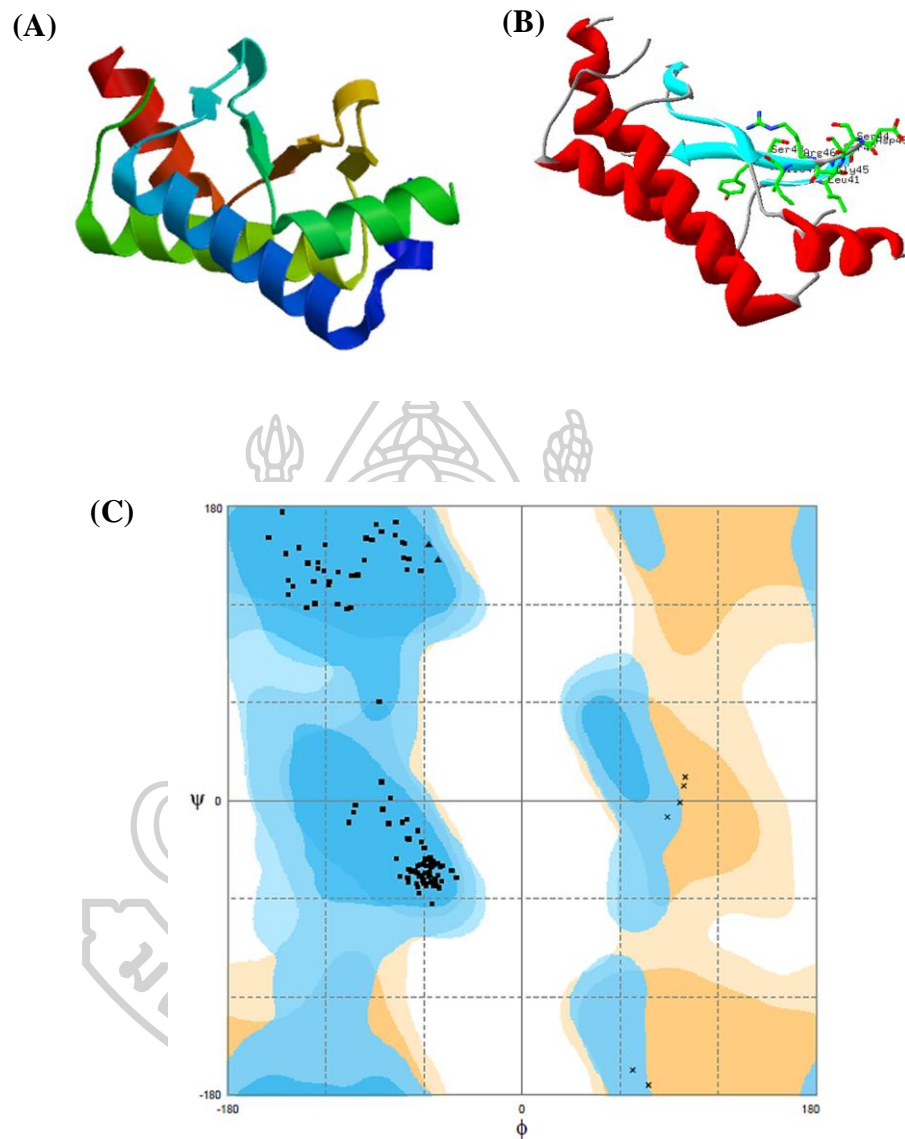


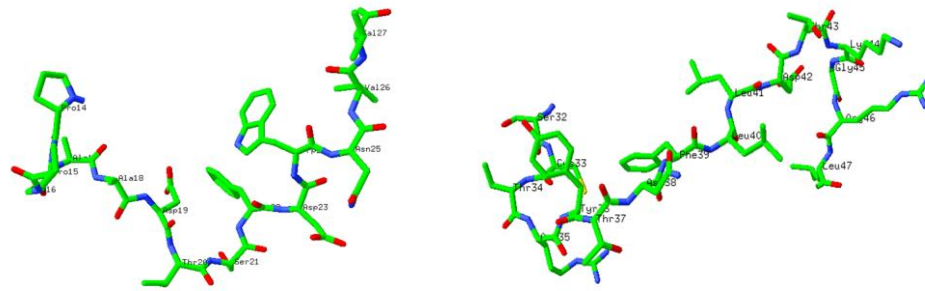
**Figure 24. (A) Modelled 3D structure of NP of Myanmar PRRSVs (B) 3D structure of NP, showing selected MHC I T-cell epitope, NIT2 (LSDSGRISY) in  $\beta$ -sheet region (C) Ramachandran plot of modelled structural template for NP showing 99.1% residues in favored region**

The 3D structures of the predicted first-line potential epitopes from Nsp2-HVII, GP5 and NP were designed by using PEP-FOLD3 server. The QMEAN z-score and residue percentage in favored region of Ramachandran plot of the selected model for individual epitope are summarized in **Table 18**. The model structure of epitopes are shown in **Figure 25**.

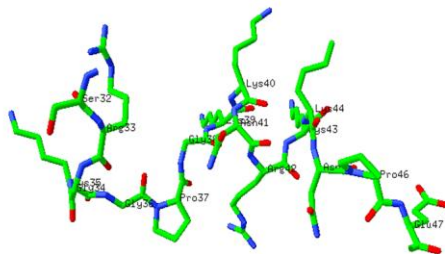
**Table 18. QMEAN z-score and residue percentage in favored region of Ramachandran plot of the selected model for individual epitope**

No.	Epitope	Quality of predicted model	
		QMEAN z-score	Percentage of residue in favored region of Ramachandran plot
<b>Nsp2-HVII</b>			
1.	Linear B-cell epitope SB3( <i>PPGAADTSFDWNVV</i> )	-1.02	87
2.	MHC I binding T-cell epitope S1T5 ( <i>LSASSQTEY</i> )	-2.62	81
3.	MHC II binding T-cell epitope S2T32 ( <i>YKAFPLAPS</i> )	-2.36	79
<b>GP5</b>			
1.	Linear B-cell epitope GB5 ( <i>SCTRYTNFLLDTKGRL</i> )	-1.65	81
2.	MHC I binding T-cell epitope G1T2 ( <i>GTDWLAQKF</i> )	-1.92	79
3.	MHC II binding T-cell epitope G2T39 ( <i>FLLDTKGRL</i> )	-1.65	81
<b>NP</b>			
1.	Linear B-cell epitope NB6 ( <i>SRGKGPGKKNRKNPE</i> )	0.24	100
2.	MHC I binding T-cell epitope N1T2 ( <i>LSDSGRISY</i> )	-0.79	89
3.	MHC II binding T-cell epitope N2T10 ( <i>LIRATASPS</i> )	-0.79	89

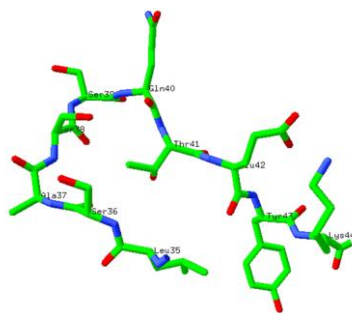




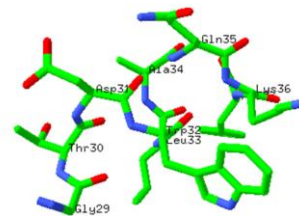
*PPGAADTSFDWNVV* (SB3 of Nsp2-HVII)    *SCTRYTNFLLDTKGR*L (GB5 of GP5)



*SRGKGP GKKNR KKNPE* (NB6 of NP)



*LSASSQTEY* (S1T5 of Nsp2-HVII)



*GTDWLAQKF* (G1T2 of GP5)

**Figure 25. Modelled peptide structure of predicted linear B-cell, MHC I and MHC II binding T-cell epitopes**

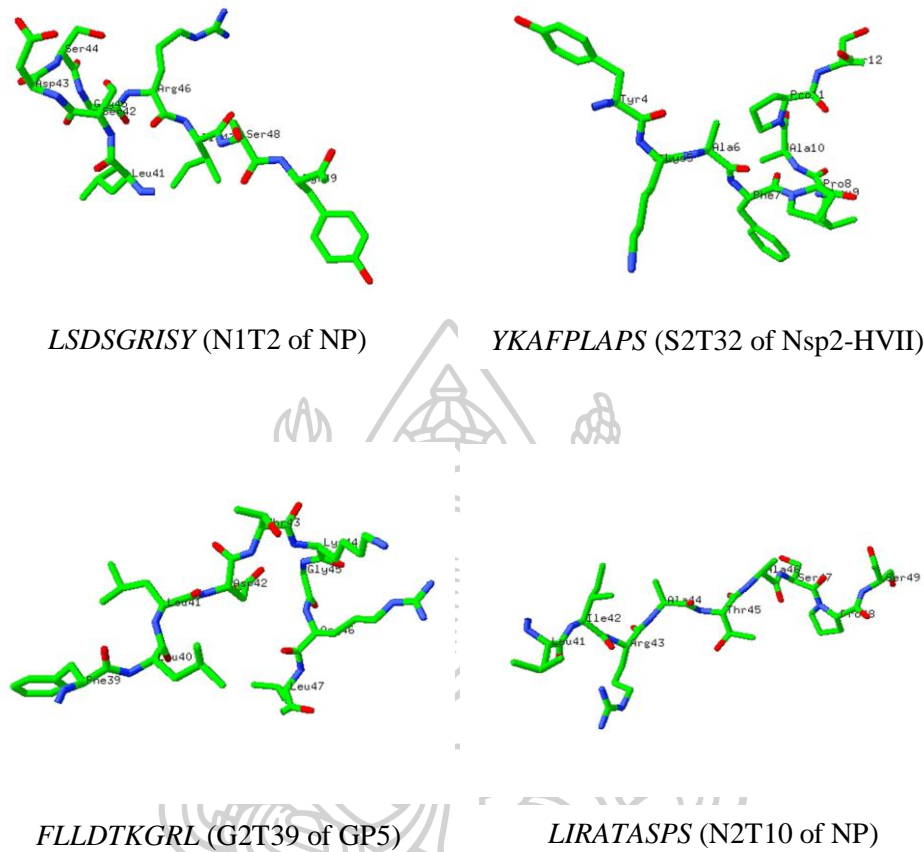


**Figure 25. Modelled peptide structure of predicted linear B-cell, MHC I and MHC II binding T-cell epitopes (continued.)**

## CHAPTER 5

### DISCUSSION

The PRRS is a devastating porcine viral infection, which is caused by the two genetically and antigenically different genotypes of PRRSV. It still persistently circulates globally and causes economic losses in the pig industry worldwide. Upon the emergence of PRRS, the causative PRRSV was continually evolving as seen from many reports including from China and Southeast Asia (23, 162-164). Since 2006, HP-PRRS has been identified in China and spread to Vietnam, Laos, Thailand, Cambodia, Philippines, Bhutan, Indonesia, Malaysia, Russia, Singapore, Myanmar, and India within a short period, by an extensive movement of infected pigs between the countries (25, 26, 28, 32, 33, 47, 165). Both NA and EU genotypes were found in these countries together with the quick evolution of the virus (27, 31, 166, 167). The first PRRS outbreak in Myanmar was reported in Mandalay region in February 2011. The disease spread rapidly to most of the area resulting in more than 34% mortality rate during this year (36, 168, 169). Thus far, little is known about the genetic characteristics of Myanmar PRRSV.

To control PRRS, the PRRSV vaccines producing from the strains that are genetically related to the field strains were generally used. But, the current PRRS vaccines cannot give substantial protective effect, especially against the heterologous virus. In 2017, Myanmar Veterinary Department allows to use NA type PRRSV MLV (Ingelvac MLV), in Myanmar (20). Because of vast genetic variability and antigenic heterogeneity of PRRSV, the type or composition of vaccine needs to be changed regularly for reflecting presently and locally circulating field strains. Therefore, various attempts have been tried to develop novel PRRSV vaccine and reverse vaccinology approach might be a novel way to develop for rapidly diverging PRRSV.

In this study, the genetic characteristics of Myanmar PRRSVs from clinical samples collected from six pig farms in five regions (Magway, Mandalay, Naypyitaw, Yangon and Ayeyarwady) upon the outbreaks in 2011 were analyzed and compared with that of NA prototype (VR-2332), EU prototype (Lelystad), LP and HP-PRRSV strains. The phylogenetic relationships between Myanmar PRRSVs and reference strains were also analyzed. Using different bioinformatics tools, the antigenicity of

*Nsp2-HVII*, ORF5, and ORF7 encoding regions (*Nsp2-HVII*, GP5, and NP, respectively) of six Myanmar PRRSVs were determined. In addition, prediction of linear B-cell, MHC I and MHC II binding T-cell epitopes from each coding region of Myanmar PRRSV (HP/MYANMAR/2303AM/2011) were conducted using various *in silico* bioinformatics tools.

### 5.1. Genetic Characterizations and Phylogenetic Analyses

High sequence homology of *Nsp2-HVII*, ORF5, and ORF7 (96.8-100% nucleotide identities) and their deduced amino acids sequences (94.9-100% amino acid identities) between the six Myanmar PRRSVs, as well as being assigned into the same lineage of subtype 3 in all phylogenetic analyses based on these genes, demonstrated that all Myanmar PRRSVs derived from the same source and did not diverge during the outbreaks. The HP/MYANMAR/0204AM1/2011 and HP/MYANMAR/0204AM2/2011 from Madaya might be the same strain because they had the same nucleotide sequences for all three genes. Nonetheless, the strain from Nyaungdon, HP/MYANMAR/2510AM/2011 showed some variations from the group, especially in *Nsp2-HVII* and ORF5. It should be noted that the clinical samples used in this study came from backyard farms where no vaccine was used, so genetic variation from the vaccine strain does not need to be considered.

When compared to VR-2332, the NA prototype, Myanmar PRRSVs showed 69.5-70.2%, 89.1-89.2%, and 93.5-94.4% nucleotide sequence identities of *Nsp2-HVII*, ORF5, and ORF7, respectively, while they showed only 47.6-48.3%, 62.8-63.3%, and 60.1-60.5% identities, respectively to Lelystad, the EU prototype. These results suggested that all Myanmar PRRSVs were closer to the NA genotype than the EU genotype. The size of full-length ORF5 and ORF7 of all six Myanmar PRRSVs were 603 and 372 bp, respectively, as those of VR-2332 and other PRRSV isolates suggesting no insertion or deletion has occurred. The discontinuous 30-amino acid deletions at position 481 and 533-561 in *Nsp2-HVII*, which considered as a molecular marker of HP-PRRSV (24, 47, 170, 171), were found in all Myanmar PRRSVs sequences supporting their derivation from HP-PRRSV.

Moreover, high sequence homologies at both nucleotide and deduced amino acid levels were observed with HP-PRRSV reference strains [JXA1, 07QN, HP/Thailand/19500LL/2010, BH58/10, 10/CAM46/2010 (*Nsp2-HVII*), and

NA/CAMC044/2010 (GP5)], particularly to HP/Thailand/19500LL/2010, BH58/10, and 1010/CAM46/2010, and NA/CAMC044/2010 revealing their close connection. When compared the amino acid sequences of Myanmar PRRSVs with those of the references HP-PRRSVs, the similarity to Thai HP/Thailand/19500LL/2010, Laotian BH58/10 and Cambodian 10/CAM46/2010, and NA/CAMC044/2010 was confirmed. These strains contained eight identical mutations (R280G, W410R, T428A, R450D, P495L, C510F, S519I, and E582K) in Nsp2-HVII and shared the same D34S mutation in GP5 and contained five identical putative glycosylation sites (N30, N33, N35, N44, and N51). This information revealed their close connection. Nonetheless, there were unique mutations found only in Myanmar PRRSVs i.e. L292F, P432S, and V621M in Nsp2-HVII (except HP/MYANMAR/2510AM/2011), and E170G in GP5 (**Figure 26**). In addition, the NP R11K and T191A mutations presented in other HP-PRRSVs were absent from Myanmar PRRSVs. These distinct features should be recognized as a marker of Myanmar PRRSVs in this study.

Given that GP5 is the major envelope protein that plays an important role in virus antigenicity and immunogenicity, the mutation in its epitopes should be focused. The decoy epitope, V<sup>27</sup>L(A/V)N<sup>30</sup>, which was conserved among all Myanmar PRRSVs and reference HP-PRRSVs may reveal its high antigenicity, but anyhow it was not involved in antibody neutralization due to previous reports (52, 53). However, isoleucine replacement at position 39 (L39I) in the primary neutralizing epitope, <sup>37</sup>SHLQLIYNL<sup>45</sup>, of all Myanmar PRRSVs and HP-PRRSVs might cause epitope conformation changes and contribute to evasion of the virus from host immune response.

From all phylogenetic trees constructed, all references HP-PRRSVs including JXA1, JXA1R, HP/Thailand/19500LL/2010, BH58/10, 07QN, and 10/CAM46/2010 (Nsp2-HVII), and NA/CAMC044/2010 (GP5) were assigned into the same subtype 3 of the NA genotype. Based on *Nsp2-HVII* and ORF5 sequences, it appeared that all Myanmar PRRSVs were closer to the HP/Thailand/19500LL/2010 BH58/10, 10/CAM46/2010, and NA/CAMC044/2010 than the 07QN, whilst the 07QN was relatively closer to the JXA1. Supporting evidence were perceived from multiple amino acid sequence alignments that JXA1 and 07QN shared the same mutations R280S, R450G, and C510R in Nsp2-HVII and D34N in GP5 (**Figure 26**). These close correlations between JXA1 and 07QN were also reported by Fang et al. (26).





Taken together, the pattern of genetic relationships between all Myanmar PRRSVs and HP-PRRSVs from Southeast Asia and the time line of the first outbreak in each country may suggest the route of transmission of PRRS. The HP-PRRSV spread from China to Vietnam in 2007. Then the virulent HP-PRRSV strains emerged in Vietnam in 2007 and the occurrence of new variants has been reported in the northern part of the country during 2007-2010 (167). The variants of Vietnamese HP-PRRSVs may be spread to Thailand and Laos in 2010, and then to Myanmar in 2011. Nilubol, et al. (2013) proposed that HP-PRRSV had been introduced to Thailand through illegal transport of infective pigs from Vietnam through Laos (33). It seems plausible to hypothesize that the HP-PRRSVs could have been introduced to Myanmar from importation of HP-PRRSV infected pigs from bordering countries, particularly, from Thailand and Laos.

To date, there has been no outbreak of PRRS reported in Myanmar since 2011 and the official vaccination program has not yet been implemented. Nevertheless, the Livestock Breeding and Veterinary Department gave permission to use the NA type modified live PRRS vaccine since September 2017 and Ingelvac PRRS MLV is currently being used in Myanmar (20). However, from our study, Myanmar PRRSVs were found to be more closely related to the JXA1R (JXA1, HP-PRRSV derived vaccine strain) than RespPRRS (VR-2332 derived vaccine strain in Ingelvac PRRS MLV).

## **5.2. *In silico* Epitope Prediction using Bioinformatics Tools**

In spite of many approaches have been investigated, little progress has been made to develop the novel PRRS vaccine which possesses effective protection against a broad range of PRRSV strains (7, 10). Neutralizing antibodies are a critical part of immune response for defense against PRRSV and there is an evidence of the substantial protection efficacy of antibody against PRRS infection in sows, glits, and piglets (73, 172, 173). Moreover, the CMI response is vital for the clearance of viral PRRS infection. It had found that the pigs recover from the experimental PRRS infection had strong lymphocyte proliferation responses and IFN- $\gamma$  is the plays an important role in the cytokine responses (73, 174). Therefore, the vaccine design becomes vital and attempts to make the PRRS vaccine, containing broadly reactive B-



cell and T-cell epitopes that elicit neutralizing antibody production and CMI responses. Reverse vaccinology approach provides to reduce time and costs using *in silico* bioinformatics tools to predict a large number of peptide epitopes. It becomes an attractive approach for the development of a novel vaccine against rapidly diverging PRRSV. Therefore, the prediction of immunodominant epitopes from immunogenically relevant proteins of PRRSV strains using bioinformatics tools becomes crucial. In the previous studies, different B-cell and T-cell epitopes from Nsp5, GP4, GP5, M, and NP were predicted by using different methods such as phage display, Pepscan peptide library, and SYFEPEITTHI and ProPed bioinformatics tools (52, 175-178). The identification of T-cell epitopes in PRRSV has been done to Nsp9, Nsp10, GP5 and M proteins (176). Various potential vaccine candidates from PRRSV proteins exhibited good protection in test animals but none has yet been approved for clinical use in the pig breeding farms.

In this study, linear B-cell, MHC I binding and MHC II binding T-cell epitopes were predicted by using the bioinformatics tools, that had not been used in the previous studies for the PRRS vaccine development. The pig has close genetic similarity to human specifically in genes that involved in immune response and there are functional similarities between SLA, and human HLA system and murine H-2 (144-146). For the predictions that do not have accessible *in silico* prediction tools for the porcine genome, the bioinformatics tools using human genome were used. Pig Matrix is a T-cell epitope prediction tool, which can be used for one SLA MHC II molecule (SLA-DRB\*0201), is developed by Gutierrez et al. in 2015, but it is not freely available.

The BCPREDS is a freely available web-based server for B-cell epitope prediction, which comprises three prediction methods, BCPred, and AAP and FBCpred. In this study, BCPred and AAP method were used to predict linear B-cell because FBCpred uses the same algorithm as BCPred except for predicting the flexible length of an epitope. The BCPred uses sequence-based Support Vector Machine (SVM) learning algorithm and is trained on the B-cell epitope database that contains epitopes from viruses, bacteria, parasites, and fungi. It has a better prediction than 11 SVM based tools. The AAP method bases on particular amino acid pairs occurred more frequently in epitope than non-epitope sequence. When compared with

ABCpred and Bepipred, commonly used B-cell prediction servers, both BCPred and APP showed better specificity and sensitivity than that of ABCpred and Bepipred (119, 120, 179). Then, the antigenicity of the predicted epitopes from all three proteins were further analyzed with VaxiJen v2.0 antigenicity prediction server at 0.5 threshold. It is the first server for alignment-independent prediction of protein antigenicity. It bases on auto cross-covariance (ACC) transformation of protein sequence into uniform vectors of principle amino acid properties and has prediction accuracy of 70-89% (147).

Among three proteins, the number of predicted linear B-cell epitopes from Nsp2-HVII was higher than that of GP5 and N protein. In accordance with the previous study, Nsp2 is a hypervariable protein and conserved regions were only found in C- and N-terminus, but it includes the highest frequency of linear B-cell epitopes when compared to GP5 and NP (175). Among 28 predicted linear B-cell epitopes from Nsp2-HVII, SB3 (*PPGAADTSFDWNVV*) had the highest antigenicity score of 1.4277 and it might be a potential vaccine candidate from Nsp2-HVII. The primary neutralizing antibodies in PRRS infection are mainly towards GP5 and the predicted linear B-cell epitopes from GP5 have great attention. The total of eight linear B-cell epitopes was predicted for GP5 and GB5 (*SCTRYTNFLDTKGRL*) had the highest antigenicity score of 0.9980 and it could be the promising vaccine candidate for antibody production. However, there have been previously reported that a partial sequence of two predicted epitopes GB1 and GB2 (*AVLANASNSNSSHIQL*, *ANASNSNSSHIQLI*) could generate natural antibodies in pigs (52, 53). This evidence strength the potential of bioinformatics tools to predict epitopes. Additionally, they contained the neutralizing motif (<sup>37</sup>SHLQLI<sup>42</sup>) which had been demonstrated in previous studies (52, 53, 74). Moreover, <sup>31</sup>ANSNSSSHIIQLIYNL<sup>45</sup> was found to be immunoreactive with more than 50% of the tested sera from experimentally infected piglets (175). For NP, which is the most conserved proteins, perceived an extensive interest to predict the epitope for diagnostic purpose regardless of its neutralizing activity, the prompt and abundant production of antibody. Among eight linear B-cell epitopes predicted from NP, NB6 (*SRGKGPGKKNRKKNPE*) scored the highest antigenicity of 1.0428 and it could be the most promising candidates from N protein.

For T-cell epitope prediction, it is generally accepted that the peptide epitope that binds to MHC molecules at an above the certain threshold will act as T-cell epitopes. Therefore, peptide affinity for MHC molecules correlates with T-cell response and T-cell epitope predictions are based on their binding affinity to MHC molecules. The MHC I molecule with peptide was recognized by cytotoxic T-cells while MHC II molecules present peptides to helper T-cells, that participate in both cytotoxic responses and antibody responses. The MHC I binding peptides are derived from intracellular protein, which is targeted to the cleavage by the proteasome, to short peptide of 8-11 length. The short peptide is transported by TAP and bind to MHC I molecule for antigen presentation (117). Therefore, a prediction based on the efficiency of proteasomal cleavage, TAP and MHC-I binding prediction is useful for identification of MHC I binding T-cell epitopes. For MHC II binding, extracellular protein derived from pathogens is take up by the receptor and targeted to endosomal cleavage to peptide length of 15-20. However, shorter or longer peptides can be presented by MHC II molecules (117).

The MHC I processing prediction server generates an overall total score from the combined efficiency of proteasomal cleavage, TAP transport, and MHC-I binding. The prediction of proteasomal cleavage was based on in vitro proteasomal cleavage data, and TAP was based on an estimation of binding affinity to TAP. Second screening by  $IC_{50}$  of selected epitopes for SLA MHC I alleles were predicted by MHC I binding prediction software from IEBD using NetMHCpan 2.0 method which can accurately predict the binding to HLA, also to those of non-human primates. It can determine epitopes that can bind to a broad range of MHC class I SLA alleles (45 SLA alleles) (135, 148, 149). From all three proteins, a total of 17 MHC I binding T-cell epitopes were selected and S1T5 (*LSASSQTEY*) from Nsp2-HV-II, G1T2 (*GTDWLAQKF*) from GP5 and N1T2 (*LSDSGRISY*) from NP, were selected as first-line potential vaccine candidate.

The MHC II binding T-cell epitopes prediction tool from IEDB, which provide the prediction of  $IC_{50}$  of the epitopes for respective HLA MHC II alleles was utilized in this study. Different algorithms are available in this tool, NetMHCIIpan2.0 was used because it has the highest accuracy among 21 MHC II binding prediction servers (150). According to the  $IC_{50}$ , a total of 191 epitopes was predicted from three

proteins. Of which, 97 epitopes had VaxiJen antigenicity score of above threshold ( $>0.5$ ) and selected as potential epitopes. Based on the number of binding HLA MHC II alleles, three epitopes S2T32 (*YKAFPLAPS*) of Nsp2-HVII, G2T39 (*FLLDTKGRL*) of GP5, and N2T10 (*LIRATASPS*) of NP were chosen as first-line potential MHC II binding T-cell epitopes.

The first-line potential epitopes, GB5 (*SCTRYTNFLLDTKGRL*), G2T39 (*FLLDTKGRL*) of GP5 and N1T2 (*LSDSGRISY*), and N2T10 (*LIRATASPS*) of NP had percentage conservancy of above 80% within reference HP-PRRSVs and they could be useful for PRRS vaccine against Asian HP-PRRSVs. Moreover, mapping of N1T2 (*LSDSGRISY*) on the predicted NP structure supported that this epitope located in  $\beta$ -sheet region and potential to be a novel vaccine candidate.

Additionally, the sequence similarity were found within the predicted epitopes. For GP5, G2T39 (<sup>144</sup>*FLLDTKGRL*<sup>152</sup>) overlapped with GB2 (<sup>137</sup>*SCTRYTNFLLD TKGRL*<sup>152</sup>), and GB1 and GB2, (<sup>26</sup>*AVLANASNSNSSHIQL*<sup>41</sup>, <sup>29</sup>*ANASNSNSSHI QLI*<sup>42</sup>) partially overlapped with G1T1 (<sup>35</sup>*NSSHIQLIY*<sup>43</sup>). For Nsp2-HVII protein, S1T1 (<sup>284</sup>*TSFDWNVVF*<sup>292</sup>) was identical to part of SB3 (<sup>278</sup>*PPGAADTSFDWNVV*<sup>291</sup>). It was suggested that these epitopes can give both B-cell and T-cell immune responses.



## CHAPTER 6

### CONCLUSION

In conclusion, based on genetic characteristics and phylogenetic analyses of *Nsp2-HVII*, ORF5, and ORF7, all six Myanmar PRRSVs in this study were of the NA-genotype and were highly-pathogenic PRRSVs. From phylogenetic analyses, they were clustered into the subtype 3 of the NA-genotype that also included other HP-PRRSVs e.g. Chinese JXA1, Thai HP/Thailand/19500LL/2010, Laotian BH58/10, and Vietnamese 07QN. Additionally, Myanmar PRRSVs were closer to Thai HP/Thailand/19500LL/2010, Laotian BH58/10, Cambodian 10/CAM46/2010, and NA/CAMC044/2010 than Vietnamese 07QN. The unique amino acid mutations found only in Myanmar PRRSVs were L292F, P431S, and V621M in *Nsp2-HVII* and E170G in GP5, which may be used as a marker for monitoring genetic diversity of newly emerging HP-PRRSV strains. This molecular study provides basic information for monitoring newly diverging strains, future epidemiological investigation, and development of effective strategies to control PRRS in Myanmar. Further studies on more isolates and gene segments are required to confirm the genetic characteristics of Myanmar PRRSV strains.

By using different bioinformatics tools, the three linear B-cell epitopes, SB3 (*PPGAADTSFDWNVV*), GB5 (*SCTRYTNFLDTKGRL*), and NB6 (*SRGKGPGKKNRKKNPE*), three MHC I binding T-cell epitopes, S1T5 (*LSASSQTEY*), G1T2 (*GTDWLAQKF*), and N1T2 (*LSDSGRISY*); and three MHC II binding T-cell epitopes, S2T32 (*YKAFPLAPS*), G2T39 (*FLLDTKGRL*), and N2T10 (*LIRATASPS*) were predicted as first-line potential PRRS vaccine candidates and they could assist in the development of novel peptide vaccine and diagnostic markers for PRRS. Implying a reverse vaccinology approach, the immunogenicity of the epitopes, predicted bioinformatically, were needed to verify through *in vivo* tests.



## REFERENCES

- 1] Holtkamp DJ, Kliebenstein JB, Neumann EJ, et al. Assessment of the economic impact of porcine reproductive and respiratory syndrome virus on United States pork producers. *Journal of Swine Health and Production*. 2013;21(2):72-84.
- [2] Nathues H, Alarcon P, Rushton J, et al. Cost of porcine reproductive and respiratory syndrome virus at individual farm level – An economic disease model. *Preventive Veterinary Medicine*. 2017;142:16-29.
- [3] Rossow KD, Collins JE, Goyal SM, et al. Pathogenesis of porcine reproductive and respiratory syndrome virus infection in gnotobiotic pigs. *Veterinary Pathology*. 1995;32:361-73.
- [4] Rossow KD. Porcine reproductive and respiratory syndrome. *Veterinary Pathology*. 1998:1-20.
- [5] Allende R, Lewis TL, Lu Z, et al. North American and European porcine reproductive and respiratory syndrome viruses differ in non-structural protein coding regions. *Journal of General Virology*. 1999;80:307- 15.
- 6] Rowland RRR, Tribble B, editors. The role of host genetics in vaccine development. *International PRRS Symposium; 2013; China*.
- [7] Kimman TG, Cornelissen LA, Moormann RJ, et al. Challenges for porcine reproductive and respiratory syndrome virus (PRRSV) vaccinology. *Vaccine*. 2009;27:3704-18.
- [8] Zhou YJ, Hao XF, Tian ZJ, et al. Highly pathogenic porcine reproductive and respiratory syndrome virus emerged in China. *Transboundary Emerging Diseases*. 2008;55(3-4):152-64.
- [9] Nguyen T. PRRS control in region. *World Organization for Animal Health Conference 2013*.
- [10] Renukaradhya GJ, Meng XJ, Calvert JG, et al. Live porcine reproductive and respiratory syndrome virus vaccines: Current status and future direction. *Vaccine*. 2015;7(33):4069-80.
- [11] Kanampalliwar AM, Soni R, Girdhar A, et al. Reverse vaccinology: Basic and Application. *Vaccines*. 2013;4:6.
- [12] Rappuoli R. Reverse vaccinology: A genome-based approach to vaccine development. *Vaccine*. 2001;19:2688-91.
- [13] Rappuoli R. Reverse vaccinology. *Genomics*. 2000;3:445-50.
- [14] Murtaugh MP, Elam MR, Kakach LT. Comparison of the structural protein coding sequences of the VR-2332 and Lelystad virus strains of the PRRS virus. *Archives of Virology*. 1995;140:1451-60.
- [15] Murtaugh MP, Xiao Z, Zuckermann F. Immunological responses of swine to porcine reproductive and respiratory syndrome virus infection. *Journal of Viral Immunology*. 2002;15:533-47.

- [16] Dea S, Gagnon CA, Mardassi H, et al. Brief Review on Current knowledge on the structural proteins of porcine reproductive and respiratory syndrome (PRRS) virus: comparison of the North American and European isolates. *Archives of Virology*. 2000;145(4):659-88.
- [17] Kappes MA, Faaberg KS. PRRSV structure: replication: origin of phenotype and genotype diversity. *Journal of Virology*. 2015:475-86.
- [18] First case of PRRS virus reported in Burma, Mizzima News. 2011, March 8.
- [19] Six New Outbreaks of PRRS in Myanmar. OIE. World Organization for Animal Health. 2011 [Available from: <http://www.thepigsite.com/swinenews/27180/six-new-outbreaks-of-prrs-in-myanmar/>].
- [20] Than Lin MLF. PRRS vaccine allowed to use in Myanmar. 2017. Personal Communication.
- [21] Hill H, Owen W, Eernisse K, et al. Prevalence of SIRS virus in Iowa swine herds. *American Association of Swine Practitioners Newsletter* 1992;4:47.
- [22] Gilbert SA, Larochelle R, Magar R, et al. Typing of porcine reproductive and respiratory syndrome viruses by a multiplex PCR assay. *Journal of Clinical Microbiology*. 1997;35:264-7.
- [23] Gao ZQ, Guo X, Yang HC. Genomic characterization of two Chinese isolates of porcine reproductive and respiratory syndrome virus. *Archives of Virology*. 2004;149:1341-51.
- [24] Zhou L, Zhang J, Zeng J, et al. The 30-amino acid deletion in Nsp2 of highly pathogenic porcine reproductive and respiratory syndrome virus emerging in China is not related to its virulence. *Journal of Virology*. 2009a;83(10):5156-67.
- [25] Metwally S, Mohamed F, Faaberg K, et al. Pathogenicity and molecular characterization of emerging porcine reproductive and respiratory syndrome virus in Vietnam in 2007. *Transboundary Emerging Diseases*. 2010;57(5):315-29.
- [26] Fang Y, Zhao T, Nguyen T, et al. Porcine reproductive and respiratory syndrome virus variants, Vietnam and China, 2007. *Emerging Infectious Diseases*. 2008;14:1774-6.
- [27] Do DT, Park C, Choi K, et al. Nucleotide sequence analysis of Vietnamese highly pathogenic porcine reproductive and respiratory syndrome virus from 2013 to 2014 based on the NSP2 and ORF5 coding regions. *Archives of Virology*. 2016;161(3):669-75.
- [28] Ni J, Yang S, Bounlom D, et al. Emergence and pathogenicity of highly pathogenic porcine reproductive and respiratory syndrome virus in Vientiane, Lao People's Democratic Republic. *Journal of Veterinary Diagnostic and Investigation*. 2012;24:349-54.
- [29] Damrongwatanapokin S, Arsayuth K, Kongkrong C, et al. Serological studies and isolation of porcine reproductive and respiratory syndrome (PRRS) virus in Thailand. *Journal of Thai Veterinary Medicine*. 1996;47:19-30.



- [30] Thanawongnuwech R, Amonsin A, Tatsanakit A, et al. Genetics and geographical variation of porcine reproductive and respiratory syndrome virus (PRRSV) in Thailand *Veterinary Microbiology*. 2004;101:9-21.
- [31] Amonsin A, Kedkovid R, Suphasawatt P, et al. Comparative analysis of complete nucleotide sequence of porcine reproductive syndrome virus (PRRSV) isolates in Thailand (US and EU genotypes). *Virology Journal*. 2009;6:143.
- [32] Jantafong T, Sangthong P, Wimontiane S, et al. Genetic diversity of porcine reproductive and respiratory syndrome virus in Thailand and Southeast Asia from 2008 to 2013. *Veterinary Microbiology*. 2015;176:3-4.
- [33] Nilubol D, Tripipat T, Hoonsuwan T, et al. Genetic diversity of the ORF5 gene of porcine reproductive and respiratory syndrome virus (PRRSV) genotypes I and II in Thailand. *Archives of Virology*. 2013;158(5):943-53.
- [34] Jantafong T, Lekcharoensuk P. Molecular characterization of complete genome of a Thai highly pathogenic porcine reproductive and respiratory syndrome virus. *Thai Journal of Veterinary Medicine*. 2014;44(4):415-25.
- [35] Rajkhowa TK, Mohanarao GJ, Gogoi A, et al. Indian porcine reproductive and respiratory syndrome virus bears discontinuous deletion of 30 amino acids in nonstructural protein 2. *Virus Diseases*. 2016;27(3):287-93.
- [36] World Organization for Animal Health, Porcine reproductive and respiratory syndrome, Myanmar (Immediate notification) 2011a, March 4 [Available from: Retrieved from [http://www.oie.int/wahis\\_2/public/wahid.php/](http://www.oie.int/wahis_2/public/wahid.php/)].
- [37] Myanmar Reports outbreaks of PRRS in Nay Pyi Daw region, *Pig Progress* 2011, April 28 [Available from: <https://www.pigprogress.net/Home/General/2011/4/Myanmar-reports-outbreaks-of-PRRS-in-Naypyidawregion-PP007293W/>].
- [38] Myanmar-Authorities ban pig and pork from Pegu. 2011 [Available from: <https://agrobenefig.wordpress.com/2011/06/01/myanmar-authorities-ban-pig-and-pork-from-Pegu-may-24-2011/>].
- [39] Myanmar 2011 [Available from: <https://agrobenefig.wordpress.com/tag/myanmar/>]
- [40] Cavanagh D. Nidovirales: a new order comprising Coronaviridae and Arteriviridae. *Archives of Virology*. 1997;142:629-33.
- [41] Snijder EJ, Meulenberg JJ. The molecular biology of arteriviruses. *Journal of General Virology*. 1998;76:961-79.
- [42] Fang Y, Treffers EE, Li Y, et al. Efficient-2 frameshifting by mammalian ribosomes to synthesize an additional arterivirus protein. *PNAS*. 2012;109:E2920-8.
- [43] Li Y, Treffers EE, Naphine S, et al. Transactivation of programmed ribosomal frameshifting by a viral protein. *PNAS*. 2014;111:E2172-781.
- [44] Fang Y, Kim D-Y, Ropp S, et al. Heterogeneity in Nsp2 of European-like porcine reproductive and respiratory syndrome viruses isolated in the United States. *Virus Research*. 2004;100:229-35.
- [45] Nelsen CJ, Murtaugh MP, Faaberg KS. Porcine reproductive and respiratory

- syndrome virus comparison: divergent evolution on two continents. *Journal of Virology*. 1999;73:270-80.
- [46] Dokland T. The structural biology of PRRSV. *Virus Research*. 2010;154:86-97.
- [47] Tian K, Yu X, Zhao T, et al. Emergence of fatal PRRSV variants: Unparalleled outbreaks of atypical PRRS in China and Molecular dissection of the unique hallmark. *PloS One*. 2007;6:e256.
- [48] Han J, Rutherford MS, Faaberg KS. Proteolytic products of the porcine reproductive and respiratory syndrome virus nsp2 replicase protein. *Journal of Virology*. 2010;84(19):10102-12.
- [49] Kapur V, Elam MR, Pawlovich TM, et al. Genetic variation in porcine reproductive and respiratory syndrome virus isolates in the midwestern United States. *Journal of General Virology*. 1996;77:1271-6.
- [50] Meng XJ, Paul PS, Halbur PG, et al. Phylogenetic analyses of the putative M (ORF6) and N (ORF7) genes of porcine reproductive and respiratory syndrome virus (PRRSV): implication for the existence of two genotypes of PRRSV in the U.S.A. and Europe. *Archives of Virology*. 1995a;140:745-55.
- [51] Wissink EHJ, Kroese MV, Maneschijn-Bonsing JG, et al. Significance of the oligosaccharides of the porcine reproductive and respiratory syndrome virus glycoproteins GP2a and GP5 for infectious virus production. *Journal of General Virology*. 2004;85:3715-23.
- [52] Ostrowski M, Jar Galeota AM, Platt KB, et al. Identification of neutralizing and non-neutralizing epitopes in the porcine reproductive and respiratory syndrome virus GP5 ectodomain. *Journal of Virology*. 2002;4241-50.
- [53] Plagemann PGW. The primary GP5 neutralization epitope of North American isolates of porcine reproductive and respiratory syndrome virus. *Veterinary Immunology and Immunopathology*. 2004;102:263-75.
- [54] Plagemann PGW. Neutralizing antibody formation in swine infected with seven strains of porcine reproductive and respiratory syndrome virus as measured by indirect ELISA with peptides containing the GP5 neutralization epitope. *Viral Immunology*. 2006;19:285-93.
- [55] Rowland RRR, Schneider P, Fang Y, et al. Peptide domains involved in the localization of the porcine reproductive and respiratory syndrome virus nucleocapsid protein to the nucleolus. *Virology*. 2003;316:135-45.
- [56] Yoo D, Wootton S, Li G, et al. Colocalization and interaction of the porcine arterivirus nucleocapsid protein with the small nucleolar RNA-associated protein fibrillarin. *Journal of Virology*. 2003;77:12173-83.
- [57] Meulenberg JJ, Bende RJ, Pol JM, et al. Nucleocapsid protein N of Lelystad virus; expression by recombinant baculovirus, immunological properties, and suitability for detection of serum antibodies. *Clinical and Diagnostic Laboratory Immunology*. 1995;2:652-6.
- [58] Lee C, Kim H, Kang B, et al. Prevalence and phylogenetic analysis of the isolated

- type I porcine reproductive and respiratory syndrome virus from 2007 to 2008 in Korea. *Virus Genes*. 2010;40:225-30.
- [59] Kedkovid R, NaAyudhya SN, Amonsin A, et al. NSP2 gene variation of the North American genotype of the Thai PRRSV in central Thailand. *Virology Journal*. 2010;7:340.
- [60] Li J, Yin Y, Guo B, et al. Sequence analysis of the NSP2, ORF5, and ORF7 genes of 11 PRRS virus isolates from China. *Virus Genes*. 2012;45:256-64.
- [61] Thuy NTD, Thu NT, Son NG, et al. Genetic analysis of ORF5 porcine reproductive and respiratory syndrome virus isolated in Vietnam. *Microbiology and Immunology*. 2013;57(7):518-26.
- [62] Albina E. Epidemiology of porcine reproductive and respiratory syndrome (PRRS): an overview. *Veterinary Microbiology*. 1997;55:309-16.
- [63] Wills RW, Zimmerman JJ, Yoon K-J, et al. Porcine reproductive and respiratory syndrome virus - a persistent infection. *Veterinary Microbiology*. 1997;55:231-40.
- [64] Edwards S, Robertson IB, Wilesmith JW, et al. PRRS ("blue-eared pig disease") in Great Britain. *AASP Newsletter*. 1992.
- [65] Robertson IB. Porcine reproductive and respiratory syndrome (blue-eared pig disease): some aspects of its epidemiology. *Proceedings Society Veterinary Epidemiology Preventive Medicine*. 1992:24-8.
- [66] Mortensen S, Madsen KS. The occurrence of PRRS in Denmark. *AASP*. 1992;4(4):48.
- [67] Lunney JK, Fang Y, Ladinig A, et al. Porcine Reproductive and Respiratory Syndrome Virus (PRRSV): Pathogenesis and Interaction with the Immune System. *Annual Review of Animal Biosciences*. 2016;4:129-54.
- [68] Wensvoort G, de Kluyver EP, Luitze EA, et al. Antigenic comparison of Lelystad virus and swine infertility and respiratory syndrome (SIRS) virus. *Journal of Veterinary Diagnostic and Investigation*. 1992;4:134-8.
- [69] Martínez-Lobo FJ, Díez-Fuertes F, Segalés J, et al. Comparative pathogenicity of type 1 and type 2 isolates of porcine reproductive and respiratory syndrome virus (PRRSV) in a young pig infection model. *Veterinary Microbiology*. 2011;154(1-2):58-68.
- [70] Keffaber K, Stevenson G, van Alstine W, et al. SIRS virus infection in nursery/grower pigs. *American Association of Swine Practitioners Newsletter* 1992;4:38-40.
- [71] Loula T. Mystery pig disease. *Agri-practice*. 1991;12:23-4.
- [72] Zimmerman JJ YK, Wills RW, Swenson SL. General overview of PRRSV: a perspective from the United States. *Journal of Veterinary Microbiology*. 1994;55:187-96.
- [73] Rahe MC, Murtaugh MP. Review: Mechanisms of Adaptive Immunity to Porcine Reproductive and Respiratory Syndrome Virus. *Viruses*. 2017;9(148).

- [74] Lopez OJ, Osorio FA. Role of neutralizing antibodies in PRRSV protective immunity. *Veterinary Immunology and Immunopathology*,. 2004;102:155-63.
- [75] Ansari IH, Kwon B, Osorio FA, et al. Influence of N-linked glycosylation of porcine reproductive and respiratory syndrome virus GP5 on virus infectivity, antigenicity, and ability to induce neutralizing antibodies. *Journal of Virology*. 2006;80:3994-4004.
- [76] Faaberg KS, Hocker JD, Erdman MM, et al. Neutralizing antibody responses of pigs infected with natural GP5 N-glycan mutants of porcine reproductive and respiratory syndrome virus. *Viral Immunology*. 2006;19:294-304.
- [77] Bautista EM, Suarez P, TW M. T cell responses to the structural polypeptides of porcine reproductive and respiratory syndrome virus. *Archives of Virology*. 1999b;144:117-34.
- [78] Meier WA, Galeota J, Osorio FA, et al. Gradual development of the interferon-gamma response of swine to porcine reproductive and respiratory syndrome virus infection or vaccination. *Journal of Virology*. 2003;309:18-31.
- [79] Lowe JE, Husmann R, Firkins LD, et al. Correlation of cell-mediated immunity against porcine reproductive and respiratory syndrome virus with protection against reproductive failure in sows during outbreaks of porcine reproductive and respiratory syndrome in commercial herds. *Journal of Veterinary Medical Association*. 2005;226:1707-11.
- [80] Diaz I, Darwich L, Pappaterra G, et al. Different European-type vaccines against porcine reproductive and respiratory syndrome virus have different immunological properties and confer different protection to pigs. *Virology Journal*. 2006;351:249-59.
- [81] Collins JE, Benfield DA, Christianson WT, et al. Isolation of swine infertility and respiratory syndrome virus (Isolate ATCC VR-2332) in North America and experimental reproduction of the disease in gnotobiotic pigs. *Journal of Veterinary Diagnostic and Investigation*. 1992;4:117-26.
- [82] Wensvoort G, Trepstra C, Pol JM, et al. Mystery swine disease in the Netherlands: the isolation of Lelystad virus. *Veterinary Quarterly*. 1991;13(3):121-30.
- [83] Mardassi H, Mounir S, Dea S. Molecular analysis of the ORFs 3 to 7 of porcine reproductive and respiratory syndrome virus, Quebec reference strain. *Archives of Virology*. 1995;140:1405-18.
- [84] Morozov I, Meng XJ, Paul PS. Sequence analysis of open reading frame (ORFs) 2 to 4 of a U. S. isolate of porcine reproductive and respiratory syndrome virus. *Archives of Virology*. 1995;140:1313-9.
- [85] Zhou L, Kang R, Zhang Y, et al. Emergence of two novel recombinant porcine reproductive and respiratory syndrome viruses 2 (lineage 3) in Southeastern China. *Veterinary Microbiology*. 2019;232:30-41.
- [86] Christopher-Hennings J, editor *Porcine Reproductive and Respiratory Syndrome (PRRSV) diagnostics in the United States: Past, present and future*. International



- PRRS Symposium; 2013; Beijing, China.
- [87] Stadejek T, Podgorska K, Jedryczko A, editors. Methods and approaches to diagnose PRRS. International PRRS Congress; 2015; Ghent, Belgium.
- [88] Report of the OIE Ad Hoc Group on Porcine reproductive and respiratory syndrome, PRRS: the disease, its diagnosis, prevention and control. World Organization for Animal Health.; 2008.
- [89] Charerntantanakul W, Platt R, Johnson W, et al. Immune responses and protection by vaccine and various vaccine adjuvant candidates to virulent porcine reproductive and respiratory syndrome virus. *Veterinary Immunology and Immunopathology*. 2006;109:99-115.
- [90] Charerntantanakul W. Porcine reproductive and respiratory syndrome virus vaccines: Immunogenicity, efficacy and safety aspects. *World Journal of Vaccine*. 2012;1(1):23-30.
- [91] Cano JP, Dee SA, Murtaugh MP, et al. Impact of a modified-live porcine reproductive and respiratory syndrome virus vaccine intervention on a population of pigs infected with a heterologous isolate. *Vaccine*. 2007;25:4382-91.
- [92] Okuda Y, Kuroda M, Ono M, et al. Efficacy of vaccination with porcine reproductive and respiratory syndrome virus following challenges with field isolates in Japan. *Journal of Veterinary Medical Science*. 2008;70:1017-25.
- [93] Scotti M, Prieto C, Alvarez E, et al. Failure of an inactivated vaccine against porcine reproductive and respiratory syndrome to protect gilts against a heterologous challenge with PRRSV. *Veterinary Research*. 2007;161:809-13.
- [94] Subramaniam S, Beura LK, Kwon B, et al. Amino acid residues in the non-structural protein 1 of porcine reproductive and respiratory syndrome virus involved in down-regulation of TNF-alpha expression in vitro and attenuation in vivo. *Virology*. 2012;432:241-9.
- [95] Lee C, Calvert JG, Welch SK, et al. A DNA-launched reverse genetics system for porcine reproductive and respiratory syndrome virus reveals that homodimerization of the nucleocapsid protein is essential for virus infectivity. *Virology*. 2005;331:47-62.
- [96] Han J, Rutherford MS, Faaberg KS. The porcine reproductive and respiratory syndrome virus nsp2 cysteine protease domain possesses both trans- and cis-cleavage activities. *Journal of Virology*. 2009;83:9449-63.
- [97] Kwon B, Ansari IH, Pattnaik AK, et al. Identification of virulence determinants of porcine reproductive and respiratory syndrome virus through construction of chimeric clones. *Virology*. 2008;380:371-8.
- [98] Renukaradhya GJ, Meng XJ, Calvert JG, et al. Inactivated and subunit vaccines against porcine reproductive and respiratory syndrome: Current status and future direction. *Vaccine*. 2015;33(3065-3072).
- [99] Fang Y, Christopher-Hennings J, Brown E, et al. Development of genetic markers

- in the non-structural protein 2 region of a US type 1 porcine reproductive and respiratory syndrome virus: implications for future recombinant marker vaccine development. *Journal of General Virology*. 2008;89:3086-96.
- [100] Xu YZ, Zhou YJ, Zhang SR, et al. Identification of nonessential regions of the nsp2 protein of an attenuated vaccine strain (HuN4-F112) of highly pathogenic porcine reproductive and respiratory syndrome virus for replication in marc-145 cell. *Virology Journal*. 2012;9(141):2-7.
- [101] Baxevanis AD. *Bioinformatics: A Practical Guide to the Analysis of Genes and Proteins*. In: Baxevanis AD, Ouellette BFF, editors. Second ed. New York: Wiley; 2001.
- [102] Ramsden JJ. *Bioinformatics: An Introduction*. In: Dress A, editor. Second Edition ed. Germany: Springer; 2009.
- [103] Selzer PM, Marhöfer RJ, Rohwer A. *Applied Bioinformatics: An Introduction*. Germany: Springer; 2008.
- [104] Menlove KJ, Clement M, Crandall KA. Similarity Searching Using BLAST. In: Posada D, editor. *Bioinformatics for DNA Sequence Analysis*. New York: Humana Press; 2009.
- [105] Rice P LI, Bleasby A. EMBOSS: The European Molecular Biology Open Software suite. *Trends in Genetics*. 2000;16(6):275-7.
- [106] Micheal I. Sequence comparison tools. In: Edwards D, Hansen D, Stajich J, editors. *Bioinformatics: Tools and Applications*. New York: Springer; 2009.
- [107] Edgar RC. MUSCLE: multiple sequence alignment with high accuracy and high throughput. *Nucleic Acids Research*. 2004;32(5):1792-7.
- [108] Fiona S, Brinkman L, Leipe DD. Phylogenetic Analysis. In: Baxevanis AD, Ouellette BFF, editors. *Bioinformatics: A Practical Guide to the Analysis of Genes and Proteins*. Second ed. New York NY: Wiley; 2001.
- [109] Brinkman FSL, Leipe DD. Phylogenetic Analysis. In: Baxevanis AD, Ouellette BFF, editors. *BIOINFORMATICS: A Practical Guide to the Analysis of Genes and Proteins*. 43. Second ed. New York: Wiley; 2001.
- [110] Pizza M, Scarlato V, Masignani V, et al. Identification of vaccine candidates against serogroup B meningococcus by whole-genome sequencing. *Science*. 2000;287(5459):1816-20.
- [111] Wilson CC, McKinney D, Anders M, et al. Development of a DNA vaccine designed to induce cytotoxic T lymphocyte responses to multiple conserved epitopes in HIV-1. *Journal of Immunology*. 2003;17(10):5611-23.
- [112] Bourdette DN, Edmonds E, Smith C, et al. A highly immunogenic trivalent T cell receptor peptide vaccine for multiple sclerosis. *Multiple Sclerosis*. 2005;11(5):552-61.
- [113] Robinson HL, Amara RR. T cell vaccines for microbial infections. *Nature Medicine*. 2005;11:25-32.
- [114] López JA, Weilenman C, Audran R, et al. A synthetic malaria vaccine elicits a



- potent CD8<sup>+</sup> and CD4<sup>+</sup> T lymphocyte immune response in humans. Implications for vaccination strategies. *European Journal of Immunology*. 2001;31(7):1989-98.
- [115] Soria-Guerra RE, Nieto-Gomez N, Govea-Alonso DO, et al. An overview of bioinformatics tools for epitope prediction: Implications on vaccine development. *Journal of Biomedical Information*. 2015; 53:405-14.
- [116] Ponomarenko JV, van Regenmortel MHV. B cell epitope prediction. *Structural Bioinformatics*. 2009:849-53.
- [117] Taylor PD, Flower DR. Innate and Adaptive Immunity. In: Flower DR, Jon T, editors. *In silico Immunology*. New York NY: Springer; 2007.
- [118] Saha S, Raghava GPS. Prediction of Continuous B-cell Epitopes in an Antigen Using Recurrent Neural Network. *Proteins*. 2006;65(1):40-8.
- [119] Chen J, Liu H, Yang J, et al. Prediction of linear B-cell epitopes using amino acid pair antigenicity scale. *Amino Acids*. 2007;33:423-8.
- [120] EL-Manzalawy Y, Drena Dobbs D, Honavara V. Predicting linear B-cell epitopes using string kernels. *Journal of Molecular Recognition* 2008;21(4):243-55.
- [121] Jespersen MC, Peters B, Nielsen M, et al. BepiPred-2.0: improving sequence-based B-cell epitope prediction using conformational epitopes. *Nucleic Acids Research*. (Web Server issue).
- [122] Ponomarenko JV, Bui H, Li W, et al. ElliPro: a new structure-based tool for the prediction of antibody epitopes. *BMC Bioinformatics*. 2008;9.
- [123] Andersen PH, Nielsen M, Lund O. Prediction of residues in discontinuous B Cell epitopes using protein 3D structures. *Protein Science*. 2006;15:2558-67.
- [124] Kulkarni-Kale U, Bhosle S, Kolaskar AS. CEP: a conformational epitope prediction server. *Nucleic Acids Research*. 2005;33(Web Server issue):W168-W71.
- [125] Rammensee H, Bachmann J, Emmerich NP, et al. SYFPEITHI: database for MHC ligands and peptide motifs. *Immunogenetics*. 1999;50(3-4):213-9.
- [126] Jardetzky TS, Brown JH, Gorga JC, et al. Crystallographic analysis of endogenous peptides associated with HLA-DR1 suggests a common, polyproline II-like conformation for bound peptides. *Processing National Academic Science USA*. 1996;93(2):734-8.
- [127] Davies MN, Flower DR. Computational Vaccinology. In: Davies MN, Flower DR, editors. *Bioinformatics for Immunomics Immunomics Reviews: (An Official Publication of the International Immunomics Society)*. 3. New York NY: Springer; 2009.
- [128] Donnes P, Elofsson A. Prediction of MHC class I binding peptides, using SVMHC. *BMC Bioinformatics*. 2002;3(25).
- [129] Liu W, Meng X, Xu Q, et al. Quantitative prediction of mouse class I MHC peptide binding affinity using support vector machine regression (SVR) models. *BMC Bioinformatics*. 2006;31(7):182.

- [130] Wan J, Liu W, Xu Q, et al. SVRMHC prediction server for MHC-binding peptides. *BMC Bioinformatics*. 2006;7(463).
- [131] Noguchi H, Kato R, Hanai T, et al. Hidden Markov model-based prediction of antigenic peptides that interact with MHC class II molecules. *Journal of Bioscience and Bioengineering*. 2002;94(3):264-70.
- [132] Davies MN, Hattotuwigama CK, Moss DS, et al. Statistical deconvolution of enthalpic energetic contributions to MHC-peptide binding affinity. *BMC Structural Biology*. 2006;20(6):5.
- [133] Wan S, Coveney P, Flower DR. Large-scale molecular dynamics simulations of HLA-A\*0201 complexed with a tumor-specific antigenic peptide: can the alpha3 and beta2m domains be neglected. *Journal of Computational Chemistry*. 2004;25:1803-13.
- [134] Sette A, Rappuoli R. Reverse vaccinology: developing vaccines in the era of genomics. *Immunity*. 2010;33(4):530-41.
- [135] Hoof I, Peters B, Sidney J, et al. NetMHCpan, a method for MHC class I binding prediction beyond humans. *Immunogenetics*. 2009;61(1):1-13.
- [136] Lundegaard C, Lund O, Nielsen M. Accurate approximation method for prediction of class I MHC affinities for peptides of length 8, 10 and 11 using prediction tools trained on 9mers. *Bioinformatics* 2008;24:1397-8.
- [137] Lin HH, Zhang GL, Tongchusak S, et al. Evaluation of MHC-II peptide binding prediction servers: applications for vaccine research. *BMC Bioinformatics*. 2008;9:S22.
- [138] Hall TA. BioEdit: a user-friendly biological sequence alignment editor and analysis program for Windows 95/98/NT. *Nucleic Acids Symposium*1999. p. 95-8.
- [139] Nielsen M, Lundegaard C, Blicher T, et al. NetMHCpan, a Method for Quantitative Predictions of Peptide Binding to Any HLA-A and -B Locus Protein of Known Sequence. *PLOS One*. 2007.
- [140] TusnaÂdy GE, Simon I. Principles Governing Amino Acid Composition of Integral Membrane Proteins: Application to Topology Prediction. *Journal of Molecular Biology*. 1998;283:489-506.
- [141] Gupta R, Brunak S. Prediction of glycosylation across the human proteome and the correlation to protein function. *Pacific Symposium on Biocomputing*. 2002;7:310-22.
- [142] Felsenstein J. PHYLIP. Retrieved from <http://evolutiongswashingtonedu/phyliptml>. 2013, April.
- [143] Page RDM. TREE VIEW: An application to display phylogenetic trees on personal computers. *Computer Applications in the Biosciences*. 1996;12:357-8.
- [144] Ollivier L, Sellier P. Pig genetics : a review (1). *Annales de génétique et de sélection animal*, INRAEditions. 1982;14(4):481-544.
- [145] Dawson HD. Comparative assessment of the pig, mouse, and human genomes: A

- structural and functional analysis of genes involved in immunity. In: McNulty PA, Dayan A, Hastings KH, Ganderup NC, editors. *The minipig in Biomedical Research*. USA: CRC Press; 2011
- [146] Dawson HD, Loveland JE, Pascal G, et al. Structural and functional annotation of the porcine immunome. *BMC Genomics*. 2013;14:332-48.
- [147] Doytchinova IA, Flower DR. Vaxijen: a server for prediction of protective antigens, tumour antigens and submit vaccines. *BMC Bioinformatics*. 8:1-7.
- [148] Peters B, Bulik S, Tampe R, et al. Identifying MHC class I epitopes by predicting the TAP transport efficiency of epitope precursors. *Journal of Immunology*. 2003;171:1741-9.
- [149] Tenzer S, Peters B, Bulik S, et al. Modeling the MHC class I pathway by combining predictions of proteasomal cleavage, TAP transport and MHC class I binding. *Cell Molecular Life Science*. 2005;62:1025-37.
- [150] Andreatta M, Karosiene E, Rasmussen M, et al. Accurate pan-specific prediction of peptide-MHC class II binding affinity with improved binding core identification. *Immunogenetics*. 2015;67(11-12):641-50.
- [151] Walters EM, Wolf E, Whyte JJ, et al. Completion of the swine genome will simplify the production of swine as a large animal biomedical model. *BMC Medical Genomics*. 2012;5(55):1-11.
- [152] Green J, Sidney J, Chung J, et al. Functional classification of class II human leukocyte antigen (HLA) molecules reveals seven different supertypes and a surprising degree of repertoire sharing across supertypes. *Immunogenetics*. 63(6):325-35.
- [153] Bui H, Sidney J, Li W, et al. Development of an epitope conservancy analysis tool to facilitate the design of epitope-based diagnostics and vaccines. *BMC Bioinformatics*. 2007;361(8).
- [154] Camacho C, Coulouris G, Avagyan V, et al. BLAST+: architecture and applications. *BMC Bioinformatics*. 2009;10:421-30.
- [155] Remmert M, Biegert A, Hauser A, et al. HHblits: lightning-fast iterative protein sequence searching by HMM-HMM alignment. *Nature Methods*. 2012;9:173-5.
- [156] Manupetit J, Derreumaux P, Tuffery P. A fast and accurate method for large-scale de novo peptide structure prediction. *Journal of Computational Chemistry*. 2010;31(4):726-38.
- [157] Shen Y, Maupetit J, Derreumaux P, et al. Improved PEP-FOLD approach for peptide and miniprotein structure prediction. *Journal of Chemical Theory and Computation*. 2014;10:4745-58.
- [158] Benkert P, Biasini M, T S. Toward the estimation of the absolute quality of individual protein structure models. *Bioinformatics*. 2011;27(3):343-50.
- [159] Lovell SC, Davis IW, Arendall WB, et al. Structure validation by  $C\alpha$  geometry:  $\phi, \psi$  and  $C\beta$  deviation. *Proteins: Structure, Function, and Genetics*. 2003;50(3):437-50.

- [160] Guex N, Petisch MC. SWISS-MODEL and the Swiss-Pdbviewer: An environment for comparative protein modeling. *Electrophoresis*. 1997;18(2714-2723).
- [161] Doan DN, Dokland T. Structure of the nucleocapsid protein of porcine reproductive and respiratory syndrome virus. *Structure*. 2003;11(11):1445-51.
- [162] Gao JC, Xiong JY, Ye C, et al. Genotypic and geographical distribution of porcine reproductive and respiratory syndrome viruses in mainland China in 1996-2016. *Veterinary Microbiology*. 2017;208:164-72.
- [163] Guo B, Chen Z, Liu W, et al. Isolation and identification of porcine reproductive and respiratory syndrome (PRRS) virus from aborted fetuses suspected of PRRS. *Chinese Journal of Preventive Veterinary Medicine*. 1996;18:1-5.
- [164] Guo Z, Chen XX, Li R, et al. The prevalent status and genetic diversity of porcine reproductive and respiratory syndrome virus in China: a molecular epidemiological perspective. *Virology Journal*. 2018;15(1):2.
- [165] An TQ, Tian ZJ, Leng CL, et al. Highly pathogenic porcine reproductive and respiratory syndrome virus in Asia. *Emerging Infectious Diseases*. 2011;17(9):1782-4.
- [166] Chen N, Cao Z, Yu X, et al. Emergence of novel European genotype porcine reproductive and respiratory syndrome virus in mainland China. *Journal of General Virology*. 2011;92:880-92.
- [167] Dietze K, Pinto J, Wainwright S, et al. Porcine reproductive and respiratory syndrome (PRRS) virulence jumps and persistent circulation in Southeast Asia. In Focus on.... Rome Food and Agricultural Organization of the United Nations. 2011;5:8.
- [168] World Organisation for Animal Health, Porcine reproductive and respiratory syndrome, Myanmar (Follow-up report No. 1) 2011b, June 29 [Available from: Retrieved from [http://www.oie.int/wahis\\_2/public/wahid.php/](http://www.oie.int/wahis_2/public/wahid.php/)].
- [169] World Organisation for Animal Health, Porcine reproductive and respiratory syndrome, Myanmar (Follow-up report No. 2). 2012, October 1.
- [170] Li Y, Wang X, Bo K, et al. Emergence of a highly pathogenic porcine reproductive and respiratory syndrome virus in the mid-eastern region of China. *Veterinary Journal*. 2007;174:577-84.
- [171] Wu J, Li J, Tian F, et al. Genetic variation and pathogenicity of highly virulent porcine reproductive and respiratory syndrome emerging in China. *Archives of Virology*. 2009;154(10):1589-97.
- [172] Osorio FA, Galeota JA, Nelson E, et al. Passive transfer of virus-specific antibodies confers protection against reproductive failure induced by a virulent strain of porcine reproductive and respiratory syndrome virus and establishes sterilizing immunity. *Virology Journal*. 2002;302:9-20.
- [173] Lopez MF, Oliveira E, Alvarez Garcia BJ, et al. Protection against Porcine Reproductive and Respiratory Syndrome Virus (PRRSV) Infection through Passive Transfer of RRSV-Neutralizing Antibodies Is Dose Dependent. *Clinical*

- and Vaccine Immunology. 2007;14(3):269-75.
- [174] Lopez Fuertes L DN, Alvarez B, Ezquerra A, Domingue J, Castro JM, Alonso F. Analysis of cellular immune response in pigs recovered from porcine respiratory and reproductive syndrome infection. *Virus Research*. 1999;64(33-42).
- [175] de Lima M, Pattnaik KA, Flores EF, et al. Serologic marker candidates identified among B-cell linear epitopes of Nsp2 and structural proteins of a North American strain of porcine reproductive and respiratory syndrome virus. *Journal of Virology*. 2006;353:410-21.
- [176] Vashisht K, Goldberg TL, Husmann RJ, et al. Identification of immunodominant T-cell epitopes present in glycoprotein 5 of the North American genotype of porcine reproductive and respiratory syndrome virus. *Vaccine* 2008;26 4747–53.
- [177] Wang YX, Zhou YJ, Li GX, et al. Identification of immunodominant T-cell epitopes in membrane protein of highly pathogenic porcine reproductive and respiratory syndrome virus. *Virus Research*. 2011;158(1-2):108-15.
- [178] Parida R, Choi IS, Peterson DA, et al. Location of T-cell epitopes in nonstructural proteins 9 and 10 of type-II porcine reproductive and respiratory syndrome virus. *Virus Research*. 2012;169:13-21.
- [179] EL-Manzalawy Y, Dobbs D, Honnavar V. Predicting flexible length linear B-cell epitopes. 7<sup>th</sup> International conference on computational systems bioinformatics; Stanford: CA; 2008. p. 121-31.







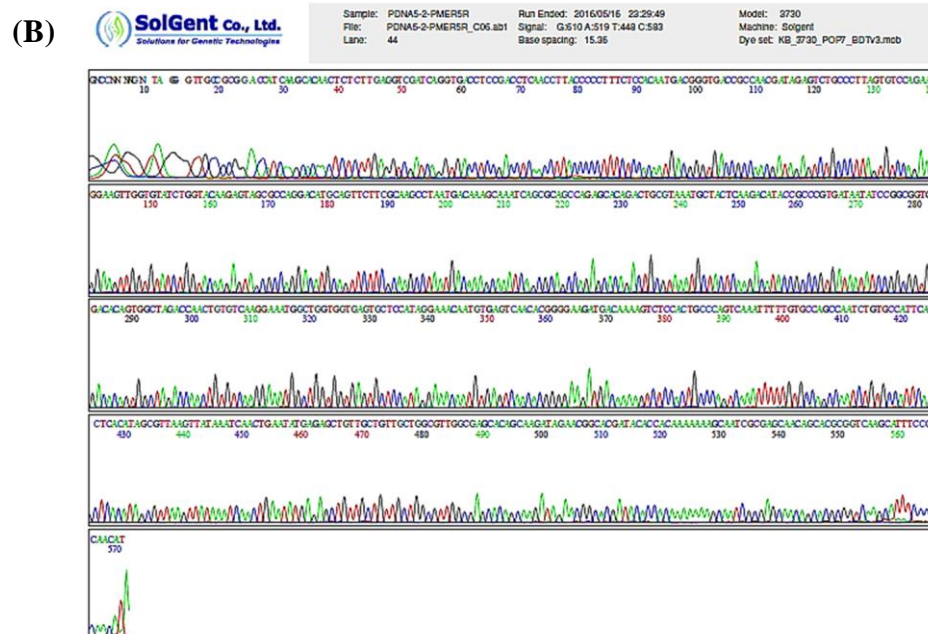
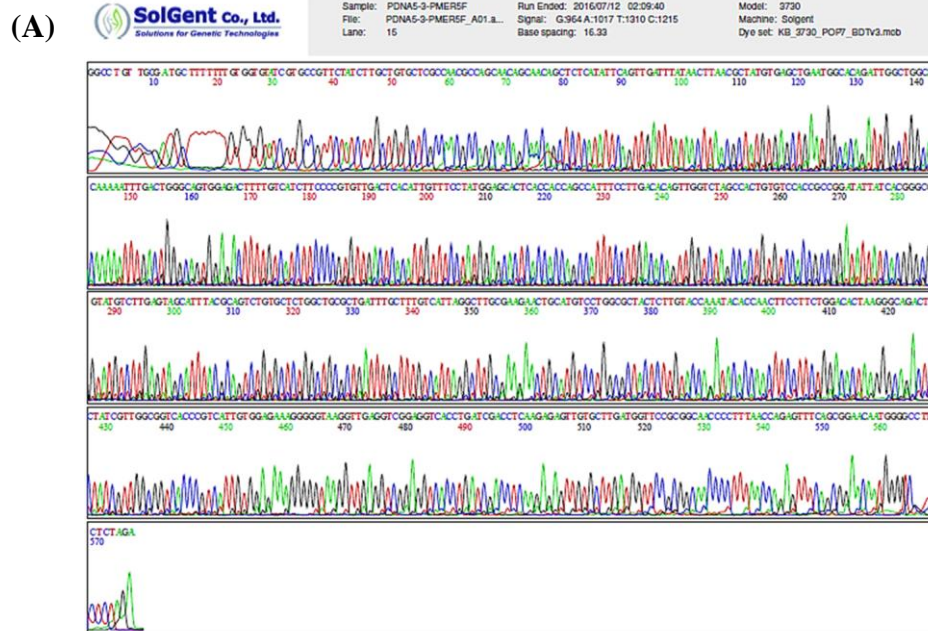
**APPENDIX I**





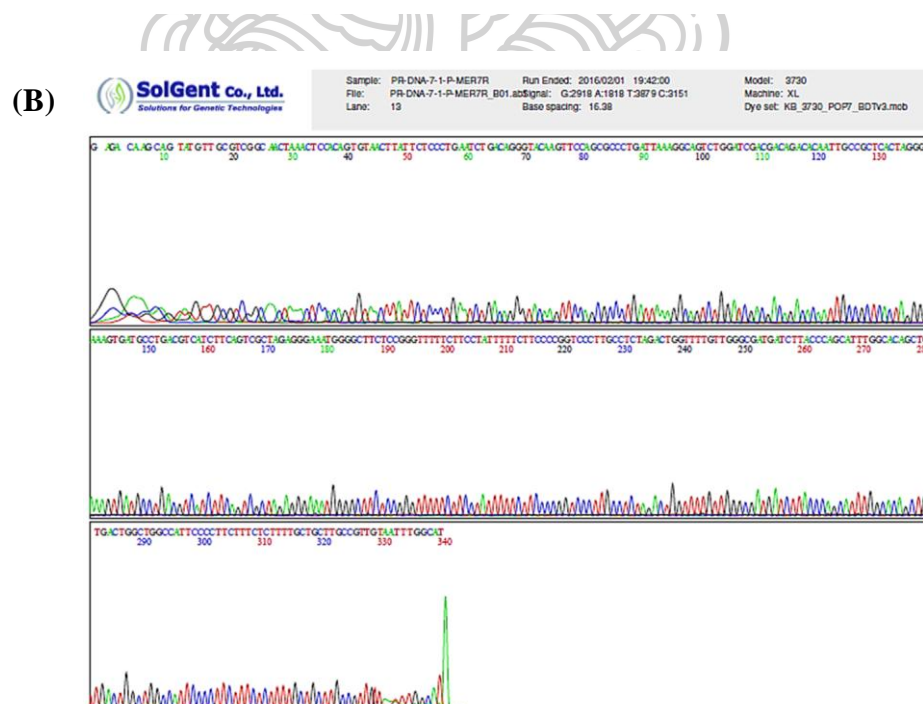
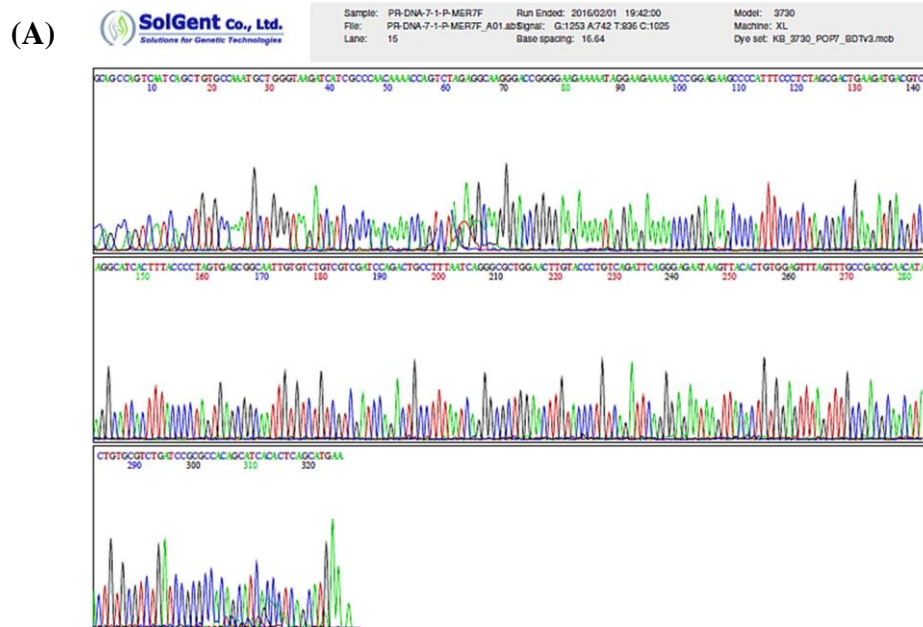
## 1.2. Sequencing chromatograms of ORF5 gene

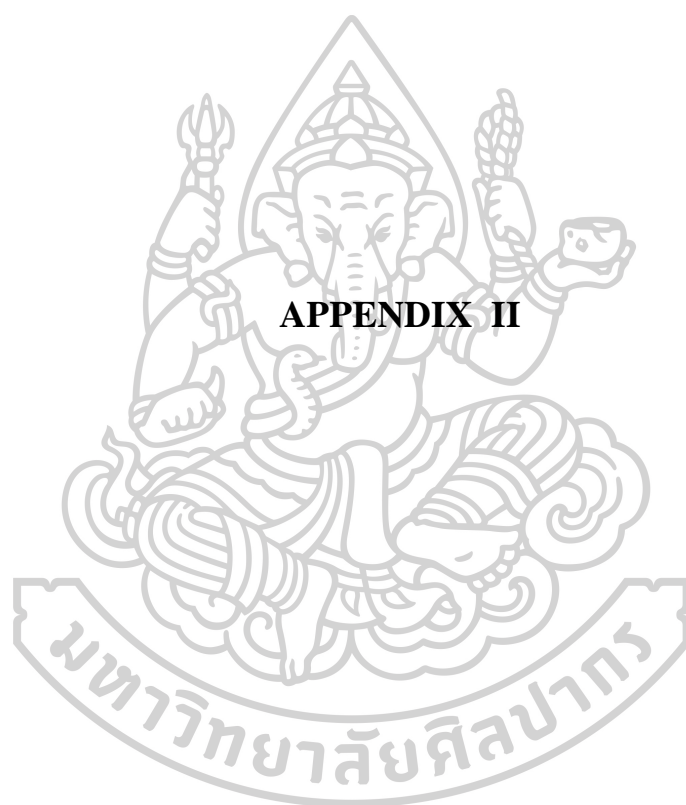
(A) Forward and (B) Reverse strands of ORF5 gene



### 1.3. Sequencing chromatograms of ORF7 gene

(A) Forward and (B) Reverse strands of ORF7 gene



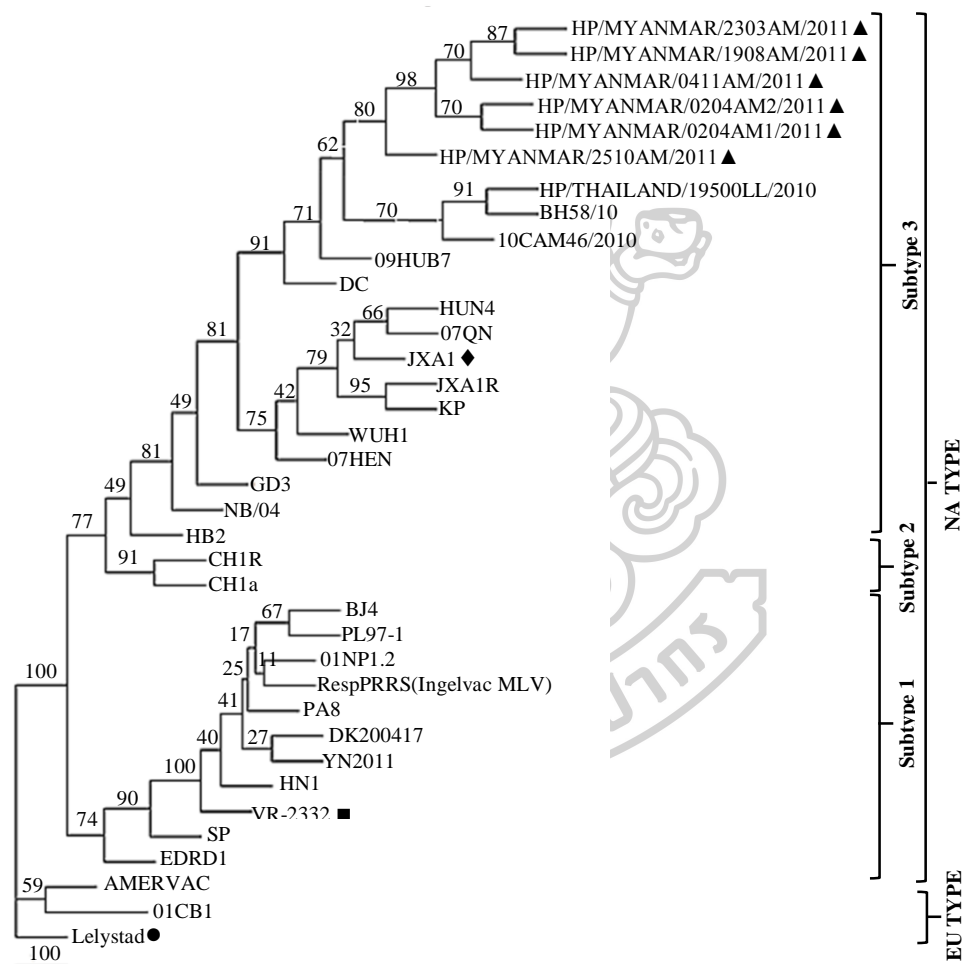


**APPENDIX II**

## 2. Phylogenetic trees

### 2.1. Phylogenetic tree of PRRSVs based on nucleotide sequences of *Nsp2-HVII* gene

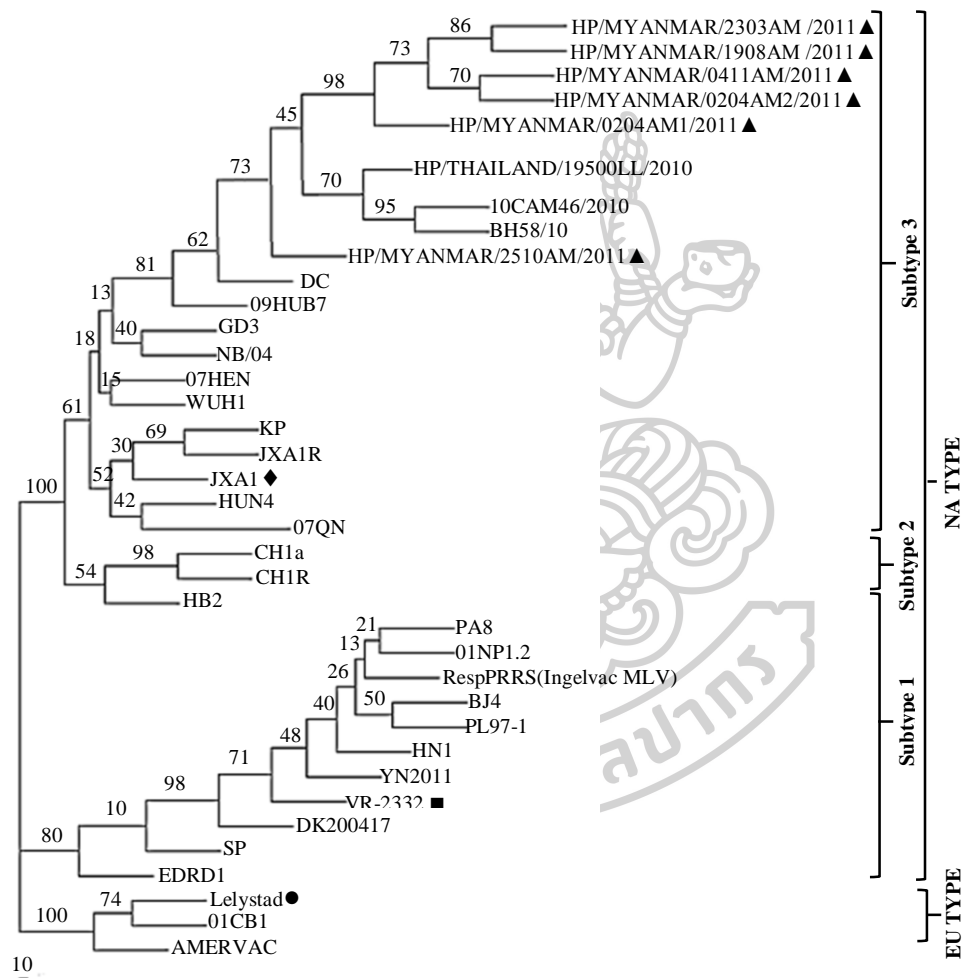
The phylogenetic tree was constructed by Maximum Likelihood method using John-Taylor-Thornton model with 1000 bootstrapping. (▲) indicates Myanmar PRRSVs, (◆) Chinese HP-PRRS, JXA1, (●) indicates EU prototype, Lelystad and (■) indicates NA prototype, VR-2332.





## 2.2. Phylogenetic tree of PRRSVs based on deduced amino sequences of *Nsp2-HVII* gene

The phylogenetic tree was constructed by Neighbor-Joining method using Kimura 2-parameter model, with 1000 bootstrapping. (▲) indicates Myanmar PRRSVs, (◆) Chinese HP-PRRS, JXA1, (●) indicates EU prototype, Lelystad and (■) indicates NA prototype, VR-2332.

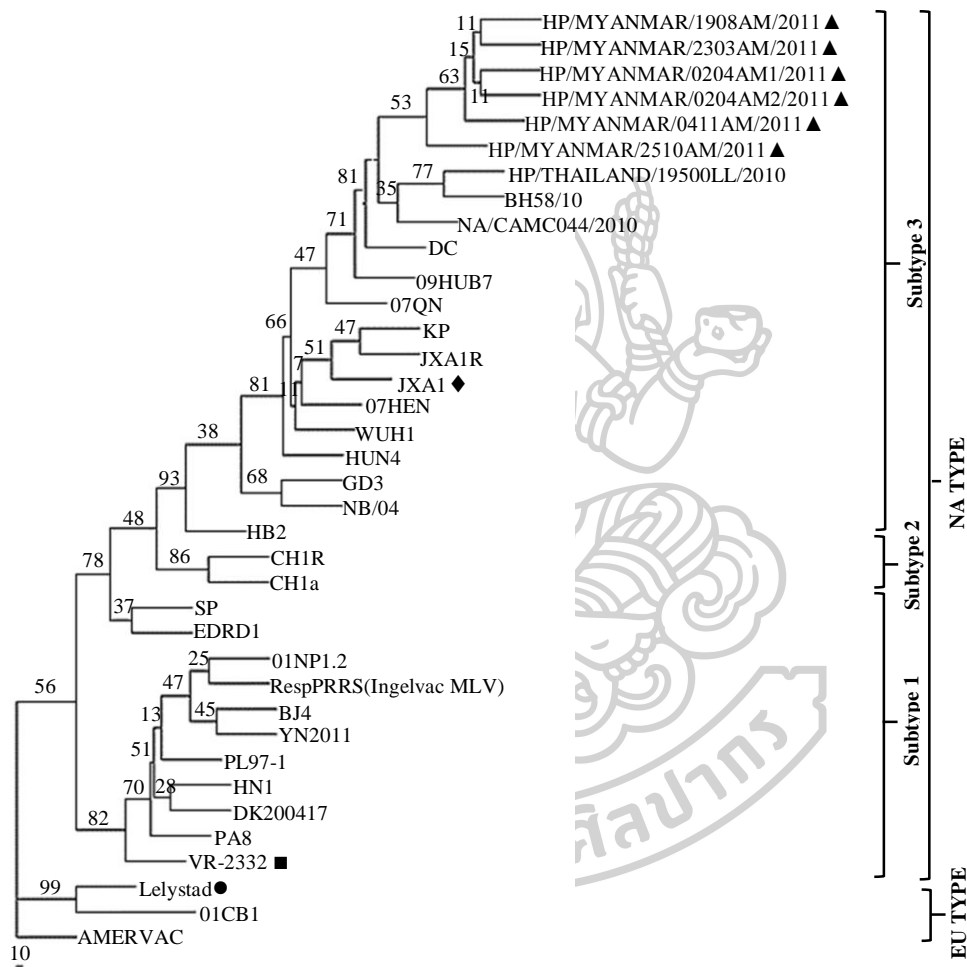






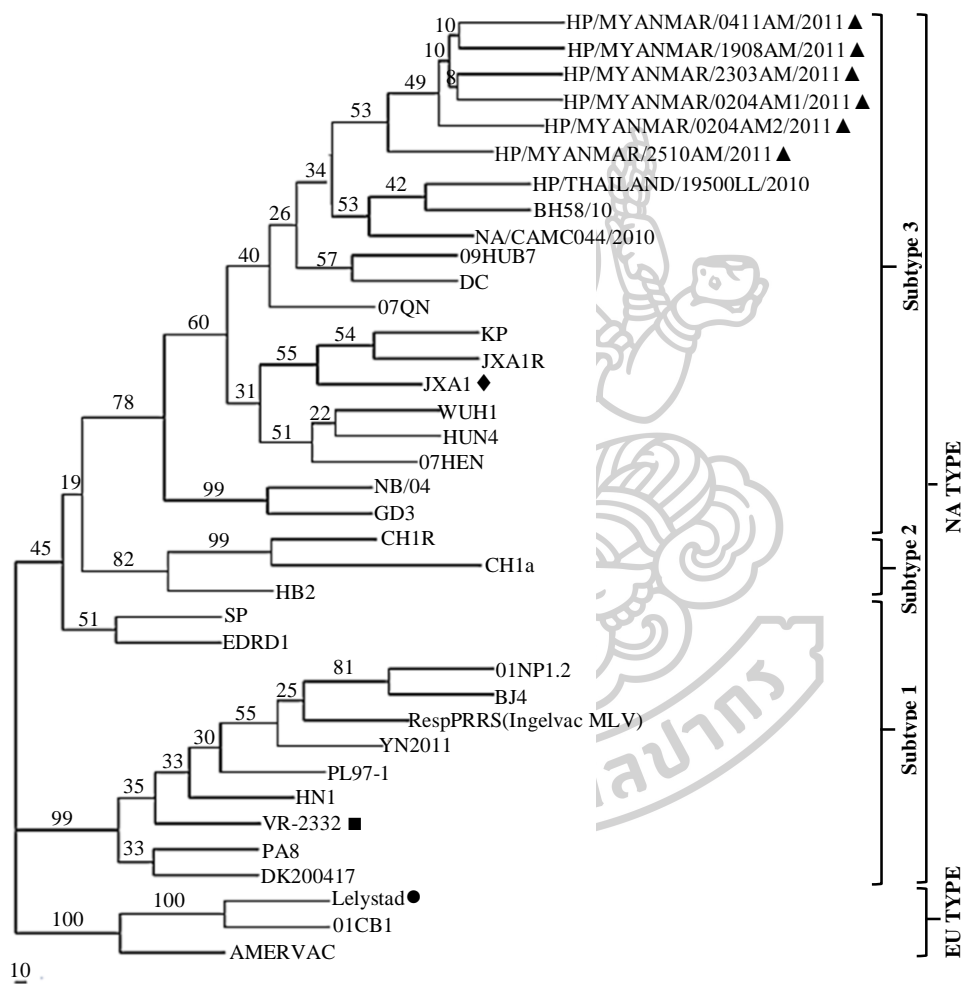
#### 2.4. Phylogenetic tree of PRRSVs based on nucleotide sequences of ORF5 gene

The phylogenetic tree was constructed by Maximum Likelihood method using John-Taylor-Thornton model with 1000 bootstrapping. (▲) indicates Myanmar PRRSVs, (◆) Chinese HP-PRRS, JXA1, (●) indicates EU prototype, Lelystad and (■) indicates NA prototype, VR-2332.



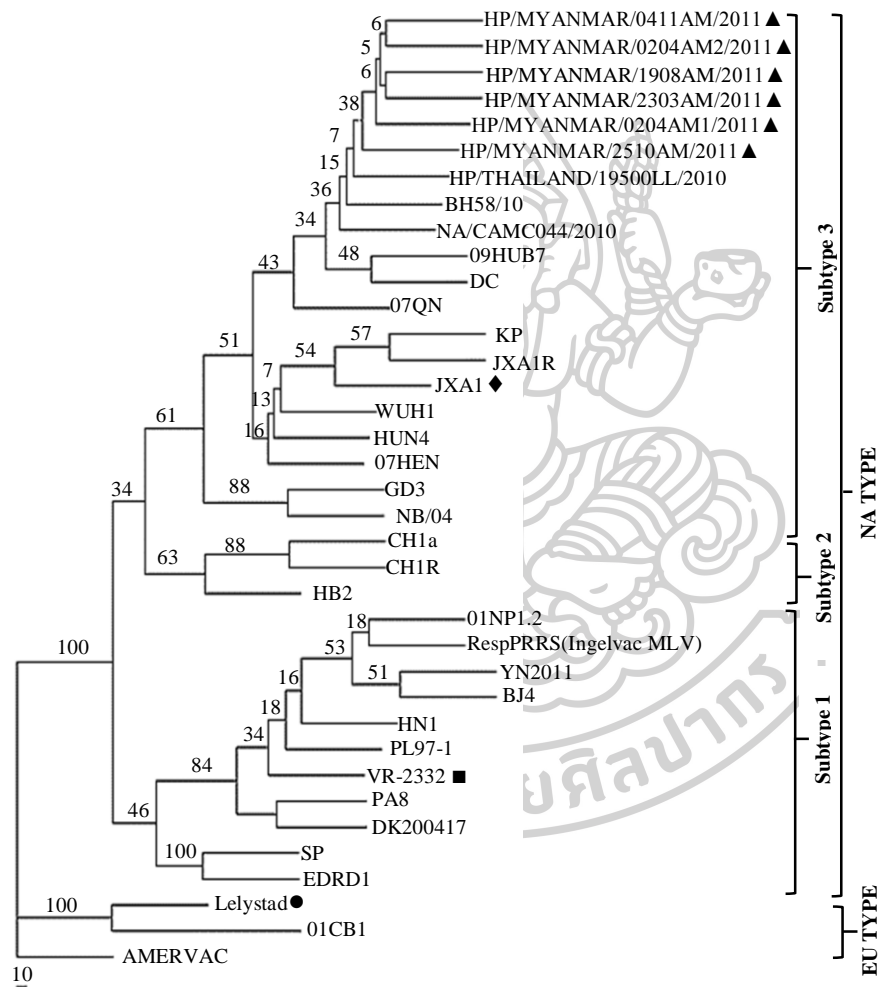
## 2.5. Phylogenetic tree of PRRSVs based on deduced amino sequences of ORF5 gene

The phylogenetic tree was constructed by Neighbor-Joining method using Kimura 2-parameter model, with 1000 bootstrapping. (▲) indicates Myanmar PRRSVs, (◆) Chinese HP-PRRS, JXA1, (●) indicates EU prototype, Lelystad and (■) indicates NA prototype, VR-2332.



## 2.6. Phylogenetic tree of PRRSVs based on deduced amino sequences of ORF5 gene

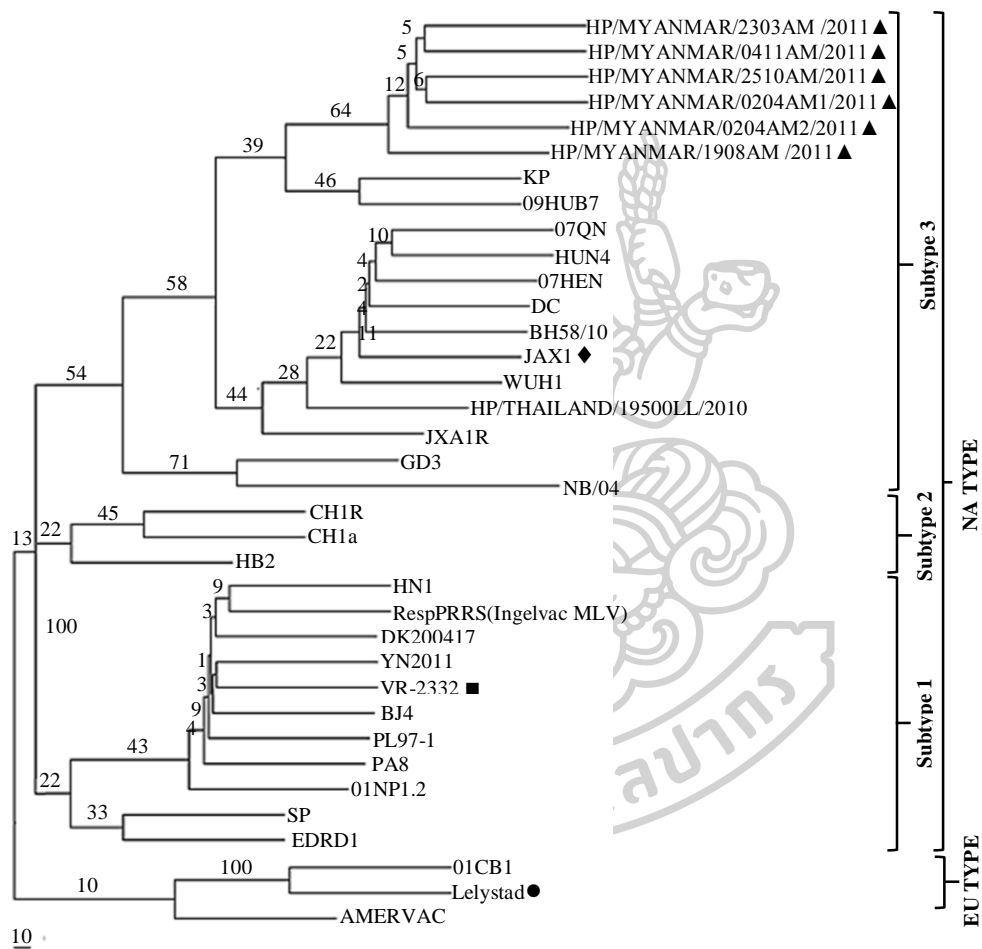
The phylogenetic tree was constructed by Maximum Likelihood method using John-Taylor-Thornton model, with 1000 bootstrapping. (▲) indicates Myanmar PRRSVs, (◆) Chinese HP-PRRS, JXA1, (●) indicates EU prototype, Lelystad and (■) indicates NA prototype, VR-2332.





## 2.8. Phylogenetic tree of PRRSVs based on deduced amino acid sequences of ORF7 gene

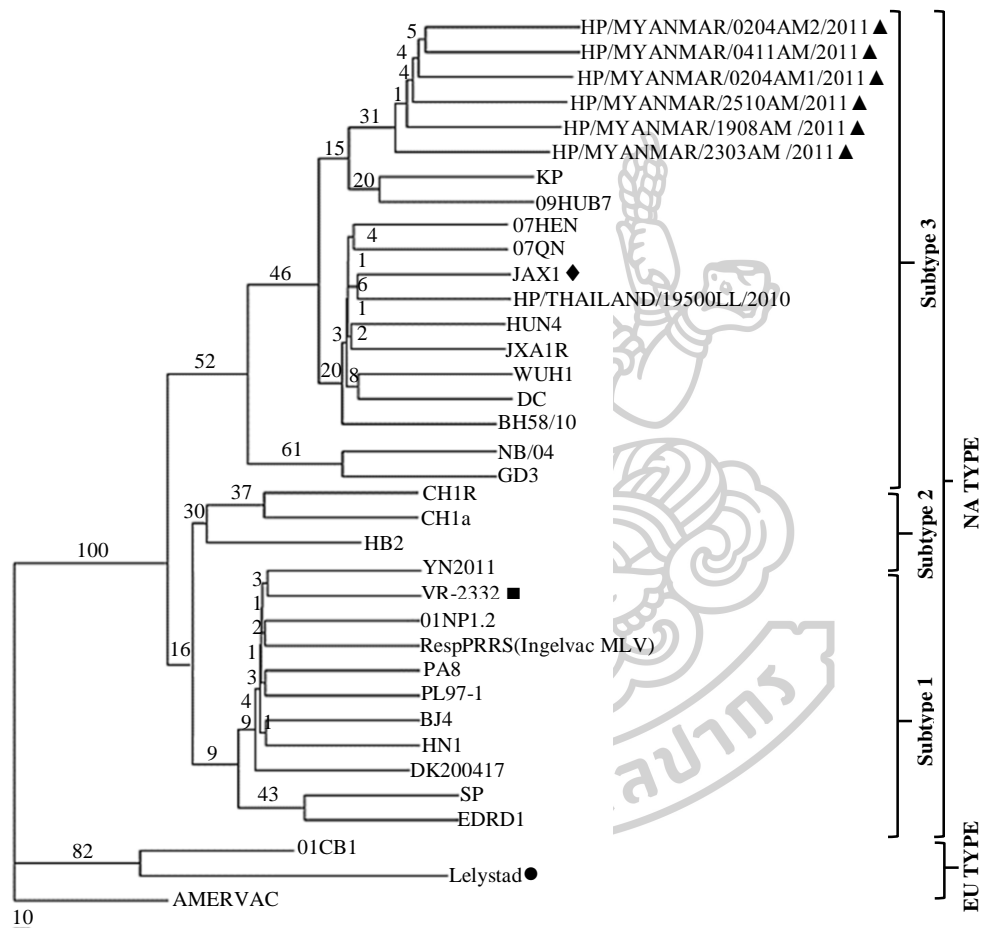
The phylogenetic tree was constructed by Neighbor-Joining method using Kimura 2-parameter model with 1000 bootstrapping. (▲) indicates Myanmar PRRSVs, (◆) Chinese HP-PRRS, JXA1, (●) indicates EU prototype, Lelystad and (■) indicates NA prototype, VR-2332.





## 2.9. Phylogenetic tree of PRRSVs based on deduced amino acid sequences of ORF7 gene

The phylogenetic tree was constructed by Maximum Likelihood method using John-Taylor-Thornton model with 1000 bootstrapping. (▲) indicates Myanmar PRRSVs, (◆) Chinese HP-PRRS, JXA1, (●) indicates EU prototype, Lelystad and (■) indicates NA prototype, VR-2332.



## VITA

**NAME** Miss Yamin Ko Ko

**DATE OF BIRTH** 17 March 1976

**PLACE OF BIRTH** Yangon, Myanmar

**INSTITUTIONS ATTENDED** Doctor of Philosophy (Ph.D.), Pharmaceutical Sciences, Silpakorn University, Thailand  
Master of Pharmacy (M.Pharm.), Pharmacology, University of Pharmacy, Yangon, Myanmar  
Bachelor of Pharmacy (B.Pharm.), Institute of Pharmacy, Yangon, Myanmar

**HOME ADDRESS** No.50, Sisone Street, Sanchaung Township, Yangon, Myanmar

**PUBLICATION** Yamin Ko Ko, Perayot Pamonsinlapatham, Aung Myint, Aung Zaw Latt, Kaythi Aye, Suang Rungpragayphan and Busaba Powthongchin. Sequence and phylogenetic analyses of Nsp2-HVII, ORF5, and ORF7 coding regions of highly pathogenic porcine reproductive and respiratory syndrome virus from Myanmar, *Transboundary and Emerging Diseases Journal*. 2019; 66.1073-1076. doi:10.1111/tbed.13118.

Yamin Ko Ko, Busaba Powthongchin, Suang Rungpragayphan, Aung Myint, Aung Zaw Latt. Phylogenetic Analysis of ORF7 Nucleotide Sequence of Porcine Reproductive and Respiratory Syndrome Virus from Myanmar. 26th Federation of Asian Pharmaceutical Associations (FAPA) Congress, 10 - 12 November 2016, Bangkok, Thailand. (Poster Presentation)